Finite element analysis of multi-channel-beam bridges

by

XiaoPeng Qin

A thesis submitted to the graduate faculty

in partial fulfillment of the requirements for the degree of

MASTER OF SCIENCE

Major: Civil Engineering (Structural Engineering)

Program of Study Committee:
F. Wayne Klaiber, Co-major Professor
Terry J. Wipf, Co-major Professor
Loren W. Zachary

Iowa State University

Ames, Iowa

2001

Copyright © XiaoPeng Qin, 2001. All rights reserved.

Graduate College
Iowa State University

This is to certify that the master's thesis of

XiaoPeng Qin

has met the thesis requirements of Iowa State University

Signatures have been redacted for privacy

TABLE OF CONTENTS

LIST OF FIGURES

LIST OF TABLES

1. INTRODUCTION

1.1. Background

Iowa ranks fifth nationally among states in quantity of bridges with nearly 25,000 structures. Seventy percent of these are on the state's secondary road system. Precast concrete deck bridge (PCDB) is one structural type commonly found on secondary roads. This structural type includes precast concrete slab, channel beam, and tee beam bridges.

In recent years, safety concerns have been raised due to the significant deterioration discovered in a large number of PCDBs. These bridges should be studied for possible reductions in their load carrying capacities and strengthening procedures needed to be developed to increase their capacities. The possibility of removing posted limitations or increasing the rating of a given bridge should also be investigated. Results from these investigations will be of interest to consultants who periodically inspect, rate, and maintain the structures.

1.2. Objective

The primary objective of this research was to determine the strength of deteriorated PCDBs, and to investigate various methods for further strengthening this type of bridge. This was addressed through both field and laboratory tests of this type of bridge, as well as, individual precast components. Theoretical models of the structures were analyzed. These models will hopefully allow engineers to predict behavior without the need of costly physical, field and laboratory testing.

This paper will mainly present the theoretical model analyses. Detailed information on the field and laboratory testing may be obtained in the reports by Ingersoll [1]. The

analytical models were intended to predict the bridges' behavior under service load, rather than determine the ultimate strength of the bridges and their components. Thus, only linear elastic analyses were conducted for this research.

1.3. Scope of Research

Ingersoll's [1] work involved laboratory tests on six old precast units, which are reinforced concrete channel beams taken from two demolished bridges, and a laboratory bridge composed of four channel beams connected with bolts and pipes. Field tests were also conducted on four multi-channel-beam bridges located in Butler, Story, and Delaware counties, which will be described in Section 1.4.

Prior to theoretical analyses, a literature review of various theories applicable to multibeam bridges was conducted. These theories include orthotropic plate theory, articulated plate theory, grillage method, and finite element method. Due to the inability of the plate theory or the grillage method for representing the structure's localized behavior, the finite element method was settled upon to fulfill the analytical aspect of this research.

Experimentally tested beams and bridges have been modeled and analyzed using ANSYS [2], a general-purpose finite element software program. Each model was verified by comparing its results with the available ACI code calculations and experimental testing results. Differences between the elastic finite element models and the actual structures that are normally deteriorated and nonlinear in behavior are addressed.

Sensitivity studies were performed when modeling the shear connections, such as bolts and pipes. Ideal model types were selected. Finally, the bridges' load distribution

factors which resulted from analyses and experimental testing for the bolt and pipe connections, were provided as the bridge engineers' design reference.

1.4. Description of the Field Tested Bridges

A typical multibeam bridge is made by placing precast beam sections side-by-side to provide a roadway over which vehicles may travel. Typically continuous longitudinal shear keys are grouted, or several separate longitudinal steel pipes are embedded on adjoining sides of each beam, to provide continuity between individual beams. For bridges with slab or box section beams, extending transverse rods through all the sections improve the entire structure's integrity through transverse prestressing. For bridges with channel section beams, the adjoining beams are often connected with transverse bolts and shear keys.

The four field bridges tested for this project fall into the channel section multibeam bridge category. Service load tests have been conducted by Ingersoll [1] on these precast reinforced concrete bridges located in Butler, Story, and Delaware counties. Three of them are single-span units; one is a two-span bridge. These bridges have been modeled using the ANSYS program, and are discussed in Chapter 5.

1.4.1. Story County Bridge

Located in Story County, the bridge is a two-lane precast reinforced concrete bridge. It is composed of 9 channel beams with an end-to-end span of 25 ft. Each of interior and edge beams has the same cross-section and reinforcing bars as presented in Figure 1.1. With a total width of 28 ft 10 in., the bridge is supported by two 1 ft 6 in. wide abutments. The bridge has only bolt connections. Figure 1.2 presents the photographs of the Story County Bridge. Figure 1.3 presents the layout of the Story County Bridge.

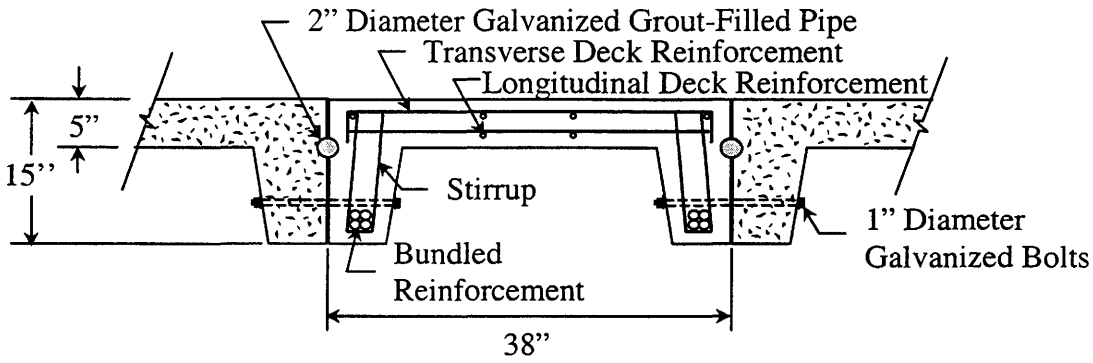

a. Interior beam

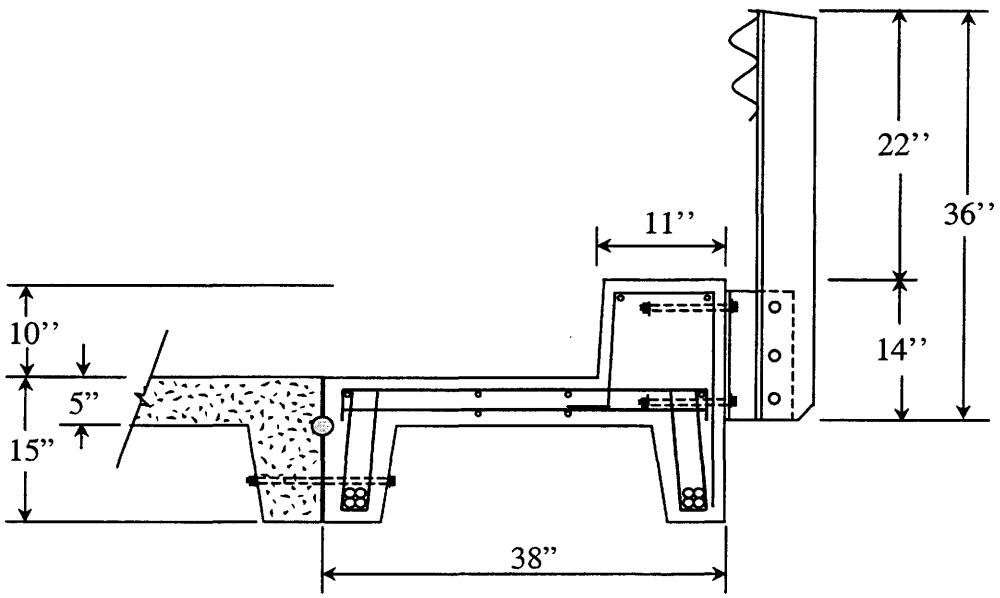

b. Exterior (or edge) beam

Figure 1.1. Typical cross-section of interior and exterior beams.

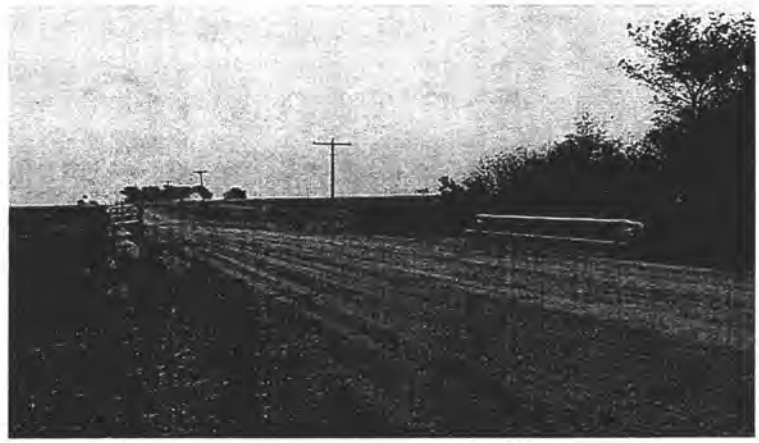

a. Plan view

b. Side view

c. Bottom view

Figure 1.2. Photographs of the Story County Bridge.

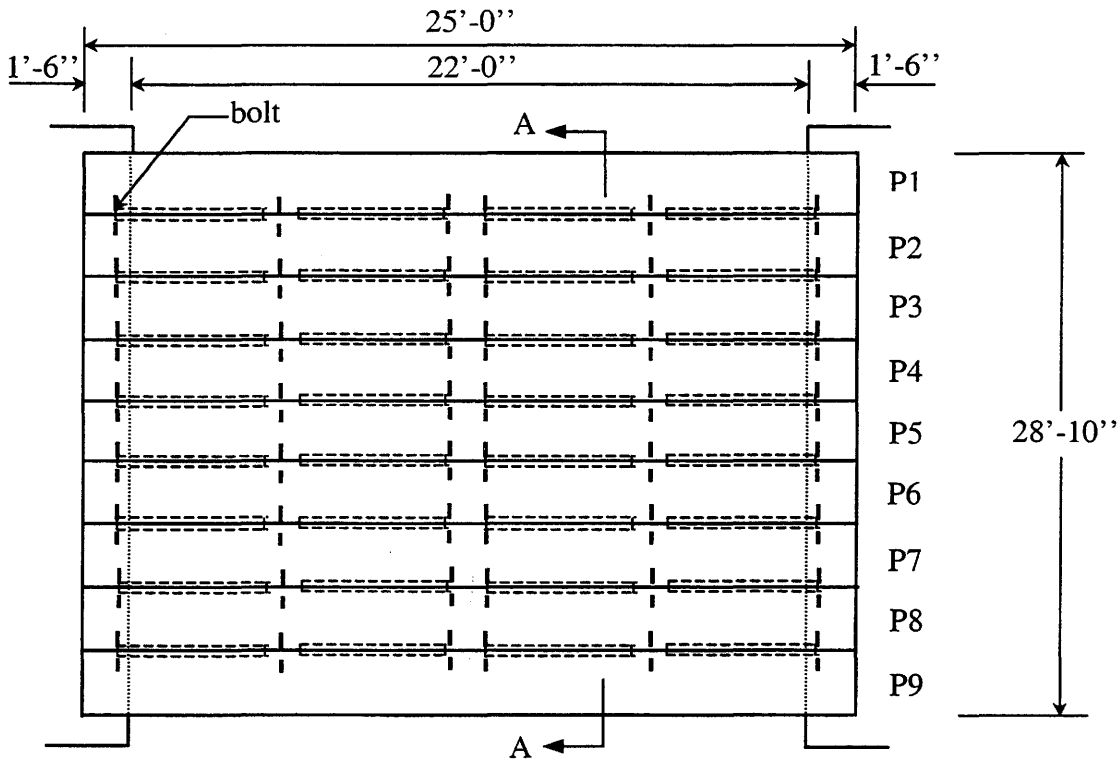

a. Plan view

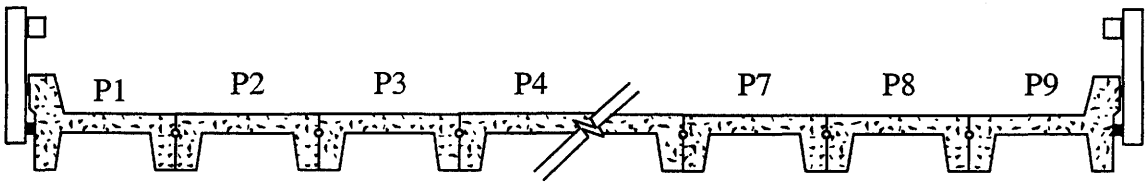

b. Section A-A

Figure 1.3. Layout of the Story County Bridge.

1.4.2. Delaware County Dairy Bridge

Located in Delaware County, the Dairy Bridge is a two-lane precast reinforced concrete bridge, illustrated in Figure 1.4. It is composed of 8 channel beams with an end-to-end span of 36 ft, including two cantilever ends. Each of interior and edge beams has the same cross-section and reinforcing bars as presented in Figure 1.1. With a total width of 25 ft 6 in., the bridge is supported by two 1 ft 9 in. wide abutments. The bridge has only bolt connections. Figure 1.5 presents the layout of the Dairy Bridge.

1.4.3. Butler County Bridge

Located in Butler County, this two-lane precast reinforced concrete bridge is composed of 10 channel beams with an end-to-end span of 31 ft. Each of the interior and edge beams has the same cross-section and reinforcing bars as presented in Figure 1.1. With a total width of 31 ft 10 in., the bridge is supported by two 2 ft wide abutments. The bridge has both bolt and pipe connections. Figure 1.6 presents the photographs of the Butler County Bridge and the layout of this bridge is illustrated in Figure 1.7.

1.4.4. Delaware County Trout Bridge

With two spans, the Trout Bridge is a two-lane precast reinforced concrete bridge located in Delaware County. Illustrated in Figure 1.8, it is composed of 9 channel beams with an end-to-end span of 31 ft for each span. Each of interior and edge beams has the same cross-section and reinforcing bars as presented in Figure 1.1. With a total width of 28 ft 10 in., the bridge is supported by three 2 ft wide abutments. The bridge has both bolt and pipe connections. Figure 1.9 presents the layout of the Trout Bridge.

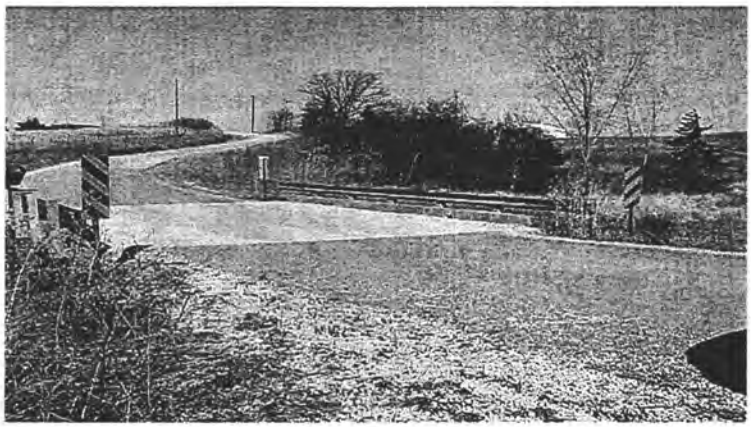

a. Plan view

b. Side view

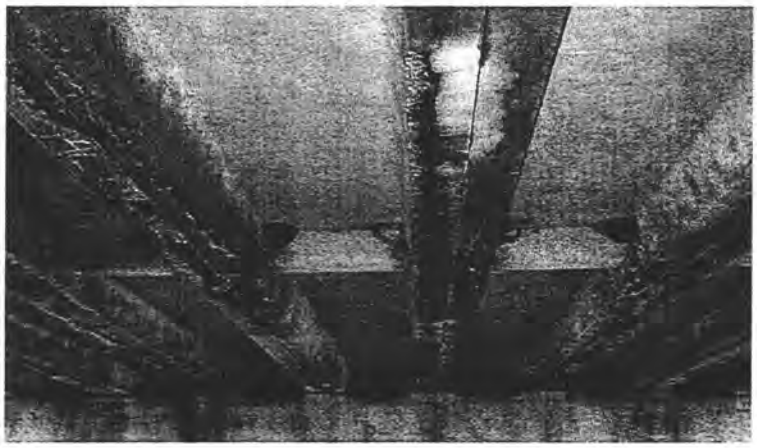

c. Bottom view

Figure 1.4. Photographs of the Delaware County Dairy Bridge.

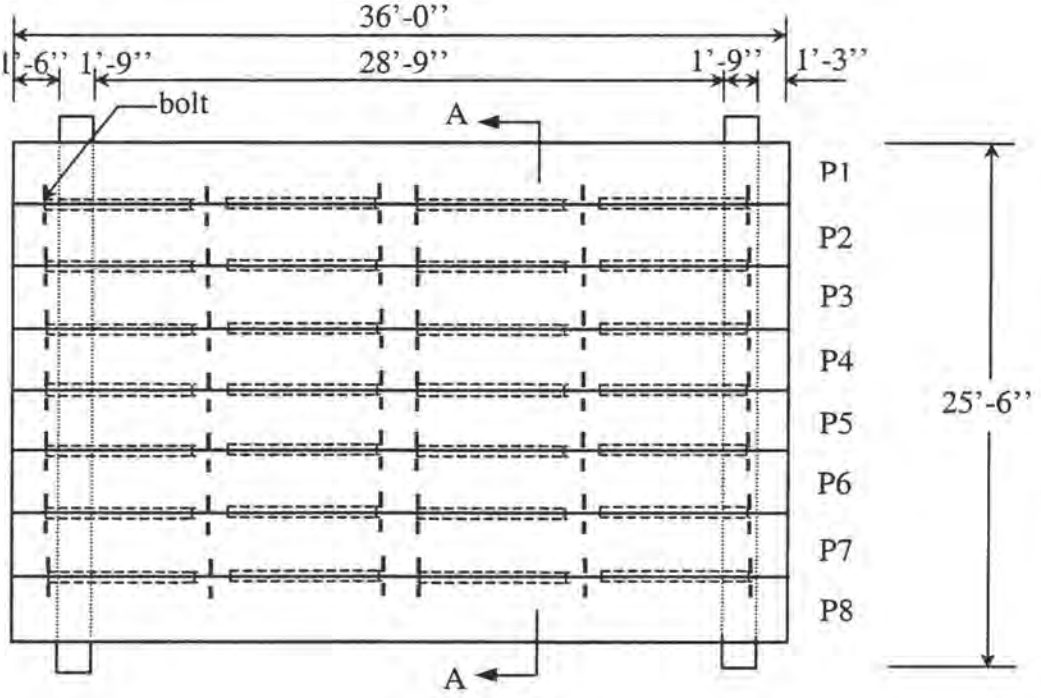

a. Plan view

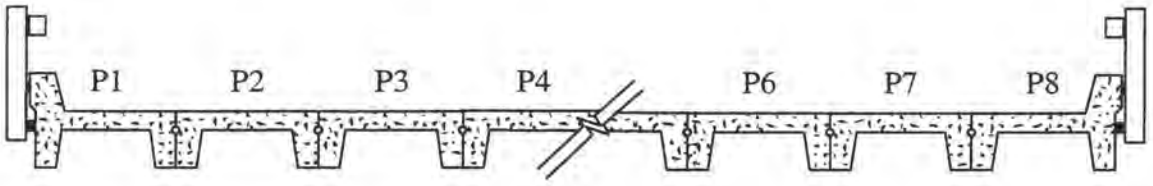

b. Section A-A

Figure 1.5. Layout of the Delaware County Dairy Bridge.

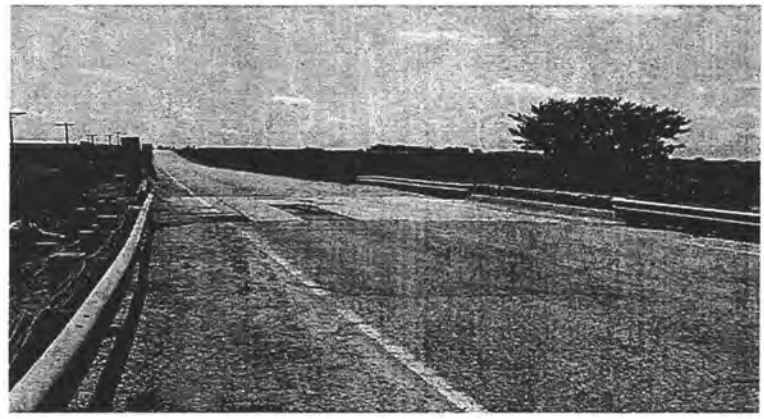

a. Plan view

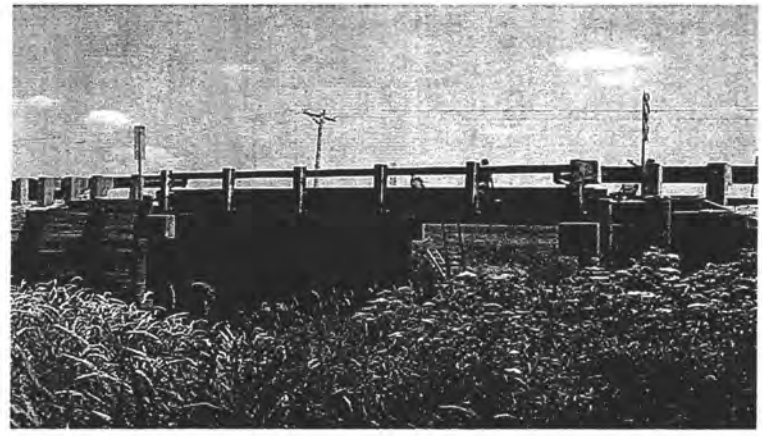

b. Side view

c. Bottom view

Figure 1.6. Photographs of the Butler County Bridge.

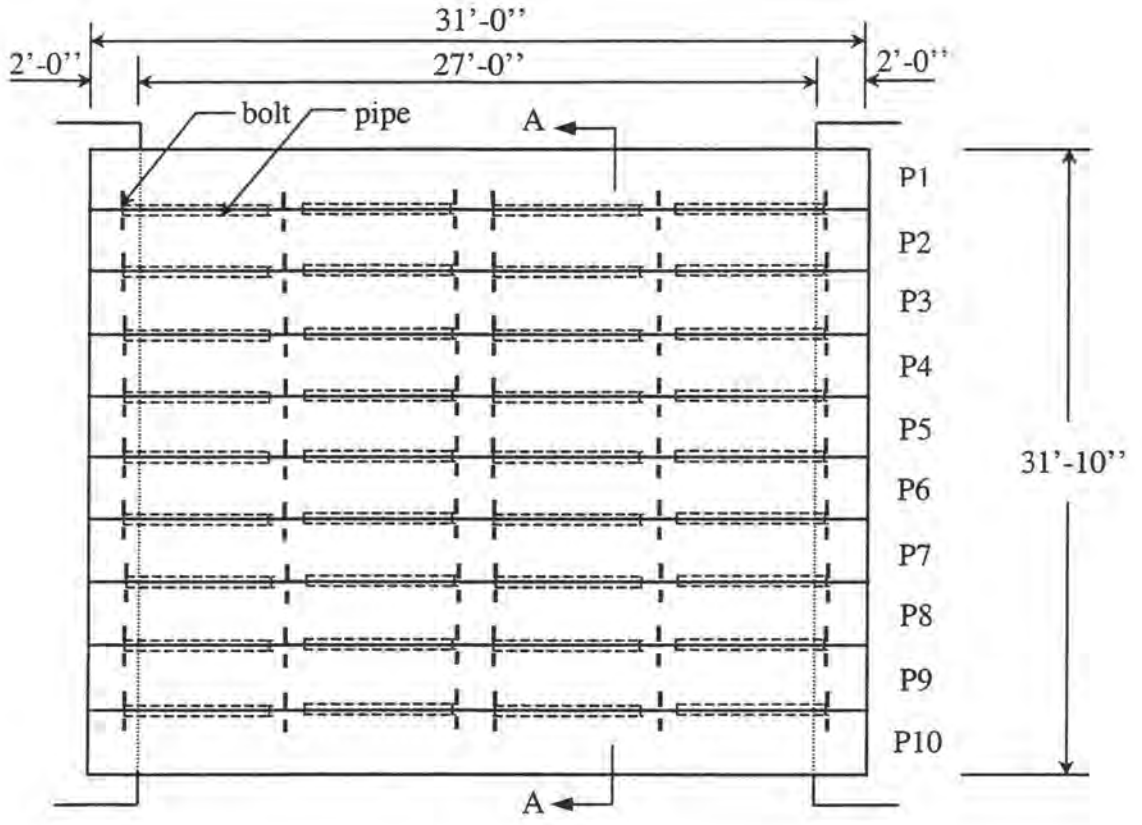

a. Plan view

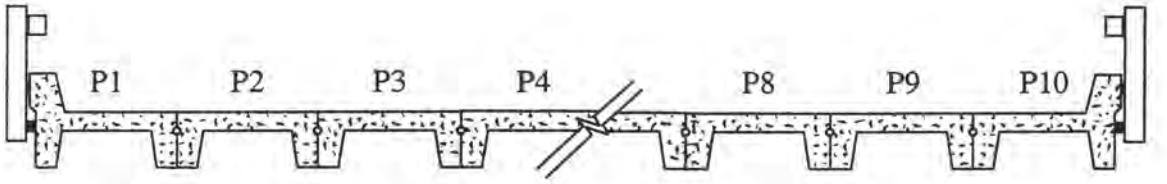

b. Section A-A

Figure 1.7. Layout of the Butler County Bridge.

a. Plan view

b. Side view

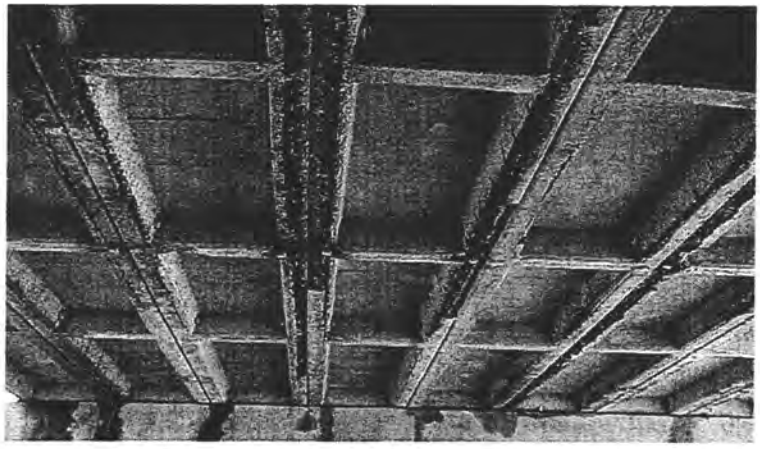

c. Bottom view

Figure 1.8. Photographs of the Delaware County Trout Bridge.

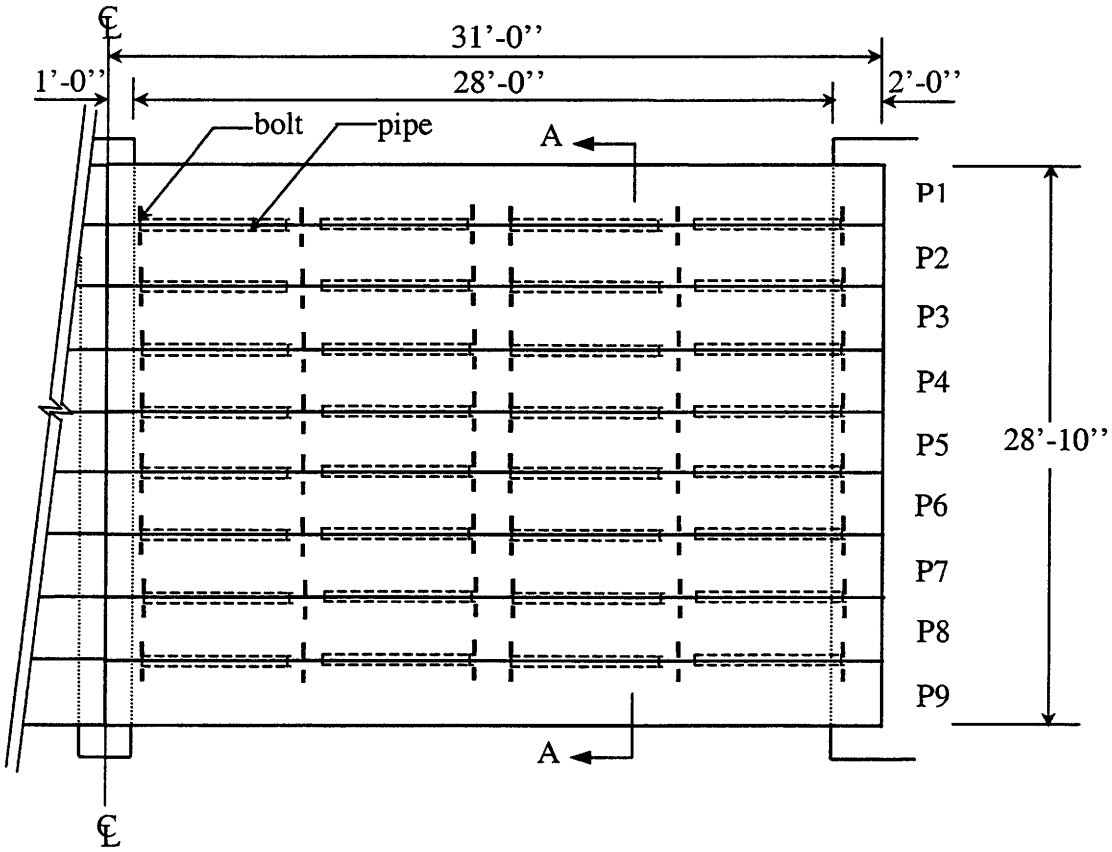

a. Plan view

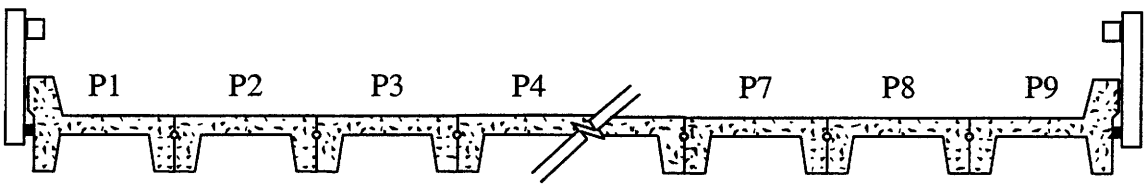

b. Section A-A

Figure 1.9. Layout of the Delaware County Trout Bridge.

2. LITERATURE REVIEW

2.1. Introduction

Four analytical methods have been developed and are used at present to perform bridge analysis. They consist of the grillage method, orthotropic plate theory, articulated plate theory, and finite element method. The appropriate application of these methods depends upon the structural behavior of the bridges under investigation.

Due to the convenience and availability of precast concrete beams, concrete multibeam bridges have been commonly used in highway and roadway construction. Numerous studies from the 1950's and 60's analyzed the structural behavior of multibeam bridges based on plate theory. With the development of computer technology and the increased availability of sufficiently powerful computers, finite element methods replaced plate theory as a means of structural analysis. A number of investigations on the finite element modeling of slab and slab-girder bridges have been well documented. However, to the author's knowledge, modeling of multibeam bridges using finite element has not been thoroughly investigated nor published.

This chapter will discuss the application of the four analytical methods in analyzing the multibeam bridges based on the related literature. A suitable analytical method will be chosen from these four to perform the analytical modeling required.

2.2. Grillage Method

The grillage method became popular in the early 1960s with the advancement of digital computers [3]. By simplifying the continuum deck as frame elements and using beam theory, grillage analysis was considered convenient due to the well-known stiffness analysis

of frames. Since beam theory and stiffness analysis are fundamental to all structural and civil engineers, this may explain why most bridge engineers are more familiar with the grillage method than with any other. In this method, imaginary cuts are taken in the longitudinal and transverse directions of the deck. Each part of the deck between these cuts is considered as a beam. The geometric properties of these beams are calculated based on the geometric section resulting from the imaginary cuts. The deck is thus idealized as a set of interconnected beams, like a grillage. In order to obtain reliable results from the grillage method, the location of these imaginary cuts must be selected with caution and care [4]. The longitudinal and transverse beam stiffnesses should be such that when prototype deck and equivalent grillage are subjected to identical loads, the two structures should deflect identically. Hambly [5] presented a comprehensive reference on modeling using the grillage method.

The grillage method has been well used to analyze the solid slab, voided slab, and slab-girder type bridges in which load distribution occurs mainly through flexure and torsion in the longitudinal and transverse directions. However, multibeam bridges differ greatly from these bridge types in that the transverse distribution of the load takes place mainly through shear force, with little or no involvement of transverse bending stiffness. Therefore, the usual grillage method suitable for analyzing slab or slab-girder bridges, is not applicable to multibeam bridges [6]. Although Hambly [5] presented an application of the grillage method for the shear-key deck, the stiffness of the shear key is difficult to obtain. Furthermore, the grillage method only provides the overall moments and shear forces. It does not provide localized deflections and stresses. In this regard, it is of limited usefulness.

2.3. Plate Theory

Plates are straight, plane surface structures of slight thickness compared to their other dimensions. The two-dimensional structural action of plates results in lighter structures and therefore offers numerous economic advantages. This has contributed considerably to the wide use of plates in all areas of engineering. Slab bridges are typical examples of the use of plates in transportation engineering. A mathematical approach to the plate theory was first formulated by Euler [7] in 1766. Since then, mathematicians, physicists, and engineers have conducted numerous studies to develop plate theory.

To apply plate theory to actual structures, one should note that the elastic properties of structural material are not the same in all directions but are instead inherently anisotropic. To make plate theory agree with experimental results and to simplify analysis, one usually assumes an orthotropic material, i.e., it has three planes of symmetry with respect to its elastic properties. The application of an orthotropic plate theory to reinforced concrete slabs was attributed to Huber [8] in 1914.

2.3.1. Orthotropic Plate Theory

In order to analyze grillages with members of negligible torsional stiffness, in 1946 Guyon [9] became the first to replace actual bridge structures with equivalent orthotropic plates. In 1950, Massonnet [10] generalized this approach to include the effects of torsion.

Consider an orthotropic plate in which the coordinate axes of x and y are taken in the middle (neutral) plane of the plate, the stress-strain relationships are provided according to Hook's law. Then the strain-displacement relationships are found based on the assumption that plane sections perpendicular to the neutral plane remain plane and perpendicular to the deflected neutral plane. It is also assumed that the plate's deflection is small compared with

the thickness of the plate. Then the stress-displacement relationships are easily derived. Bending moments, twisting moments, and shear forces of the plate are formed due to the stresses. To satisfy the equilibrium requirement, a differential equation of the plate is produced. Timoshenko et. al. [11] presented a detailed derivation of this governing differential equation for the orthotropic plate.

The differential equation was modified for the case of multibeam bridges in which the torsional stiffness is not necessarily the same in the x and y direction. A close-form solution to this equation is difficult to obtain. The famous Levy's method [11] was used to solve the differential equation. Guyon [9] and Massonnet [10] developed distribution coefficient methods based on the orthotropic plate theory to find a simplified approximate solution. Morice et. al. [12] and Rowe [13] generalized the principles of the method and provided charts to formulate a design procedure based on this method.

The prerequisite for applying the orthotropic plate theory to the analysis of multibeam bridges is that the transverse connections between beams provide a degree of continuity sufficient to make the bridges behave as a plate. For instance, orthotropic plate theory is quite applicable to a multibeam bridge with a continuous, reinforced concrete composite slab. However, in the case of a multibeam bridge whose transverse load distribution is obtained through concrete shear keys, mild steel shear connectors, or transverse prestressing, the orthotropic plate theory is questionable because of the low transverse stiffness of the pseudo slab [14]. To make the orthotropic plate theory applicable in this case, one must assume that the deck is continuous in both longitudinal and transverse directions. In the transverse direction, the thickness of the slab would change from a maximum value equal to the depth of the individual beam to a value less than the depth at the joints between the beams. Cusens

[14] suggested measuring effective depth to the center of the shear key. In calculations on a pseudo-slab with mild steel connectors, Best [15] assumed the concrete in the joints would be cracked to the level of the connector. The uncracked part of the concrete section was used to compute the second moment of area per unit length of span.

Based upon the orthotropic plate theory, in 1981 Bakht et. al. [16] presented a simplified method for determining transverse shear intensity in the shear keys of multibeam bridges using the AASHTO [17] and Ontario [18] highway bridge design vehicles. Applicable to right single span bridges, this method involves calculating the value of a dimensionless characterizing parameter from the bridge properties, and the reading of the design values of transverse shear intensities from provided charts.

2.3.2. Articulated Plate Theory

The Guyon-Massonnet distribution coefficient methods based on the orthotropic plate theory is valid only if one-half of the sum of the longitudinal and transverse torsional stiffnesses does not exceed the square root of the product of the corresponding flexural stiffness [14]. However, certain types of multibeam bridges do not satisfy this requirement, and may be assumed to possess no transverse stiffness, thus behaving as an articulated plate which is a particular class of orthotropic plate. In these bridges, load distribution takes place mainly by shear forces.

Assuming the transverse bending stiffness, transverse torsional stiffness, and the bending coupling stiffness of the plate are zero, in 1961, Spindel [19] presented the differential equation of the articulated plate. Once again, the solution was provided using Levy's method. The distribution coefficients were also formulated to make the solution easier to find.

2.3.3. Comparison between the Plate Theory and Experimental Results

Little [20] performed laboratory tests for load distribution in a model prestressed concrete bridge in 1955. Meanwhile, significant laboratory work was performed at Fritz Laboratory at Lehigh University to investigate the multibeam bridge and the orthotropic plate theory [21][22]. A 10 ft 9 in. wide and 16 ft spanned bridge model with nine rectangular beams was built. Prestressing was applied in both the longitudinal and transverse directions. Concrete was grouted to the large keyways along the sides of the beams. Fifty-eight different tests were conducted to determine the stiffness properties of the bridge, the influence of the degree and location of lateral post-tensioning, the interaction of shear keys, and slippage between the adjacent beams. Lateral load distribution in the inelastic range of the bridge was also tested up to the point of destruction.

Roesli [21] and Walther [22] conclude that the correlation between theory and test results is very close as long as little slippage developed between adjacent beams. When the relative displacement between adjacent beams becomes decisive, an empirical modification to the orthotropic plate theory was necessary.

In 1963, Best [15] performed tests on a bridge model with a 17 ft 10 in. span and a 11 ft 10 in. width. The model was formed with 13 longitudinal precast, pre-tensioned rectangular beams with transverse continuity produced by mild steel shear loop in the concrete joints. A scale model of the HB abnormal load vehicle [13] was applied, up to 25% above the working load. Results from both orthotropic and articulated plate theories were compared to the experimental results. Best [15] concluded that when the load was applied at or near the edge of the bridge, agreement between the experimental results and both the orthotropic and articulated plate theories is very good. However, when the load was applied

at or near the center of the bridge, the articulated plate theory agrees with laboratory results much better than does the orthotropic plate theory. After rotation, slope, and transverse shear values were compared, he concluded that the articulated plate theory should be used for analyzing this type of bridge.

Cusens and Pama [14] performed laboratory tests on a bridge model similar to that of Walther [22] and Best [15]. They concluded that the articulated plate theory gave a good prediction of the deflection distribution coefficient profile of the slab towards the unloaded edge, while orthotropic plate theory showed marked superiority near the loaded edge of the slab [14].

Observing that, due to its low transverse flexural stiffness, orthotropic plate theory is often inapplicable in practice, Pama and Cusens [23] focused instead on the articulated plate theory. Adding the effects of longitudinal torsion and Poisson's ratio, they improved upon the articulated plate theory formulated by Spindel [19], which considered only transverse torsion effects. They also included the effects of edge beam stiffening, finding these particularly significant under eccentric loading.

2.4. Khachaturian's Method

Although based on a similar assumption that the transverse stiffness of the pseudo-slab is zero and that beams are connected to each other along the span by hinges (i.e., joints), the approach of Duberg, Khachaturian and Fradiger [24] is nonetheless different from Spindel's [19]. In their unique method, a small longitudinal length of a beam element was taken. External vertical forces are then applied, along with the statically indeterminate distributed forces acting at the joints. Differential equations for the deflection of the element

are obtained using the engineering theory of bending and restrained torsion. All of the forces may be expressed in a form of a Fourier series that satisfies the boundary conditions. Integration of the differential equations results in the total deflection of the beam element in terms of the joint forces.

Similar expressions may be derived for all the beam elements of the bridge. Then, in order to eliminate the deflection terms, compatibility equations, which satisfy the deflection continuity between adjacent beam elements, may be derived and substituted for the deflection equations, thus obtaining simultaneous equations in terms of joint forces. Each joint contains three unknown joint forces, and three simultaneous equations may be derived in terms of these unknowns. Generally, if the bridge contains m joints, there will be 3m unknown forces in m joints, and 3m equations available for their solution.

Due to concentrated loads acting at various points in the bridge, the shears, moments, and stresses in each element may be calculated according to the ordinary theory of bending and torsion, once the forces in each joint are determined.

In 1967, Khachaturian, Robinson and Pool [25] adapted their method to multibeam bridges constructed with channel beams. Because the torsional behavior of open sections is different from that of closed sections, the behavior of a channel section differs from that of a box or slab section. In this instance, an energy method was used and the Fourier series for joint forces were divided into two parts to satisfy convergence requirement.

Based on Khachaturian's method, Powell, Ghose, and Buckle [26] developed a general, computer-oriented method for the analysis of multibeam bridges with elements of slab and box sections. The effects of edge beam stiffening were included in this program.

However, Cusens and Pama [27] pointed out that Khachaturian's method gave only the average value at the center of each beam, whereas, their improved articulated plate theory gave a clearer indication of the actual distribution of bending across the transverse section. They also mentioned that, with proper parameters in the articulated plate theory, results almost identical to those derived from Khachaturian's method were obtained, but that their improved articulated plate theory was simpler for structural designers to use.

In 1984, Jones and Boaz [28] developed an analytical tool based on Khachaturian's method for a skewed and discretely connected multibeam bridge with standard prestressed, precast double-tee sections. The connection response is modeled by linear and rotational springs that resist relative displacement between adjacent beams. The governing system of equations for the total structure is generated after development of the single beam and connection responses.

2.5. Finite Element Method

Finite element method is a numerical procedure for analyzing structures that are too complicated to study satisfactorily using classical analytical methods. Instead of writing the differential equation of the continuous structure as adopted in the grillage method and plate theory, finite element approach discretizes the structure into a series of elements. In each element, a smooth displacement function related to the element's coordinates is provided. Satisfying the compatibility requirement at the connected nodes of the adjacent elements, a piecewise-smooth displacement function of the entire structure is formed. After the load and support conditions are applied to the discretized structure, simultaneous linear algebraic equations resulted from the assemblage of the entire structure can be solved to determine the

nodal displacements. Element strains, thus stresses, can be calculated from the nodal displacements. In a word, the finite element method is a method of piecewise approximation in which the approximating (displacement) function is formed by connecting simple functions, each defined over a small region (element) [29].

Since first used in the 1960s for reinforced concrete, the finite element analysis has been studied to represent many special features of reinforced concrete, including: constitutive relationships, failure theories, multi-axial stress theories, reinforcement modeling, behavior on the interface between reinforcement and concrete, crack representation, and the mechanisms of shear transfer [30]. The method has also produced many widely used general finite computer programs such as ABAQUS, ANSYS and ADINA.

The mathematical theory and formulation of the method were well documented by Zienkiewicz [31] in 1971. No further attempt is made to explain them here.

Numerous research papers have been published that present the investigation of this powerful method including, undoubtedly, its application to the analysis of bridges. In their 1985 summary of the subject, Jategaonkar, Jaeger, and Cheung [4] introduced element types for modeling solid slabs, pseudo slabs and slab-girder bridges, including cellular and steel decks. They also described the relationship of the grillage analysis to the finite element method, as well as mentioning their limitations. It may be noted that, although a number of studies have modeled slab-girder bridges, there is little available literature modeling multibeam bridges.

Since any analytical method relies on theories and assumptions that are not universally applicable, finite element programs are themselves not foolproof, a caveat noted in much of the finite element literature. In applying the principles of finite element modeling,

one should carefully examine mesh sizes, element types, and support conditions, among other factors. Alternative results, obtained from different analytical bases or from experiments, should be available for comparison.

2.6. Discussion and Summary

From the literatures presented above, it can be seen that numerous investigations were conducted to analyze multibeam bridges using plate theory. Little work has been done using grillage method and finite element method to analyze multibeam bridges. As for a multibeam bridge with channel beams, only Khachaturian et. al. [25] provided detailed study using their own method. Although it is believed that Cusen et. al. [27] also investigated the multibeam bridge with channel beams to compare their modified articulated plate theory with Khachaturian's approach, no detailed information was provided.

All the analytical methods discussed above are not independent with each other. They are actually related with each other. For instance, grillage model can be regarded as a particular derivation of plate theory by separating the continuum plate into a series of interconnected beams. It can also be regarded as a special case of finite element model by using beam elements in both longitudinal and transverse directions to model the bridge's deck.

The grillage method was not adopted to perform the analysis of multibeam bridges with channel beams for the following reasons:

1. It is not well suited to multibeam bridges in which the transverse distribution of the load takes place mainly through shear force and the transverse bending stiffness is very small.

2. Although Hambly [5] presented the application of the grillage method for the shear-key deck, the stiffness of the shear key is difficult to obtain.
3. It only yields the overall moments and shear forces and it does not provide localized deflections and stresses.

Neither of the plate theories will be used to perform the analysis for this research project for the following reasons:

1. The assumption that the deck behaves like a plate, orthotropic or articulated, is not well suited to multibeam bridges with channel beams having only bolt connections.
2. The simplified solution was presented with a series of tables and charts, because of the complexity of the solving process directly. Unfortunately, no information is given on how to apply this method to multibeam bridges with channel beams.
3. No matter how complicated the plate theory chosen, the results are still coarse, only including the overall moment and shear forces.

Although Khachaturian et. al. [25] presented their investigation of multibeam bridges with channel beams, their process is complicated and needs a specific computer program to use conveniently. Also, the localized behavior of the structure cannot be presented using their approach.

Therefore, the most advanced and refined analytical approach, the finite element method, was adopted for this project due to the following advantages:

1. The general-purpose finite element software, ANSYS, is available. The user friendly operating interface of the software makes it easy to use and the results can be conveniently deciphered.

2. Localized behavior, such as that of bolt connections, deflections and stresses at any position of the channel beams, can be easily obtained.
3. Multiple elements are available in ANSYS which allows the model to be optimized relatively rapidly.

It should be noted that in the multibeam bridges, slip between the adjacent panels is a possible occurrence. This makes accurate analysis difficult. It is also the reason why the previous researchers usually made an assumption that no slip occurred between the adjoined beams.

3. MODELING OF REINFORCED CONCRETE CHANNEL BEAMS

3.1. Introduction

Reinforced concrete channel beams were modeled first using ANSYS since they are the basic units of multi-channel-beam bridges. A structure can be modeled using one-, two-, or three-dimensional elements or combinations of these elements, depending upon its physical complexity and behavior. The ANSYS program has a library of 189 element types serving different purposes. It is important to determine which of these are most appropriate.

To model the reinforced concrete channel beams, calculations based on the American Concrete Institute Concrete Code (ACI 318-99) [32] were completed. Next, a study was conducted to determine the beam's full range of responses under service loads using the Type 3 rating vehicle [33]. This was followed by a sensitivity study on support conditions and span length of the finite element models. Several element types in ANSYS were then investigated to model the reinforced concrete channel beams. The analytical results from the finite element models were compared to the experimental results and the theoretical calculations based on ACI 318-99. Ideal model types were selected to pursue the subsequent modeling of the laboratory multi-channel-beam bridge presented in Chapter 4.

3.2. Laboratory Test Description

Laboratory tests were conducted on six reinforced concrete channel beams. Three beams were taken from the demolished Butler County Bridge and the remaining three were taken from the demolished Cedar County Bridge. Material properties of these two groups of beams were tested and averaged, as shown in Table 3.1. The ends of the beams sit on steel girders, W21 x 8, with plastic bearings to form the contact surfaces. Using hydraulic jacks,

two point loads were applied three feet in each direction from the midspan of the beams. A 1 ft x 1 ft hardboard bearing pad acted as the reaction surface between the jacks and the beam. All six beams were load tested until they failed. The test setup is illustrated in Figure 3.1.

Table 3.1. Material properties and span lengths of the beams.

Number of Group	Taken From	Span Length (ft)	Elastic Modulus of Concrete, E_c (ksi)	Elastic Modulus of Reinforcement, E_s (ksi)
1	Cedar County	25	5,700	26,600
2	Butler County	31	4,490	26,605

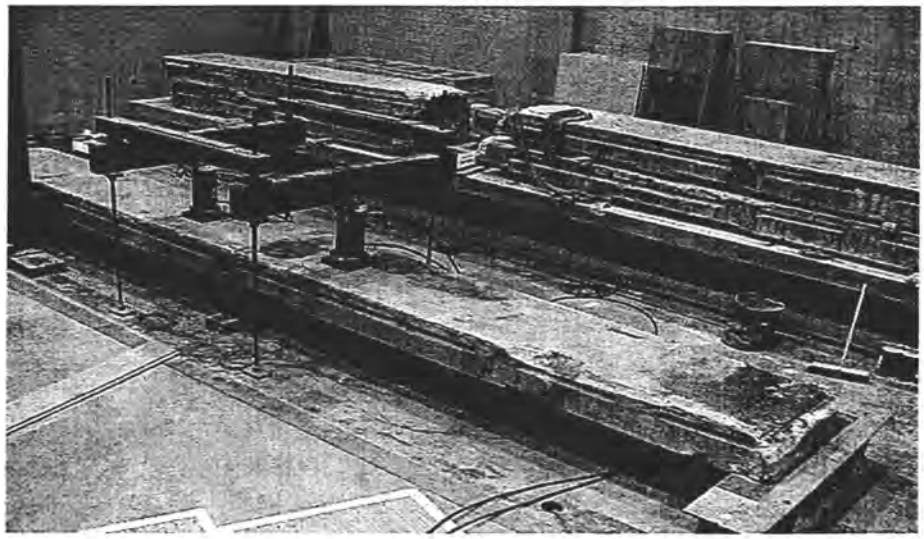

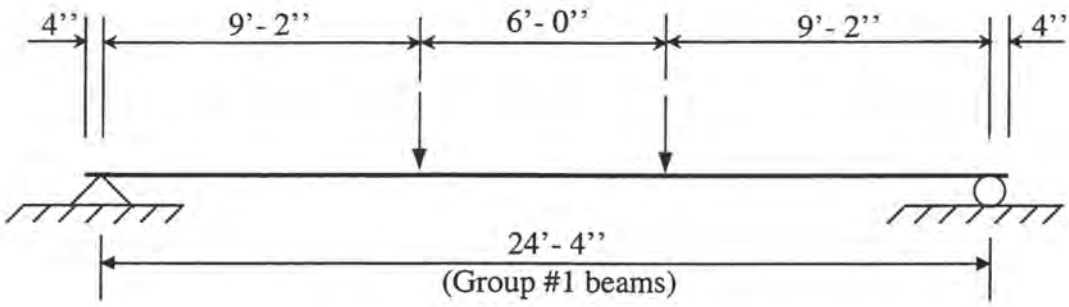

Figure 3.1. Laboratory test setup.

3.3. Theoretical Calculations and Parameter Study

This section presents calculations of the beams' deflections and strains based on ACI 318-99, which will be compared to the results from the finite element models and laboratory tests in subsequent sections. Calculations were also made to determine the beams' response under service load.

The following are sample calculations for the Group #1 beams, from the Cedar County Bridge as presented in Table 3.1. Due to their similarity, calculations for the Group #2 beams will not be presented here. The results for all of the beams are summarized in Table 3.2.

3.3.1. Formulas of the Deflection and Strain

A cross-section of the channel beam and the transformed beam sections are shown in Figure 3.2.

Step 1: Calculate M_{cr} (cracking moment)

$A = (38)(5)+(12)(10) = 310 \text{ in}^2$

$x = [(38)(5)(2.5)+(12)(10)(10)] / 310 = 5.4 \text{ in}^2$

$I_g = (38)(5)(3) / 12+(38)(5)(5.4-2.5)(2)+(12)(10)(3) / 12+(12)(10)(10-5.4)(2)$

$= 5533 \text{ in}^4$

$f_c' = (5700 / 57)^2 / 1000 = 10 \text{ ksi}$

$f_r = 7.5\sqrt{f_c'} = 7.5\sqrt{10000}/1000 = 0.75\text{ksi}$ ACI (9 - 9)

$M_{cr} = f_r I_g / y_t = (0.75)(5533) / (15-5.4) / 12 = 36.02 \text{ ft-kip}$ ACI (9-8)

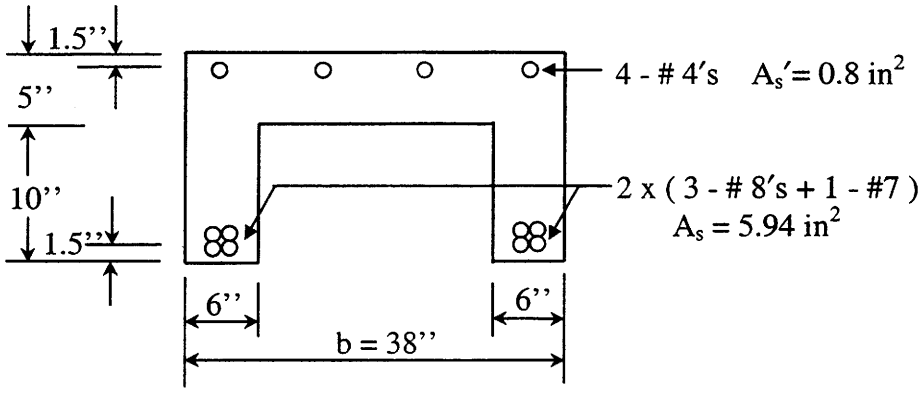

a. Channel beam cross-section

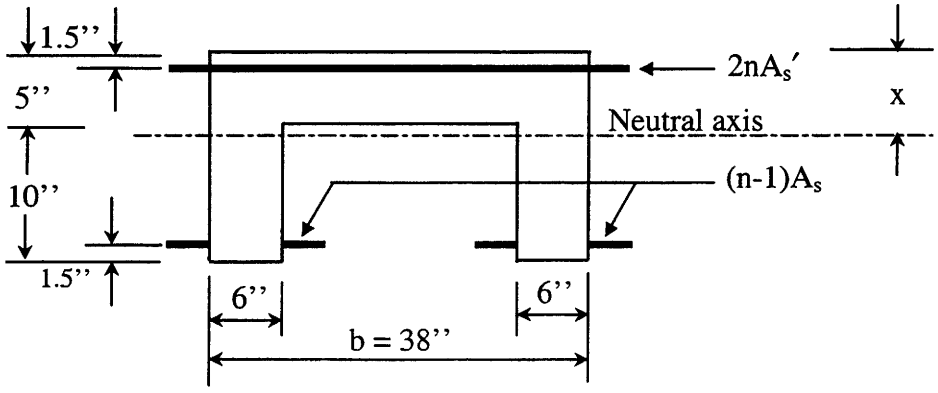

b. Uncracked transformed beam section

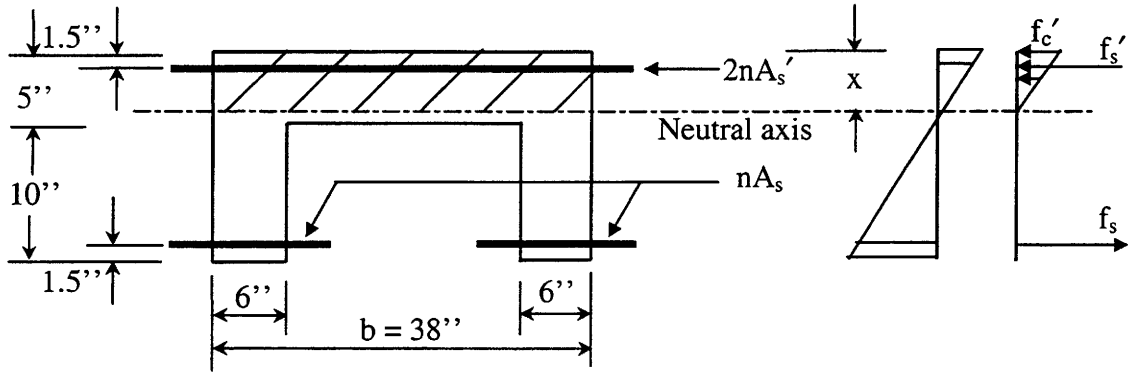

c. Cracked transformed beam section

Figure 3.2. The transformed channel beam section.

Step 2: Calculate I_{uncr} (moment of inertia of the uncracked transformed beam section)

$n = E_s / E_c = 26600 / 5700 = 5 < 6$, so $n = 6$

$(n-1)A_s = (5)(5.94) = 29.7\ in^2$ $\qquad 2nA_s' = (2)(6)(0.8) = 9.6\ in^2$

Refer to Figure 3.2(b) $\qquad A = (38)(5)+(12)(10)+29.7+9.6 = 349.3\ in^2$

$x = [(38)(5)(2.5)+(12)(10)(10)+(29.7)(13.5)+(9.6)(1.5)] / 349.3 = 6.0$ in.

$I_{uncr} = (38)(5)^3 / 12+(38)(5)(6.0-2.5)^2+(12)(10)^3 / 12+(12)(10)(10-6.0)^2$

$+(29.7)(13.5-6.0)^2+(9.6)(6.0-1.5)^2 = 7508\ in^4$

Step 3: Calculate I_{cr} (moment of inertia of the cracked transformed beam section)

Refer to Figure 3.2(c), the tension forces are equal to the compression forces,

$$\frac{1}{2}bxf_c'+2nA_s'\frac{x-1.5}{x}f_c' = nA_s\frac{13.5-x}{x}f_c'$$

$$\frac{1}{2}(38)x+2(6)(0.8)\frac{x-1.5}{x} = 6(5.94)\frac{13.5-x}{x}$$

Thus, $x = 4.05$ in.

$I_{cr} = (38)(4.05)^3 / 3+(2)(6)(0.8)(4.05-1.5)^2+(6)(5.94)(13.5-4.05)^2 = 4087\ in^4$

Step 4: Calculate I_e (effective moment of inertia), D (deflection) and S (strain).

$$I_e = \left(\frac{M_{cr}}{M_a}\right)^3 I_g + \left[1-\left(\frac{M_{cr}}{M_a}\right)^3\right] I_{cr} \qquad \text{ACI (9-7)}$$

$$D = \frac{5}{48}\frac{M_a l^2}{E_c I_e}$$

$$S = \frac{M_a}{I_e}y$$

where M_a is the bending moment of the beam,

y is the distance from the calculated position to the neutral axis along the depth of the cross-section of the beam.

Step 5: Calculate M_n (nominal moment strength of the beam).

Assume the concrete in compression reaches its ultimate strain of 0.003, and the bottom reinforcement reaches its yielding strain. After the first trial, it was found that x is less than 1.5 in, which means the top reinforcement is also in tension, hence,

$$0.85f_c'\beta_1 bx = \frac{x-1.5}{x}(0.003)E_sA_s'+f_yA_s$$

$$(0.85)(10)(0.65)(38)x = \frac{x-1.5}{x}(0.003)(26600)(0.8)+40(5.94)$$

Thus, x = 1.12 in.

The strain of the bottom tensile reinforcement is

$$\frac{13.5-x}{x}(0.003) = 0.033 > \frac{f_y}{E_s} = \frac{40}{26600} = 0.0015$$

which satisfies the assumption that the bottom reinforcement yields, therefore,

$$M_n = f_yA_s(13.5-\frac{0.85x}{2}) = 40(5.94)[13.5-\frac{0.85(1.12)}{2}]/12 = 257.88ft-kip$$

3.3.2. Parameter Study

To determine the beam's overall range of responses under service load, standard AASHTO HS20-44 and Type 3 vehicles [33] were used. Due to short spans of the beams, the Type 3 vehicle was selected to calculate the maximum bending moment produced by the

service load. Wheel configuration and weight distribution for this vehicle are illustrated in Figure 3.3. The position of the Type 3 vehicle loading to produce the maximum moment is shown in Figure 3.4. For the Group #1 beams, the maximum moment per wheel line produced by the Type 3 rating vehicle is $M_{TYPE3} = 87.09$ ft-kip.

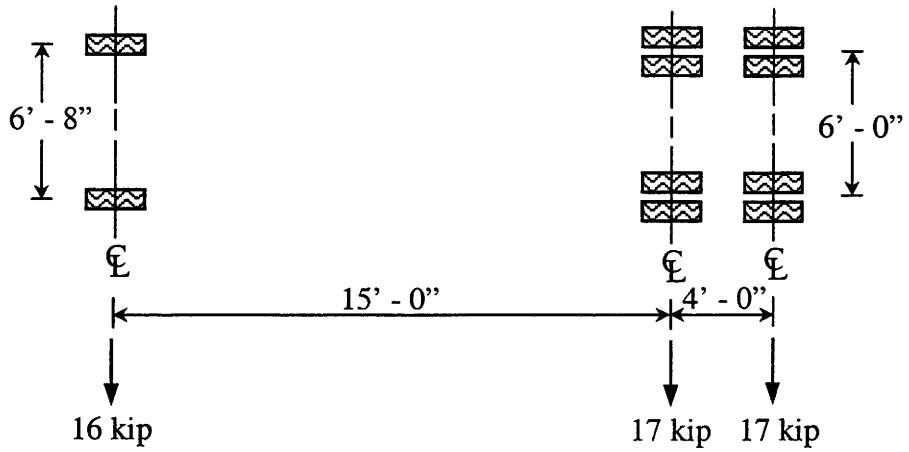

Figure 3.3. Wheel configuration and weight distribution of Type 3 rating vehicle.

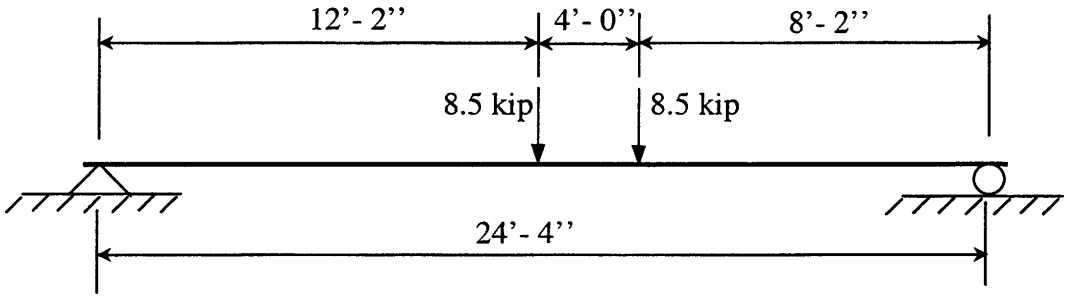

Figure 3.4. Position of the Type 3 rating vehicle to produce the maximum moment.

Analysis should, at a minimum, be conducted up to this maximum bending moment value for the multibeam bridges with channel beams similar to the beams from Cedar County (Group #1). Table 3.2 presents the summary of the theoretical calculations based on ACI

318-99 for the two groups of beams tested in the laboratory. It should be noted that in practice, the actual bending moment of the beam due to this wheel load is less than half of the value calculated due to the load distribution of the bridge, as presented in Chapter 5. For a precast bridge composed of the beams similar to Group #1, the maximum moment per wheel line produced by the Type 3 rating vehicle is approximate 40 ft-kip. Similarly, for a bridge composed of the beams similar to Group #2, it is approximate 55 ft-kip. Referring to Table 3.2, it can be seen that this maximum moment is only either a little beyond (for Group #1) or two times (for Group #2) the beam's cracking moment. The maximum moment is either 16% or 21% of the beam's nominal moment capacity. This linear elastic analysis is sufficient to provide information of the investigated bridges under service loading.

Table 3.2. Summary of theoretical calculations of the tested beams.

Number of Group	I_g (in^4)	I_{UNCR} (in^4)	I_{CR} (in^4)	M_{CR} (ft-kip)	M_n (ft-kip)	$M_{TYPE3, MAX}$ (ft-kip, per wheel line)
1	5533	7508	4087	36.0	257.9	87.1
2	5533	7508	4087	28.3	256.4	115.0

3.4. Sensitivity Study

The complex support conditions of a beam in practice are usually idealized in analytical models. A sensitivity study is usually required to investigate the idealization of beam's support conditions and span length. For the sake of simplicity, a one-dimensional finite element model was used for this task.

One end of the beam is always hinged, which means the three translational degrees of freedom (DOF) of the end are constrained. For the other end of the beam, the following scenarios were studied:

1. The other end is a roller, noted as "U_z" in Figure 3.5(a), which means the translational DOFs of this end are constrained only in the global z direction.
2. The translational DOFs of the other end are constrained in the global y and z directions, noted as "U_{yz}" in Figure 3.5(a).
3. The other end is hinged, noted as "U_{xyz}" in Figure 3.5(a), which means the translational DOFs of this end are constrained in the global x, y, and z directions.

Two scenarios were included for the span length sensitivity study. One is noted as "center span" where the span length was taken as the center-to-center distance between supports; the other is noted as "clear span" where the span length was taken as the face-to-face distance between supports. Figure 3.5(b) presents an illustration.

The results of the sensitivity study are shown in Figure 3.5(c). It can be seen that the model is very sensitive to the longitudinal (y axis) constraint in the other end. Removing this constraint resulted in a 128% increase of deflection. While the transverse (x axis) constraint in the other end has very little influence on the beam's behavior. Since there is no indication that the longitudinal displacement of the beam is totally constrained in practice, the "U_{yz}" and "U_{xyz}" support cases were not investigate further. Instead, the "U_z" support case was adopted as a modeling assumption for this study.

Compared to the total length of the beam, the bearing length is very small. This is the reason why the difference between the center span case and the clear span case is not significant. The center span case produced a deflection 8% more than the clear span case for

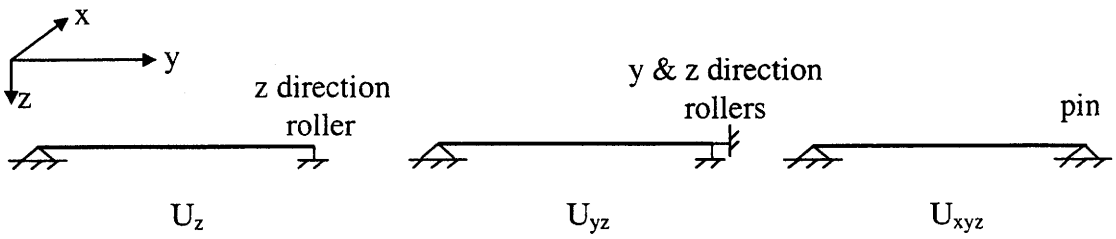

a. Support condition

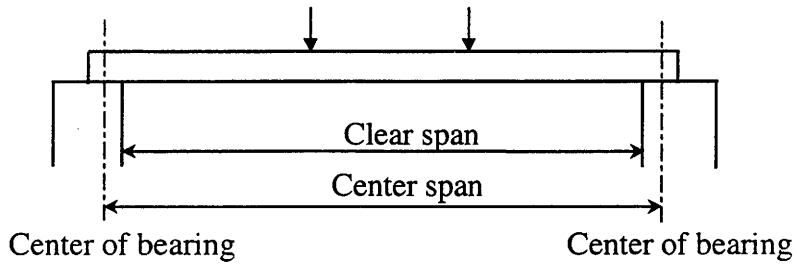

b. Span length

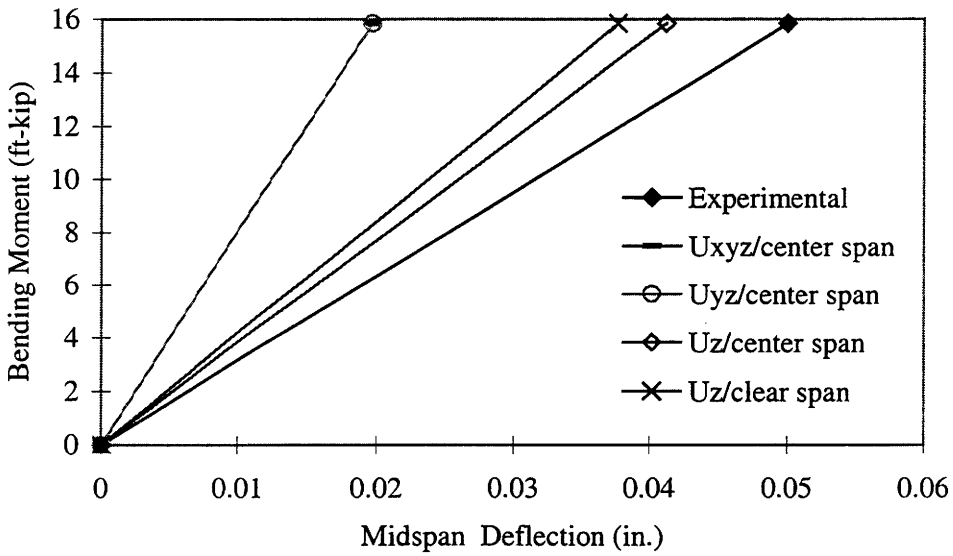

c. Deflection vs bending moment

Figure 3.5. Support condition and span length sensitivity.

this beam. The center span case was selected for the remainder of this study because it is a typical adoption in many theoretical methods. It also provided a slightly more conservative result, when compared to the clear span case.

The "U_z/center span" model was adopted for the remaining analysis. It should be noted, from Figure 3.5(c), that this model result more accurately reflects the experimental data than the other models.

3.5. Element Type Selection

3.5.1. One-dimensional Model (Beam4 Model)

A one-dimensional element connects two or more linear nodes. The Beam4 element in the ANSYS program falls into this category. It is a uniaxial element with tension, compression, torsion, and bending capabilities. It has six degrees of freedom at each node: translations in the nodal x, y, and z directions and rotations about the nodal x, y, and z axes. It is defined by two nodes, the cross-sectional area, two area moments of inertia (IZZ and IYY), two thickness (TKY and TKZ), an angle of orientation about the element x-axis, the torsional moment of inertia (IXX), and the material properties [2]. Figure 3.6 gives an illustration of the Beam4 element.

In modeling reinforced concrete beams, the Beam4 element has the distinct advantage that it has the capability of including the post-cracking behavior by inputting the calculated effective moment of inertia based on the ACI code. The disadvantage of this model is that it cannot represent the exact shape of the beam. Because of this, the localized behavior of the bolt connections in the bridge cannot be investigated accurately using the Beam4 element. Due to this drawback, the one-dimensional model was not used for this project.

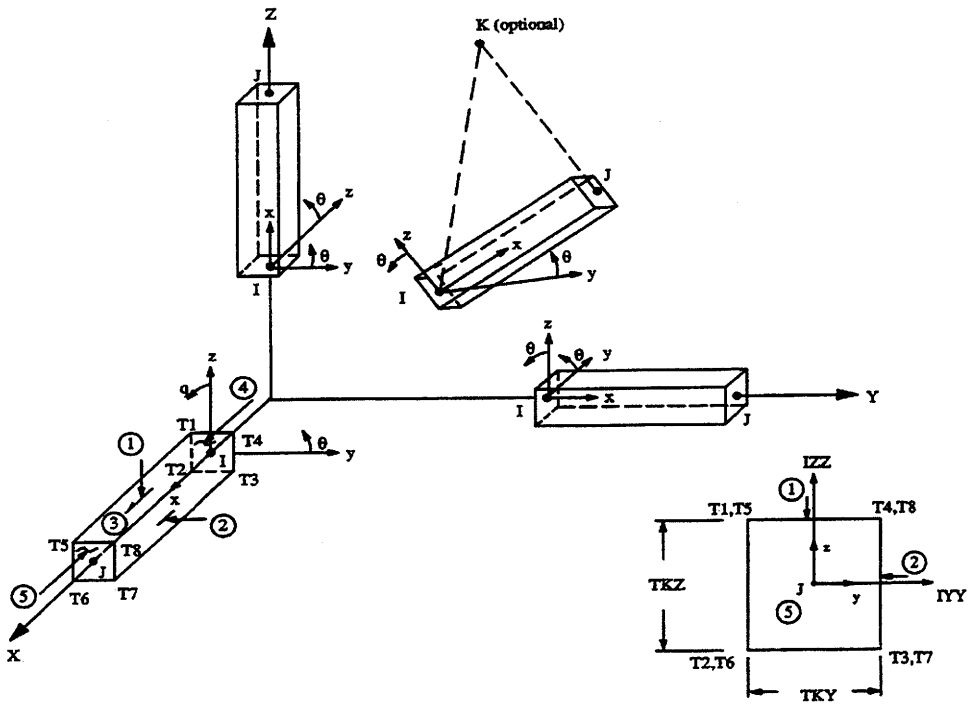

Figure 3.6. Beam4 element [2].

3.5.2. Two-dimensional Model (Shell63-Beam4 Model)

A two-dimensional element connects three or more nonlinear, planar nodes. The Shell63 element, which has both bending and membrane capabilities, falls into this category. This element has six DOFs at each node: translations in the nodal x, y, and z directions and rotations about the nodal x, y, and z axes. It is defined by three or four nodes, its thickness, and its orthotropic material properties [2], as shown in Figure 3.7.

The Shell63-Beam4 model, illustrated in Figure 3.8, is a combination of the Shell63 and Beam4 elements. In this model, the Shell63 element was used to represent the "deck" of the channel beam, which receives direct vehicle contact, while the Beam4 element was used to represent the "leg" portion of the beam. The "deck" element was rigidly connected to the "leg" element.

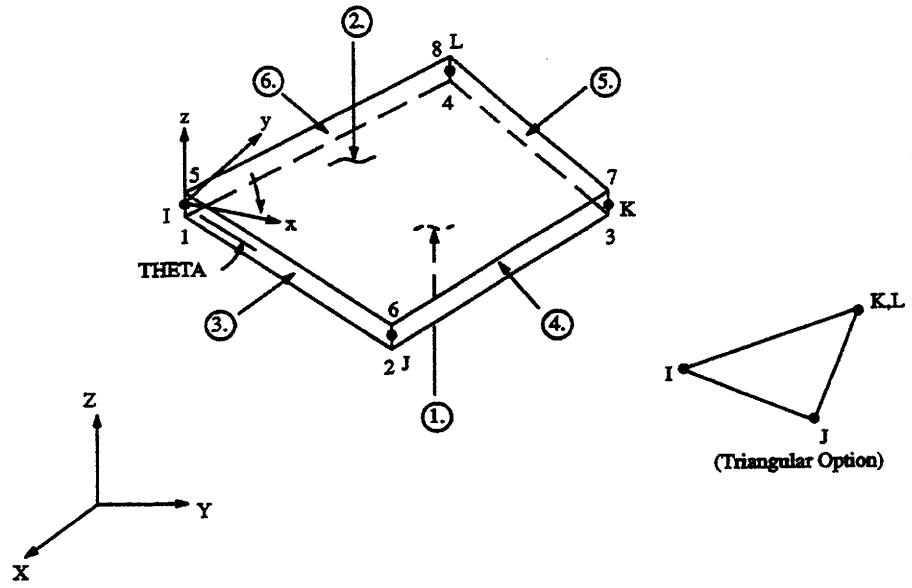

Figure 3.7. Shell63 element [2].

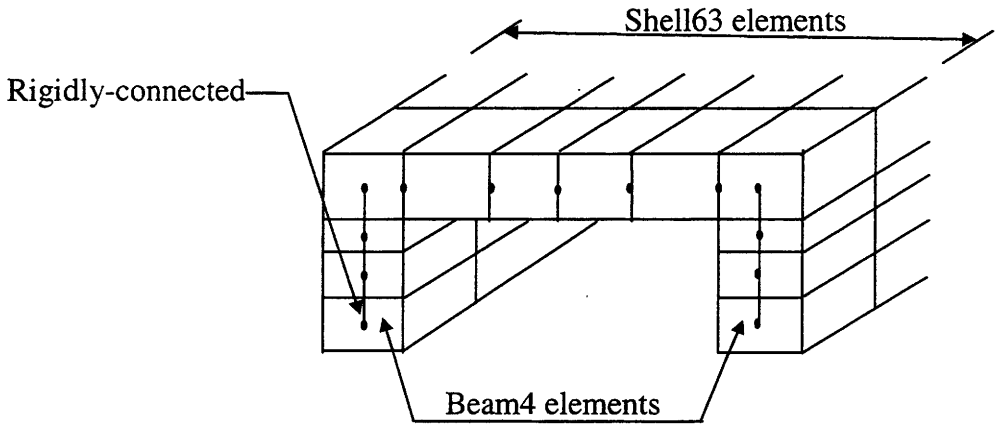

Figure 3.8. Shell63-Beam4 model.

This model may be effective for a slab-girder bridge. However, it may not be suitable for analyzing a multi-channel beam bridge since it artificially separates the monolithic channel beam into two parts with rigid connections. It also does not adequately account for

the rotation of the cross-section of the channel beam. Therefore it does not satisfy the assumption of plane sections' remaining plane in the beam theory. Figure 3.9 shows the discrepancy between the discontinuous strain profile along the depth of the cross-section of the beam resulting from this model and the continuous strain profile predicated from the beam theory. This two-dimensional model was deemed unsatisfactory for analyzing this specific bridge type and was not adopted.

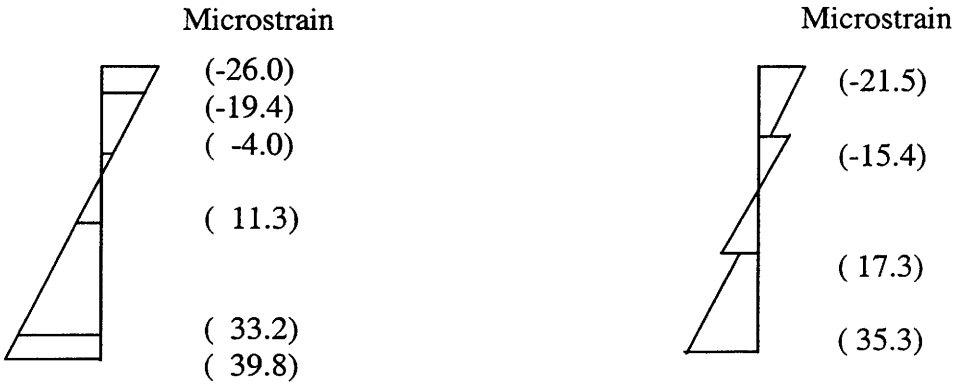

a. Beam theory b. Shell63-Beam4 model

Figure 3.9. Comparison between the beam theory and the Shell63-Beam4 model.

3.5.3. Three-dimensional Model

3.5.3.1. Solid45-Link8 Model

A three-dimensional element connects four or more non-planar nodes that can form a volume. The family of Solid elements in the ANSYS program fits this description. The Solid45 element, illustrated in Figure 3.10, is defined by eight nodes, each with three DOFs: translations in the nodal x, y, and z directions [2].

The Link8 element is a one-dimensional, uniaxial, tension-compression element with three DOFs at each node: translations in the nodal x, y, and z directions. It is defined by two nodes, the cross-sectional area, an initial strain, and the material properties, as shown in Figure 3.11.

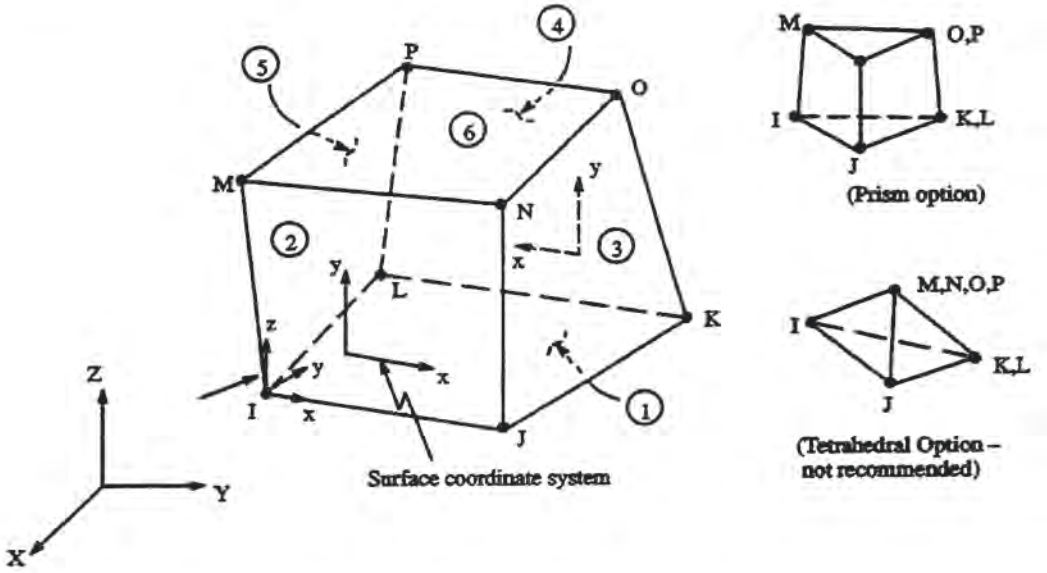

Figure 3.10. Solid45 element [2].

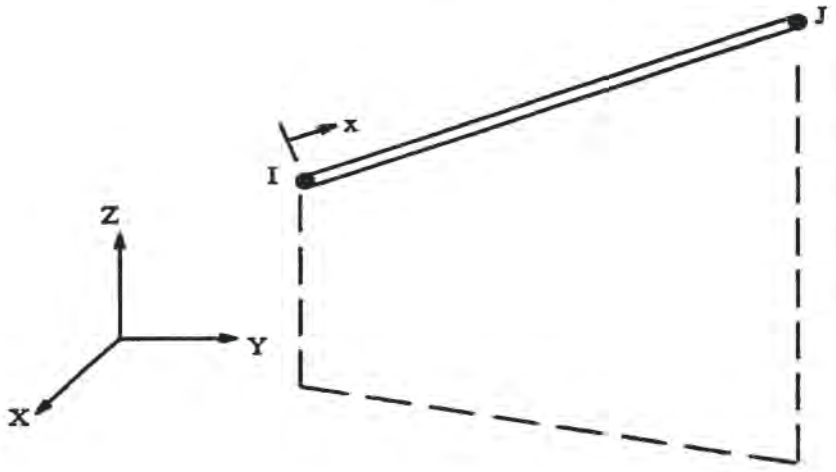

Figure 3.11. Link8 element [2].

The Solid-Link model, as illustrated in Figure 3.12, is a combination of the Solid45 and Link8 elements. In this model, the Solid45 element was used to model the concrete portion of the beam, and the Link8 element was used to model the reinforcing bars embedded in the concrete. A reinforcing bar (Link8 element) is considered to be an axial member built into the isoparametric element (Solid45 element) so that the displacements of the two elements are equal. This represents a perfect bond between the concrete and reinforcement.

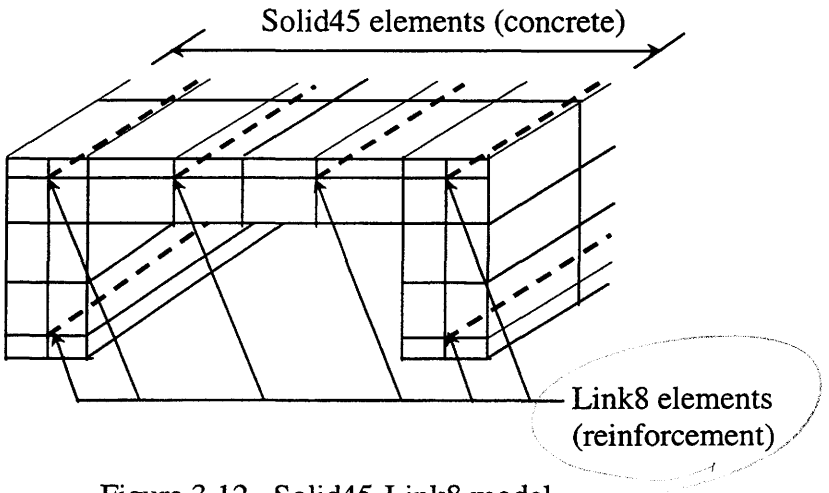

Figure 3.12. Solid45-Link8 model.

The Solid45-Link8 model represents the actual shape of the beam. The elements are connected to each other at the nodes, thus forming a monolithic channel beam model. Reinforcement is also included at the appropriate position with the desired area and material property. The model has an uncracked moment of inertia, I_{uncr}. Results from this model were compared with theoretical results from beam theory calculations. Under the same loading, this model predicted a maximum deflection of 0.0387 in., while beam theory using I_{uncr} resulted in a 0.0390 in. displacement. Strain profiles along the depth of the cross-section from the model and beam theory are illustrated in Figure 3.13. By comparing the two strain

profiles, it can be concluded that this model is very accurate in modeling the reinforced concrete channel beam in the uncracked condition. Based on its accuracy, this three-dimensional model was selected as an appropriate model before crack propagation.

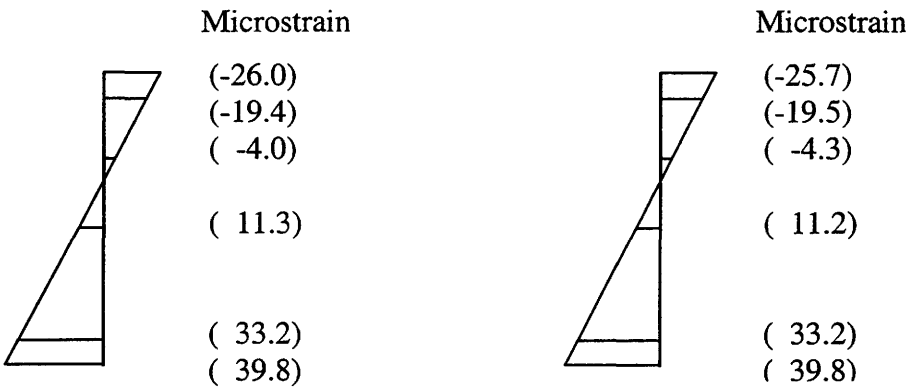

a. Beam theory b. Solid45-Link8 model

Figure 3.13. Comparison between the beam theory and Solid45-Link8 model.

The disadvantage of this model type is that it does not include the post-cracking behavior of the beam, which limits its application only to an elastic range study of reinforced concrete beams. Since this research only includes linear elastic analysis, as discussed in Section 3.3, this limitation did not impact the project.

3.5.3.2. Solid73-Pipe16 Model

The difference between the Solid73 and the Solid45 element is that the Solid73 element has six DOFs at each node instead of the three DOFs of Solid45. The Solid73 element includes the translations in the nodal x, y, and z directions, similar to the Solid45 element, but adds the rotations about the nodal x, y, and z axes [2]. The Pipe16 element is a one-dimensional element with tension-compression, torsion, and bending capabilities. It has six DOFs at each of the two nodes it connects: translations in the nodal x, y, and z directions

and rotations about the nodal x, y, and z axes. The basic input data include the pipe outer diameter (OD), wall thickness (TKwall), and material properties [2]. Figure 3.14 provides the details of this element type. The geometry of the Solid73-Pipe16 model, as illustrated in Figure 3.15, is the same as that of the Solid45-Link8 model.

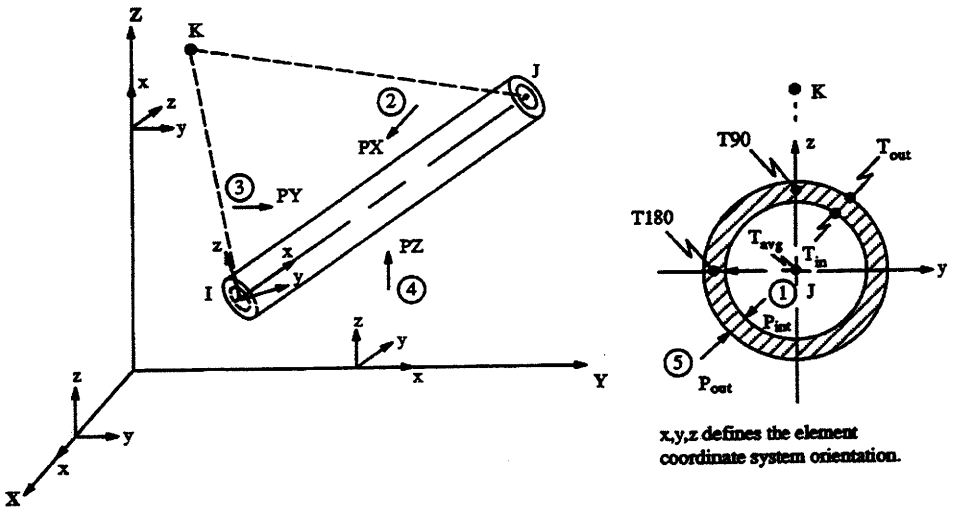

Figure 3.14. Pipe16 element [2].

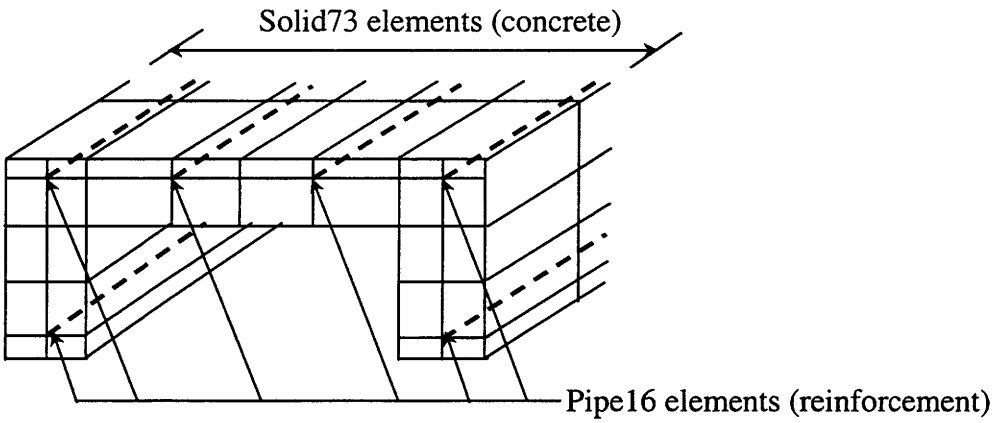

Figure 3.15. Solid73-Pipe16 model [2].

This elastic Solid73-Pipe16 model is more refined than the Solid45-Link8 model in that it has six DOFs, which include the rotational behavior of the nodes. The deflection and strain profiles derived from this model are very close to those derived from the Solid45-Link8 model. The main reason for constructing this model was to investigate the connections between the beams in a bridge, which will be presented in Chapter 4.

3.6. Discussion of Results

Differences in the results from the elastic three-dimensional finite element models, the experimental results, and the theoretical calculations based on ACI 318-99 with the maximum produced by single lane Type 3 vehicle loading, determined in Section 3.3.2, are presented in this section. Figure 3.16 presents the comparison of the midspan deflections and strain profiles along the depth of cross-section for the Group #1 of the laboratory tested beams, while Figure 3.17 presents data on Group #2 of the tested beams.

3.6.1. Deflection Reading

From Figures 3.16(a), it can be seen that the results from the Solid45-Link8 model are very close to the Solid73-Pipe16 model. These two models always slightly underestimate structural behavior of the tested beams. This may be attributed to their stiffness. As previously noted, a perfect bond between the concrete and reinforcing bars was assumed in these models. They do not include the slip of reinforcing bars or the deterioration in the actual beams. As shown in Figure 3.13, the Solid45-Link8 and Solid73-Pipe16 models results match the calculations based on I_{uncr} closer than the results based on I_e. The relative difference of the models and the laboratory test is less than 30% in the linear elastic stage. This difference will increase gradually after the crack occurred, due to both the nonlinear

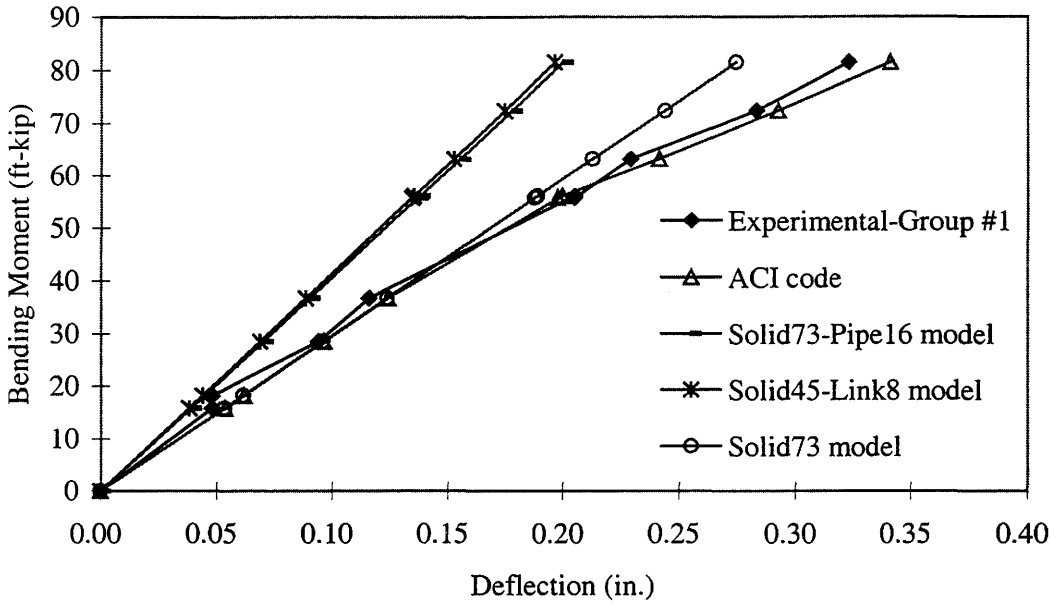

a. Midspan deflection

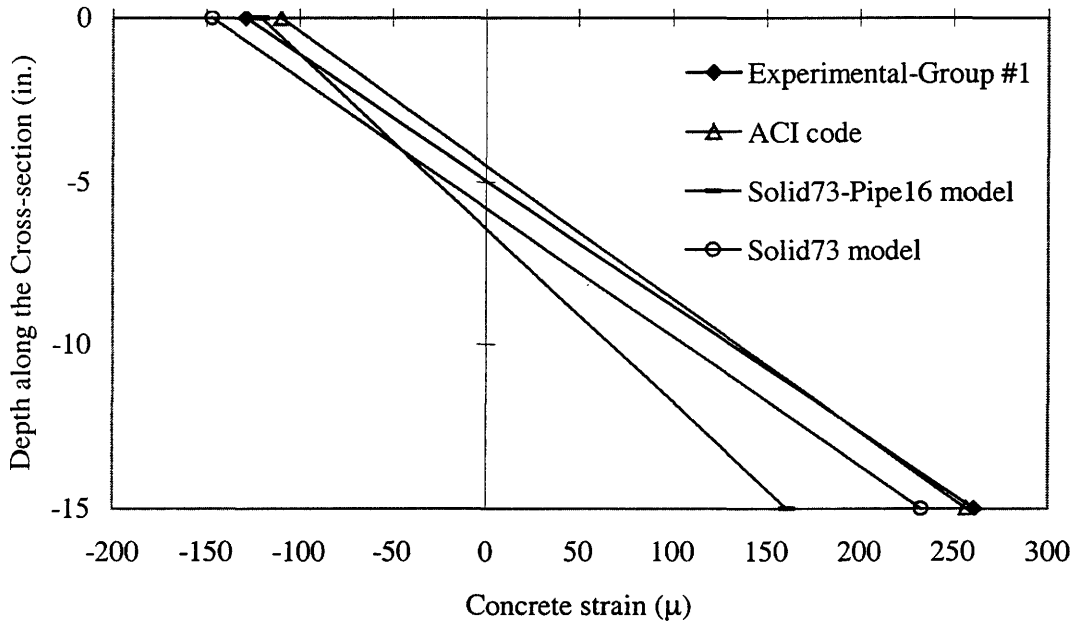

b. Strain profiles along the depth of cross-section

Figure 3.16. Comparison for Group #1 beams.

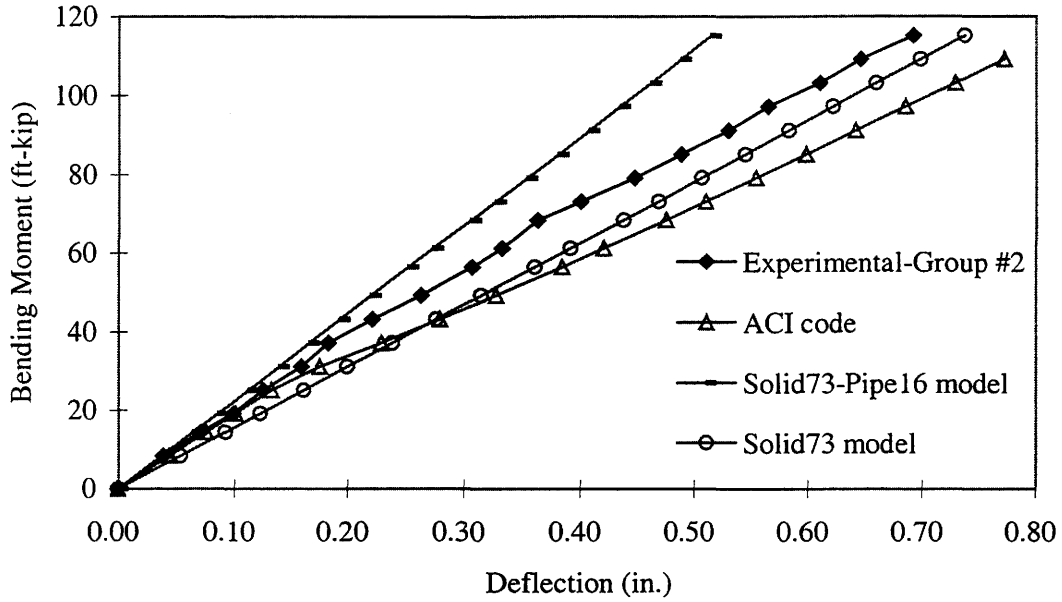

a. Midspan deflection

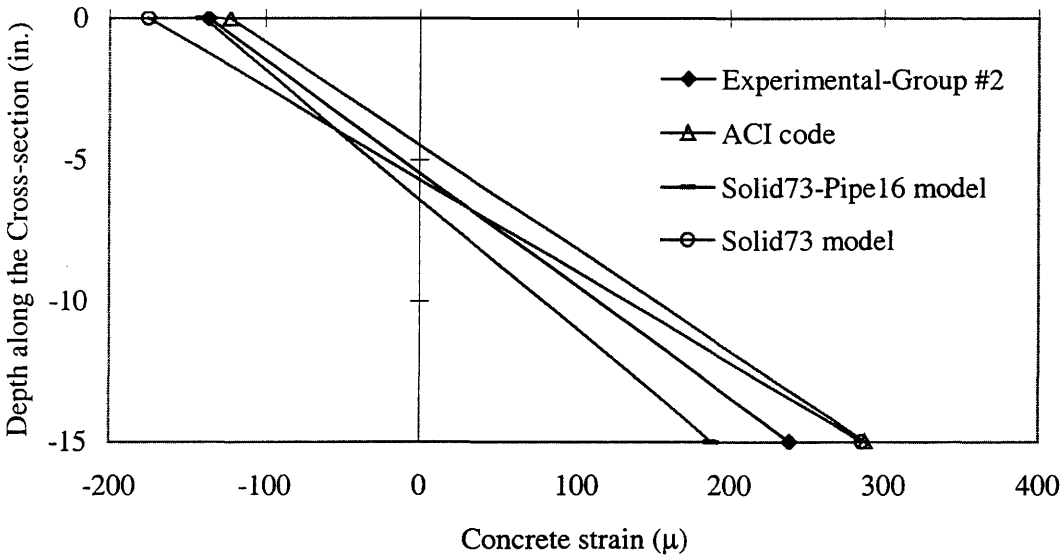

b. Strain profiles along the depth of cross-section

Figure 3.17. Comparison for Group #2 beams.

behavior of the actual beams and the stiffness of the elastic models which do not consider the effects of cracking.

Based on these observations, a model neglecting reinforcement was constructed to represent a beam with an I_g rather than I_{uncr}. In this model, there was only the Solid73 element to represent the concrete; the Pipe16 element (used to represent the reinforcement) was removed. The results from this Solid73 model are included in Figures 3.16(a) and 3.17(a). Within the linear elastic stage, the Solid73 model is very close to the calculations based on the ACI code. Due to this, it is more consistent with the experimental result than the models including reinforcement for Group #1 beams. For Group #2 beams, the experimental results are between the models that include and neglect reinforcement.

3.6.2. Strain Reading

Figure 3.16(b) presents the strain profiles along the depth of Group #1 beams when a bending moment of 63.18 ft-kip was applied. Referring to the calculated cracking moment shown in Table 3.2, this beam has cracked. With the cracked neutral axis, results based on the ACI code are very similar to the experimental result. Since the finite element models are elastic, they always underestimate the strain values. However, the curvature value, which resulted from the finite element model neglecting reinforcement (the Solid73 model), is very close to the experimental result. The finite element model with reinforcement model (the Solid73-Pipe16 model) produced the smallest curvature and tensile strains and the lowest neutral axis (greatest distance from top fibers) due to it having the greatest stiffness.

Similar results are illustrated in Figure 3.17(b) when a bending moment of 61.2 ft-kip was applied to Group #2 beams. The finite element model neglecting reinforcement (the Solid73 model) predicted a compressive strain at the top of the beam very close to the

experimental result. The curvature of the beam, based on the experimental data, is between those from the finite element models with reinforcement and without reinforcement. Once again, the elastic finite element model with reinforcement (the Solid73-Pipe16 model) underestimated the beam's tensile strain and curvature.

3.7. Chapter Summary

The Solid45-Link8 and Solid73-Pipe16 models are appropriate for modeling the individual reinforced concrete channel beams. They were selected for modeling the multi-channel-beam bridges for the following reasons:

1. They represent the actual physical shape of the beams and their components.
2. Within the elastic range, results from the finite element analyses agree with results based on the ACI code fairly well.
3. They provide compatibility in modeling of the critical connection components.

Observing that the analytical models have a stiffness which is usually greater than actual beams, a model neglecting reinforcement was also constructed to predict the behavior of a structure with an I_g instead of I_{uncr}. For the subsequent analyses, both models including reinforcement and models neglecting reinforcement will be used to perform a study of the effect of reinforcement on deflections and strains.

4. MODELING OF A LABORATORY BRIDGE

4.1. Introduction

Prior to investigating the overall structural behavior of the field multi-channel-beam bridges, a laboratory bridge was constructed in the structural engineering laboratory of Iowa State University. This bridge was composed of four reinforced concrete channel beams connected by steel pipes and bolts. Tests were conducted on this laboratory bridge.

Finite element models of this laboratory bridge were then developed using the ANSYS program. Sensitivity studies on modeling of bolts and pipes were conducted. Deflections and strains derived from the analytical models were compared to experimental results. Ideal model types were selected to pursue modeling of the field multi-channel-beam bridges presented in Chapter 5.

4.2. Laboratory Test Description

Four reinforced concrete channel beams taken from the demolished Cedar County Bridge were connected to construct the laboratory multibeam bridge. The beams are similar to Group #1 beams tested in Chapter 3 and are illustrated in Table 3.1 and Figure 3.2(a). End to end span length of this bridge was 25 ft. The ends of the laboratory bridge were supported by concrete girders. A point load was applied at the midspan of each panel. The laboratory test setup is shown in Figure 4.1. Figure 4.2 presents the layout of this bridge. The material properties of this laboratory bridge are E_c=5,700 ksi and E_s=26,600 ksi, similar to the Group #1 beams in Table 3.1. The influences of the two most popular connections used with the multi-channel-beam bridges were investigated: (1) bolt connections and (2) bolt plus pipe connections.

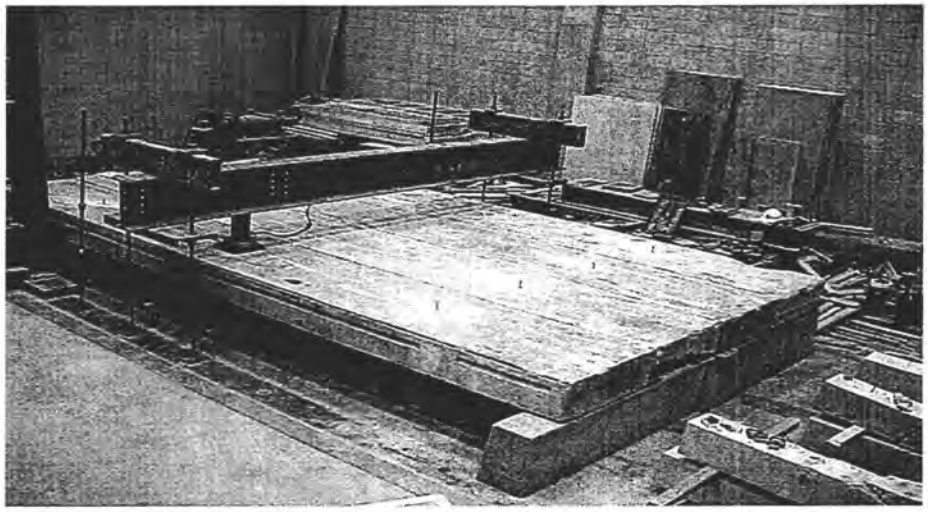

Figure 4.1. Laboratory test setup.

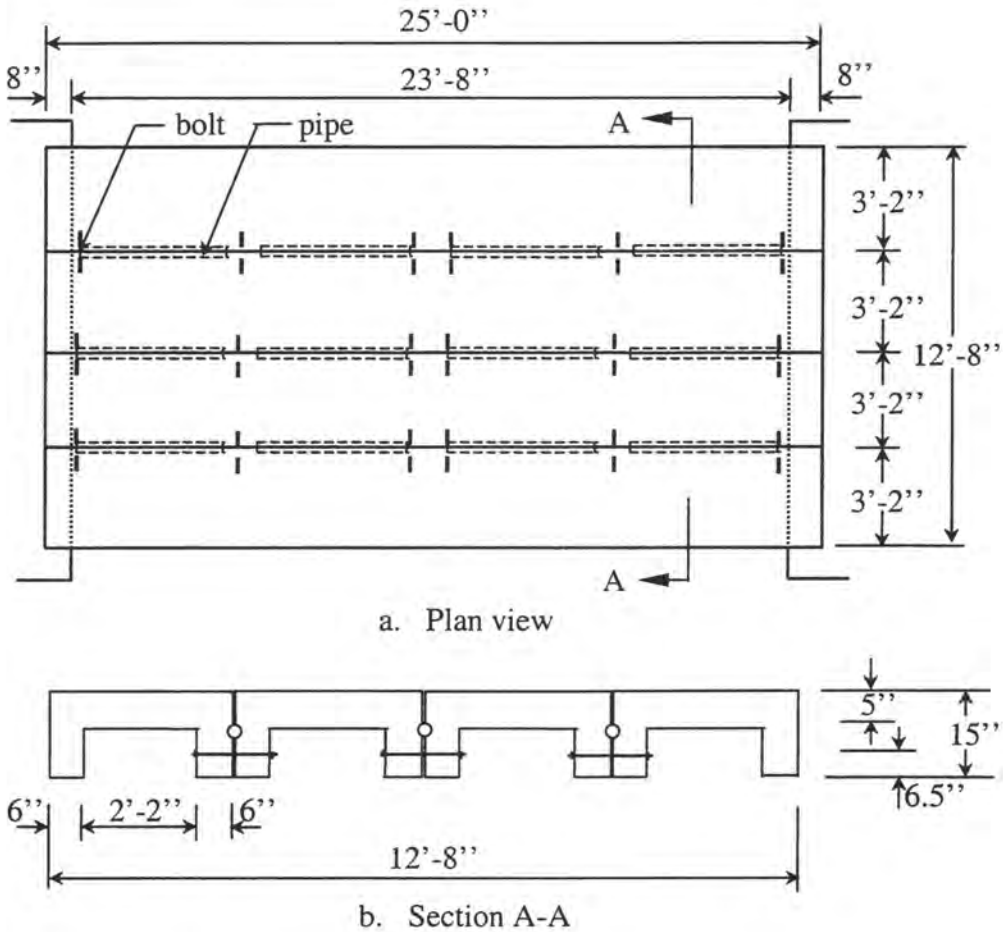

Figure 4.2. Layout of the laboratory bridge.

4.3. Modeling of Bolt Connections

4.3.1. Mechanism of Load Transfer through Bolts

Consider the analytical model of two channel beams (Panel A and Panel B) with a bolt connection, and an external vertical load, P, applied to Panel A as shown in Figure 4.3(a). Due to P, Panel A will deflect downward, creating contact stresses between the bolt and Panel A from point 1 to point 2, and the bolt and Panel B from point 2 to point 3. Figure 4.3(b) shows the contact stresses on the bolt. To achieve equilibrium, the force V_1 from point 1 to point 2 must equal the force V_2 from point 2 to point 3. Therefore, Panel B is subjected to a downward force V_2, while the load on Panel A is $P-V_1$. In other words, a portion of the load P is transferred from Panel A to Panel B.

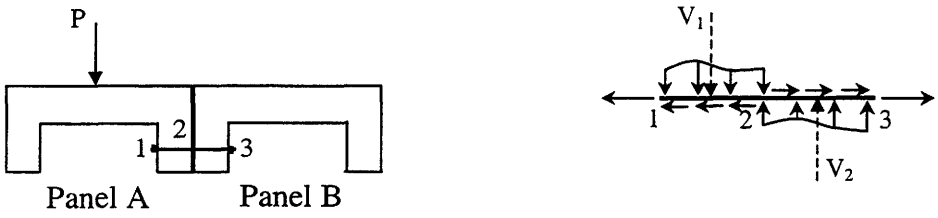

a. Cross-section b. Stresses on the bolt

Figure 4.3. Mechanism of load transfer through bolts.

Due to the complexity of loading cases, support conditions, and the degree of fixity in bolt connections, the value of load transfer through bolt connections is hard to determine using the classical analytical approaches. However, finite element analysis provides a possible method to analyze the bolts and obtain fairly reproducible results.

The bolt is also subject to a bending moment, resulting from the contact stresses shown in Figure 4.3(b). Due to this bending moment, the bolt has an additional rotational degree of freedom.

4.3.2. Element Type Selection

As presented in Chapter 3, the Solid45-Link8 model with 3 DOFs closely resembles the Solid73-Pipe16 model with 6 DOFs for the channel beam analyses. Both are practical for modeling reinforced concrete channel beams. This section will determine the preferred model for the multibeam bridge analyses.

In the Solid45-Link8 model, the Link8 element was used to model both the reinforcing bars and the bolt connections. In the Solid73-Pipe16 model, the Pipe16 element was used to model both the reinforcing bars and the bolt connections. Based on laboratory tests, the modulus of elasticity of the concrete was determined to be 5,700 ksi, the modulus of elasticity of the reinforcing bars 26,500 ksi, and the modulus of elasticity of the bolts 29,000 ksi. Figure 4.4 and Table 4.1 presents details of the two models. The nominal diameter of the positive reinforcing bars was assigned to the Pipe16 elements that represent the positive reinforcement. Identical mesh sizes, support conditions, load position, and load magnitude were applied to the two models. Deflection profiles from the two models are shown in Figure 4.5.

From Figure 4.5, it can be seen that the Link8 element cannot represent the true bending behavior of the bolt because it has no rotational nodal DOFs. Using the Solid45-Link8 model, Panel 2 deflects under load P while the other panels do not deflect. Thus, load P is not transferred between the adjoining panels. The Solid73-Pipe16 model uses the Pipe16 element with rotational nodal DOFs to model the bolt connections. This model provides load

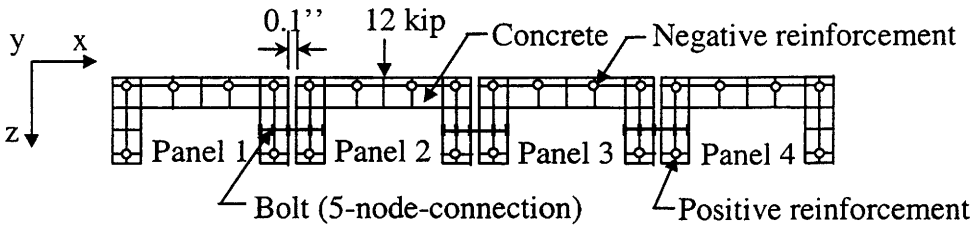

a. Cross-section of the models

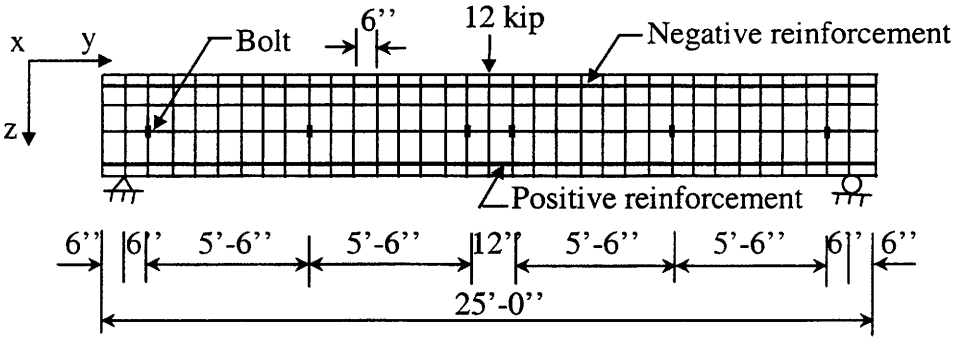

Note: One end has pin supports (x, y, z translations are restrained), the other end has roller supports (z translations is restrained).

b. Side view of the models

Figure 4.4. Details of the Solid45-Link8 and the Solid73-Pipe16 models.

Table 4.1. Element types and input properties of the analytical models.

Model Type	Concrete	Negative Reinforcement (1- #4)	Positive Reinforcement (3- #8s and 1- #7)	Bolt (Dia=5/8 in.)
Solid45-Link8	Solid45	Link8 - Areas (in^2)		
(3 DOFs)		0.20	2.97	0.31
Solid73-Pipe16	Solid73	Pipe16 - Dia (in.)		
(6 DOFs)		0.50	1.95	0.625

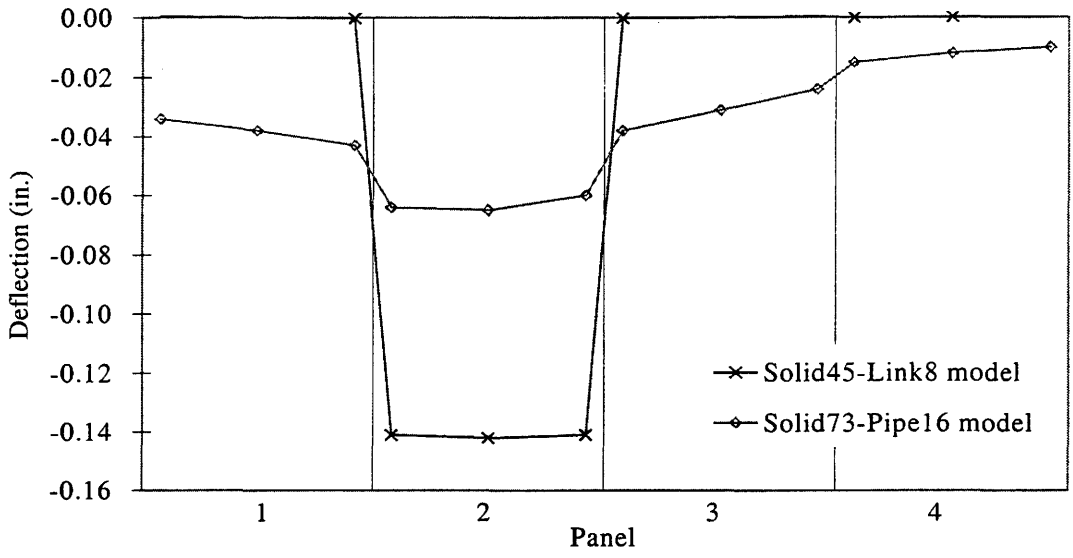

Figure 4.5. Comparison of the Solid45-Link8 and Solid73-Pipe16 models.

transfer between the panels. Therefore, the Solid73- Pipe16 model, instead of the Solid45-Link8 model, is best when analyzing a multibeam bridge with bolt connections. Before using the Solid73-Pipe16 model, a node connection sensitivity study needs to be performed.

4.3.3. Node Connection Sensitivity Study

The Solid73-Pipe16 model is sensitive to the number of nodes connected by the bolt (Pipe16 element). It is assumed that the more nodes connected by the Pipe16 element, the more loads are transferred through the element. However, there is no current information on how many nodes are required to best represent the behavior of the bolts. Moreover, an unavoidable practical problem—the amount of bolt slip—makes accurate analysis difficult. Thus, a sensitivity study was conducted using four bolt connection scenarios, 2-nodes-, 4-nodes-, 5-nodes-, and 7-nodes-connection as described in Figure 4.6. Figure 4.7 compares deflection profiles from these scenarios to the results from the laboratory test.

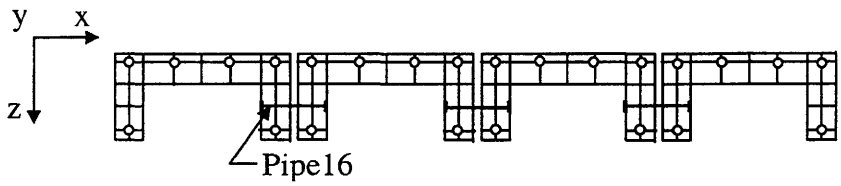

a. 2-nodes-connection model

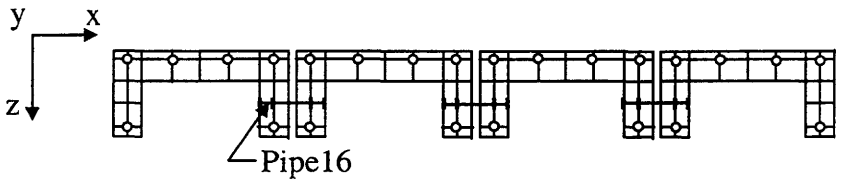

b. 4-nodes-connection model

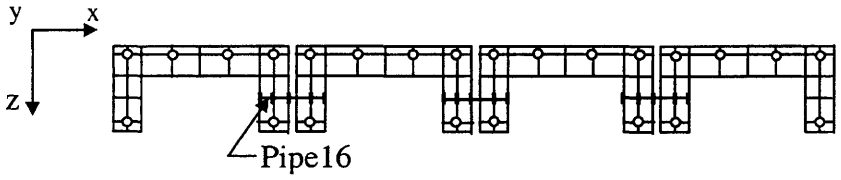

c. 5-nodes-connection model

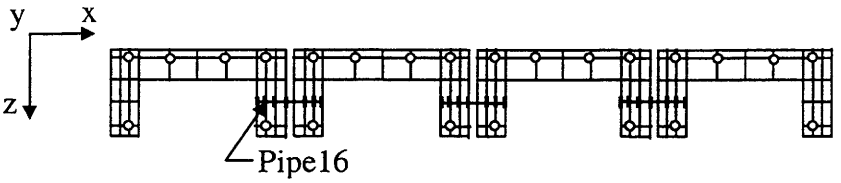

d. 7-nodes-connection model

Figure 4.6. Node connection scenarios of bolt model.

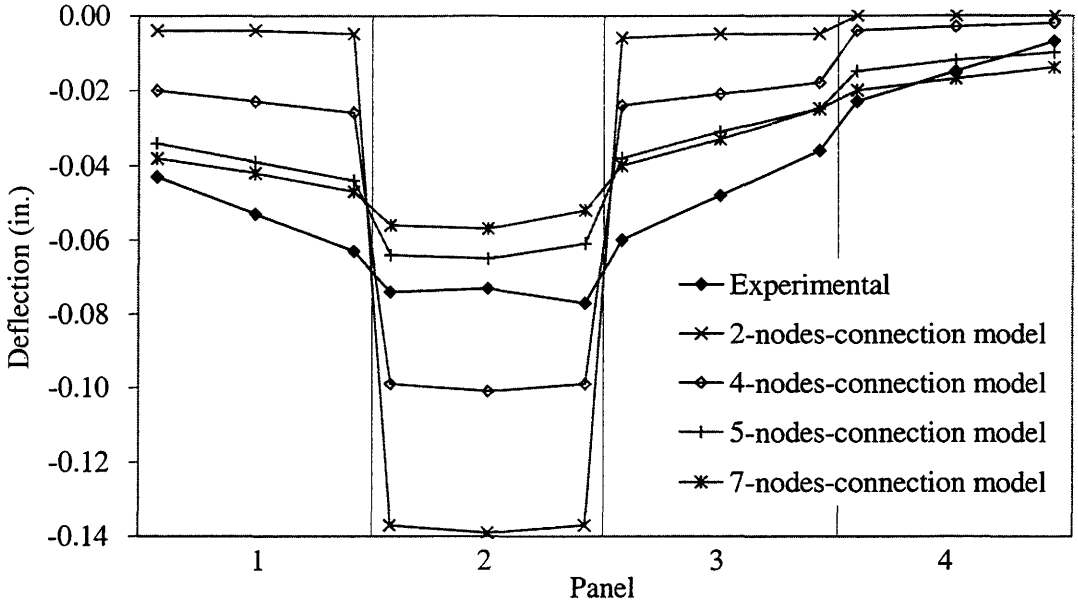

Figure 4.7. Comparison of node connection scenarios of bolt model.

To investigate the load transfer through the bolts, nodal forces of a bolt that is at the midspan of the bridge and between Panel 2 and Panel 3 resulted from the four models were recorded. Since shear is the main force to be transferred, Figure 4.8 illustrates the vertical nodal forces of the bolt elements to determine the amount of transferred shear through this bolt.

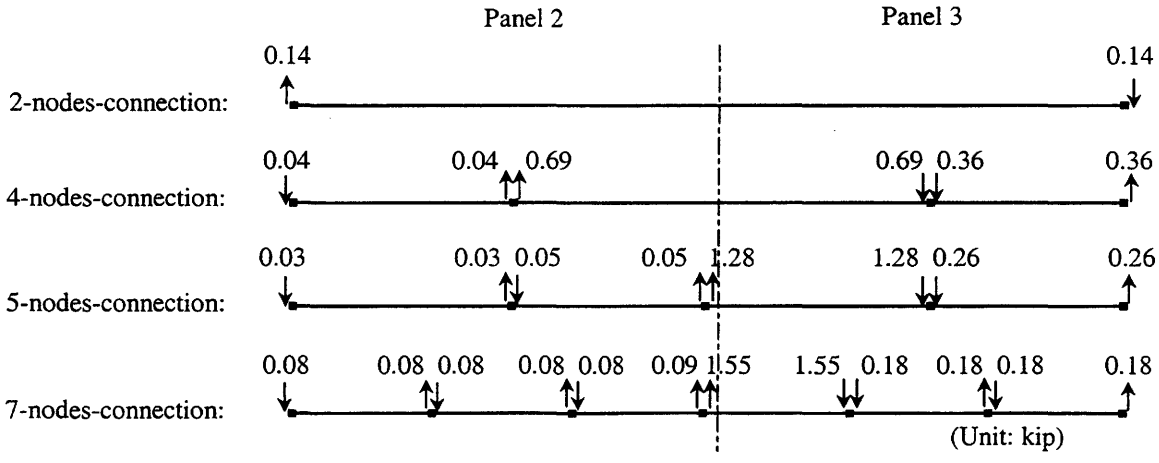

Figure 4.8. Vertical nodal forces of a bolt resulted from the models.

4.3.4. Discussion of Results

4.3.4.1. Model Selection

From Figure 4.7, it can be seen that when the number of connected nodes increased from four to five, the maximum deflection of Panel 2 decreased by 32%. When it increased from five to seven, the maximum deflection of Panel 2 decreased by 18%. It can be predicted that if the number of connected node increases from seven to eight or nine, no significant difference of Panel 2's maximum difference will occur. Therefore, the 7-nodes-connection Pipe16 element is determined fine enough to model the bolt connection. For the laboratory bridge, both the 5-nodes-connection and 7-nodes-connection models are more consistent with the laboratory testing results than the other models. The 5-nodes-connection model was preferred since it has fewer elements than the 7-nodes-connection model but also has a good accuracy. The 5-nodes-connection model was chosen to model the laboratory bridge with bolt connections.

Figure 4.8 shows the shear transfer through the bolt in different models. In the 2-nodes-connection model, an upward nodal force of 0.14 kip at node 1 (Panel 2) and a downward nodal force of 0.14 kip at node 2 (Panel 3) were produced. This means a downward (shear) force of 0.14 kip was transferred from Panel 2 to Panel 3. In the 4-nodes-connection model, a force of 0.69 kip was transferred. The transferred shear increases with the number of connected nodes of the bolt elements. In the 7-nodes-connection model, a maximum force of 1.55 kip was transferred. This verifies the assumption made in Section 4.3.3 that the more nodes connected in the model, the larger transferred loads.

4.3.4.2. Reason for Differences

From Figure 4.7, it can be seen that the elastic models slightly underestimate the laboratory bridge's behavior. This may be attributed to the nonlinear behavior of the actual structures or the stiffness of the analytical model. The beam analysis performed in Chapter 3 can be used to address this issue, since this laboratory bridge is composed of the channel beams which fit in Group #1 beams presented in Chapter 3.

Based on the assumption that the deflection is proportional to the load resisted, Panel 2 accounts for a 38.9% of the total load on the bridge. This percentage was obtained by dividing the sum of all panels' deflections by the deflection of Panel 2 that resulted from the laboratory test. Since the total applied load was 12 kip, Panel 2 is calculated to resist a load of 38.9%x12 or 4.67 kip. Under this load at the midspan, a maximum bending moment, 4.67x24.33/4 or 28.4 ft-kip, was produced in Panel 2. This is less than the calculated cracking moment of 36.02 ft-kip. From Figure 3.17(a), it can be seen that Panel 2 deflected approximate 0.09 in. during the laboratory test, while the ANSYS elastic Solid73-Pipe16 model predicted a deflection of 0.07 in. Similar results for Panel 2 were obtained from the laboratory test and the Solid73-Pipe16 model with 5-nodes-connection bolt. This degree of accuracy proves the 5-nodes-connection model is appropriate for modeling the laboratory bridge.

The beam was not cracked when tested to 12 kip. The difference between the experimental and analytical results is mainly due to the stiffness of the analytical model. Based on the discussion in Section 3.6, a model neglecting reinforcement was constructed to present beams with a gross moment of inertia, I_g. In the Solid73-Pipe16 model, the Pipe16 elements modeling the reinforcement were removed and those modeling the bolt connections

remained. This model is known as "model w/o reinforcement". Figure 4.9 presents the effect of the reinforcement on the deflections of the laboratory bridge with only bolt connections.

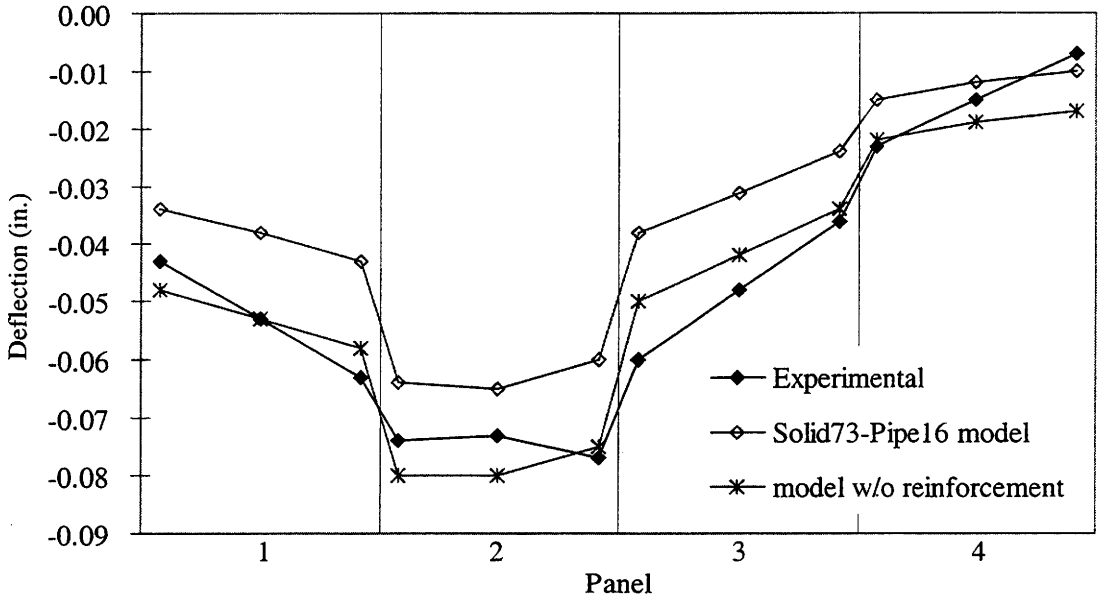

Figure 4.9. Effect of the reinforcement on deflection.

From Figure 4.9, it can be seen that the results from the model neglecting reinforcement are very close to the experimental data. The maximum deflection predicted by the model neglecting reinforcement is 0.08 in., within 7% of the experimental result. In Panel 2, which received the load directly, the experimental data are between the two models. Both of the analytical models underestimated the deflection of Panel 3 by 33% and 17%, respectively. The difference between the results from the models and the experimental data for Panel 1 and Panel 2 is minimal.

Figure 4.10 presents the strain profiles along the depth of the laboratory bridge with only bolt connections. A neutral distance of 4.5 in. from the top fibers of the beam was obtained from the laboratory test. Referring to Section 3.3.1, the beam has not cracked. The laboratory test resulted in the maximum curvature and the smallest neutral distance. The analytical model neglecting reinforcement predicted a curvature value very close to the experimental data. The model including reinforcement underestimated the structure's behavior in both tensile strain and curvature.

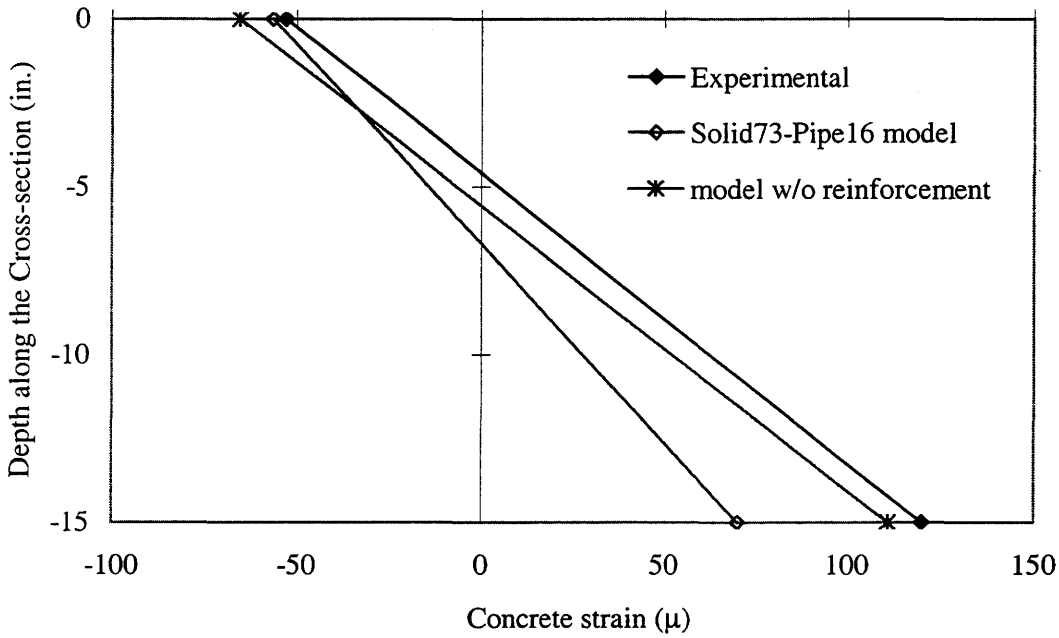

Figure 4.10. Comparison on strain profile.

Due to the nonlinear behavior of the structure, greater deviation occurred between the experimental and analytical results when a greater load was applied. Figure 4.11 illustrates this behavior. Compared to the experimental data, in this loading range, the maximum relative differences of the analytical models with or without reinforcement are approximately

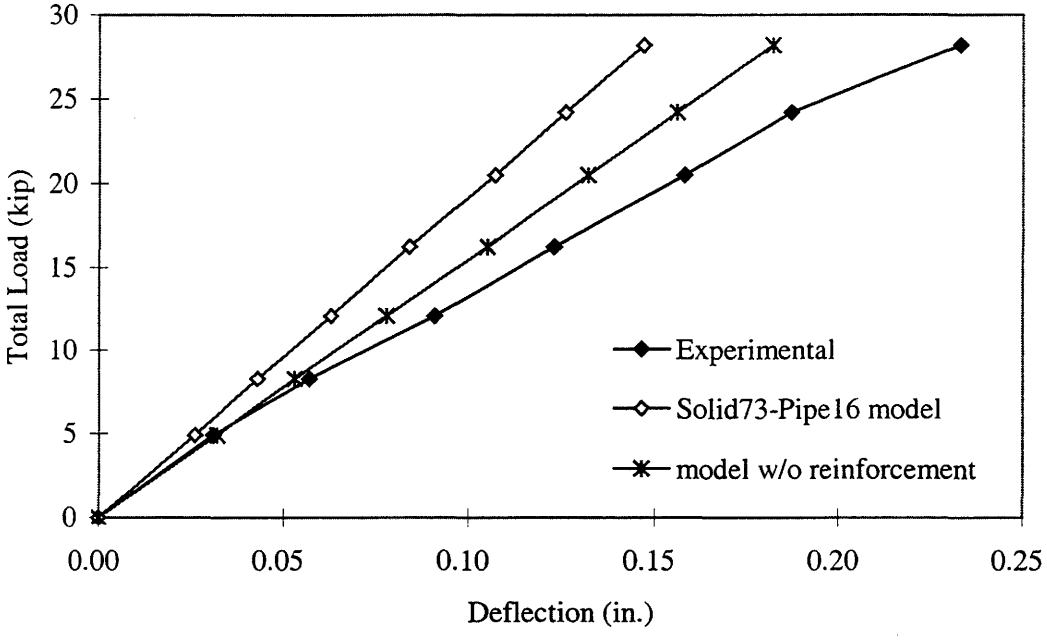

Figure 4.11. Differences on deflection.

30% or 15%, respectively.

4.4. Modeling of Bolt plus Pipe Connections

4.4.1. Mechanism of Load Transfer through Pipes

Consider the analytical model of two channel beams (Panel A and Panel B) with a steel pipe connection, as shown in Figure 4.12. Under a vertical load, P, contact stresses and shear stresses (or friction stresses) develop perpendicular to and along the surface of the pipe. Dut to these stresses, a certain amount of P will be transferred from Panel A to Panel B. To simplify the analysis, the pipe is usually idealized as a hinged connection. Only shear is transferred between the adjacent panels.

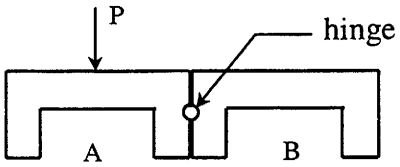

Figure 4.12. Mechanism of load transfer through pipe.

4.4.2. Element Type Selection

Based on the hinge assumption, the Combin7 element of the ANSYS program was selected to model the steel pipe connections. The Combin7 element is a three-dimensional pin joint which may be used to connect two or more parts of a model at a common point. The capabilities of this element include joint stiffness, friction, and certain control features [2]. Details of this element are shown in Figure 4.13.

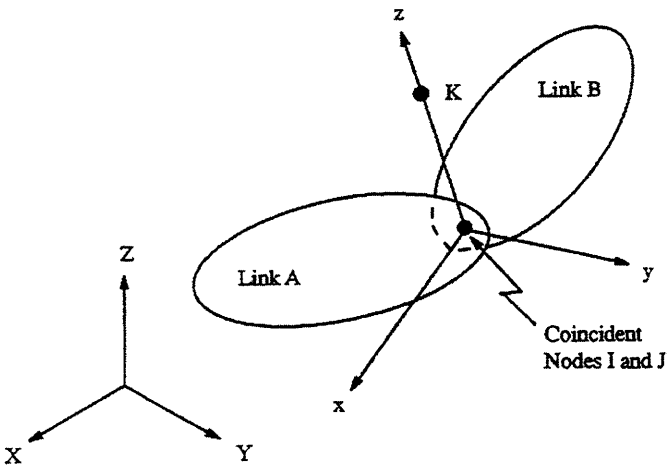

Figure 4.13. Combin7 element [2].

4.4.3. Translational Stiffness Sensitivity Study

It was determined that the model was sensitive to the translational stiffness, K1, of the Combin7 element. Due to the complexity of the contact behavior of the beams and pipes,

it is difficult to determine K1. A sensitivity study was performed in an attempt tp predict K1. Five scenarios were investigated, in which K1 was assumed to be 5, 10, 15, 20, and 100 kip/in, respectively. The deflection profiles from these five models are shown in Figure 4.14. When K1 is set to 5 kip/in, load transfer between panels is negligible, whereas when K1 is 100 kip/in, the panels are very rigidly connected. It can be seen that 10 to 20 kip/in would be an appropriate range for K1. Although no experimental verification is available, results from the laboratory bridge testing with only bolt connections presented in Section 4.3 can be used as a reference. It is assumed that the pipes should at least as effective as the bolts. Based on this assumption, K1=20 kip/in was selected due to it properly producing rotation in the adjoining panels.

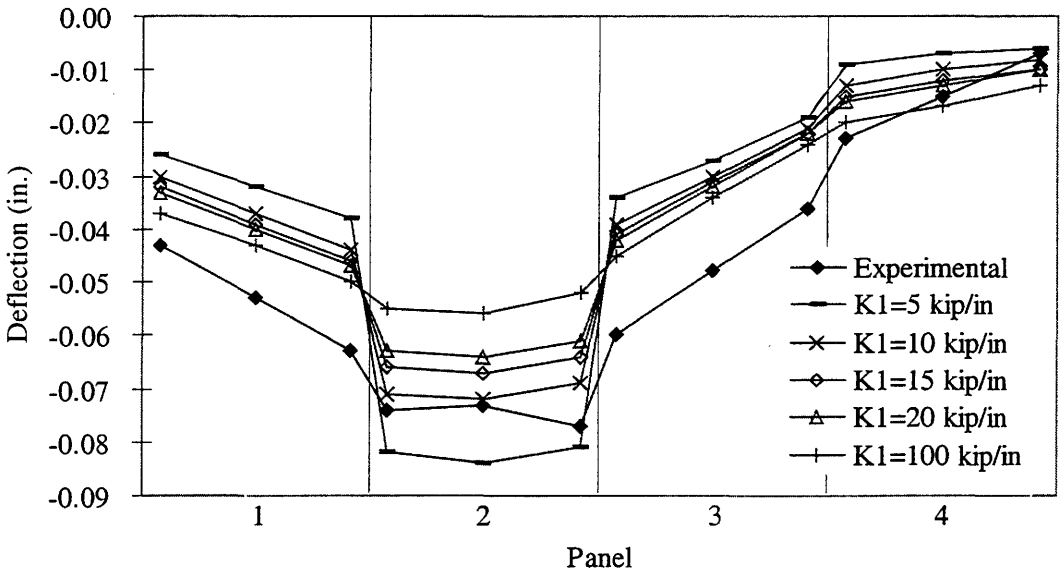

Figure 4.14. Sensitivity study on translational stiffness of the Combin7 element.

4.4.4. Models of the Laboratory Bridge with Bolt plus Pipe Connections

Based on the individual investigations into the modeling of bolt and pipe connections, the Solid73-Pipe16-Combin7 model was constructed to model the laboratory bridge with both bolt and pipe connections. A cross-section of this model is illustrated in Figure 4.15. The Solid73 and Pipe16 elements were used to model the concrete and reinforcement, respectively. The 5-nodes-connection Pipe16 element was used to model the bolt connections and the Combin7 element with a translational stiffness K_1=20 kip/in was used to model the pipe connections. The laboratory testing procedure and setup was the same as described in Section 4.2.

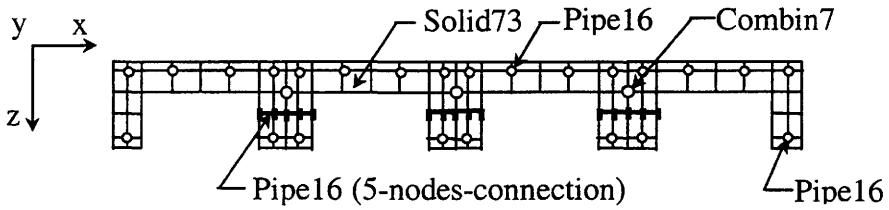

Figure 4.15. Cross-section of the Solid73-Pipe16-Combin7 model.

A model neglecting reinforcement was also constructed to study the effect of reinforcement. Figures 4.16 and 4.17 illustrate the comparison of deflection and strain profiles resulting from both the laboratory tests and analytical models. Due to the symmetry of the structure, only the loads applied to Panel 1 and Panel 2 are presented. These loads are named LC1 and LC2, respectively.

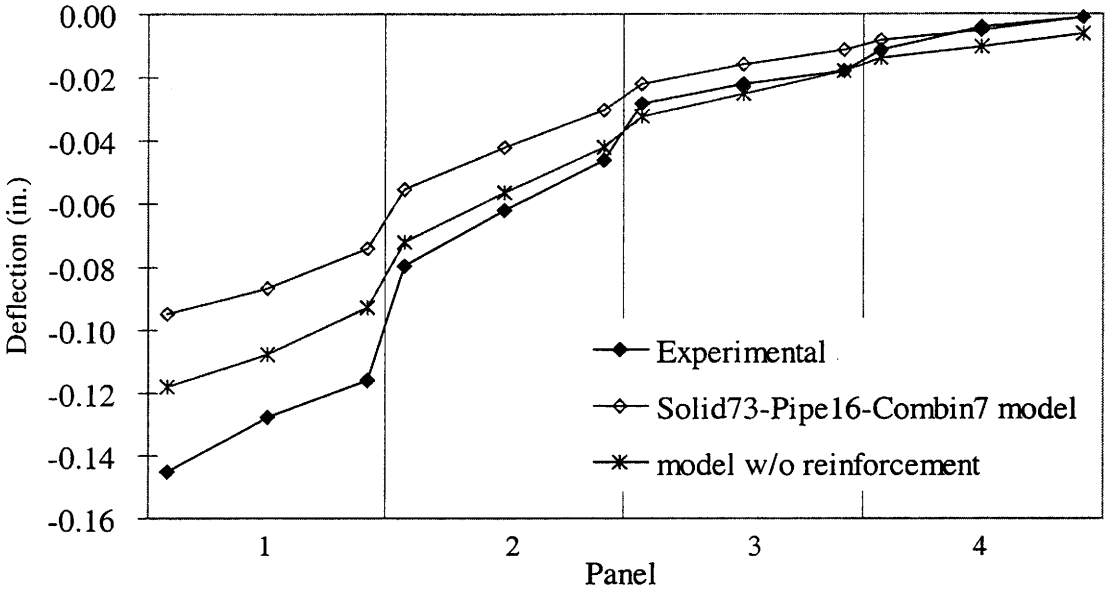

a. LC1

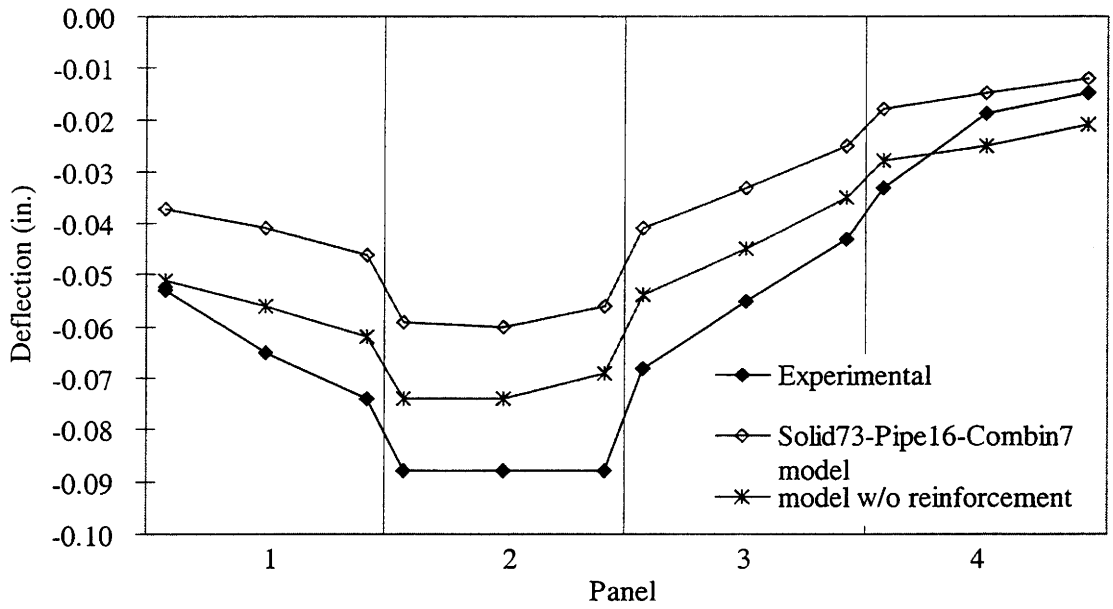

b. LC2

Figure 4.16. Comparison of deflection profiles.

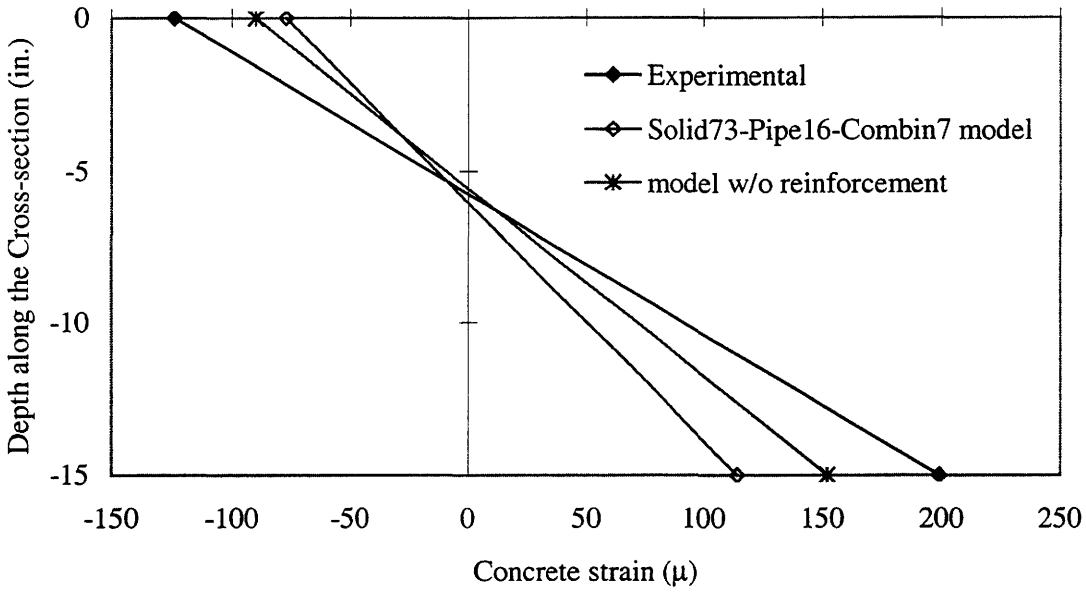

a. LC1

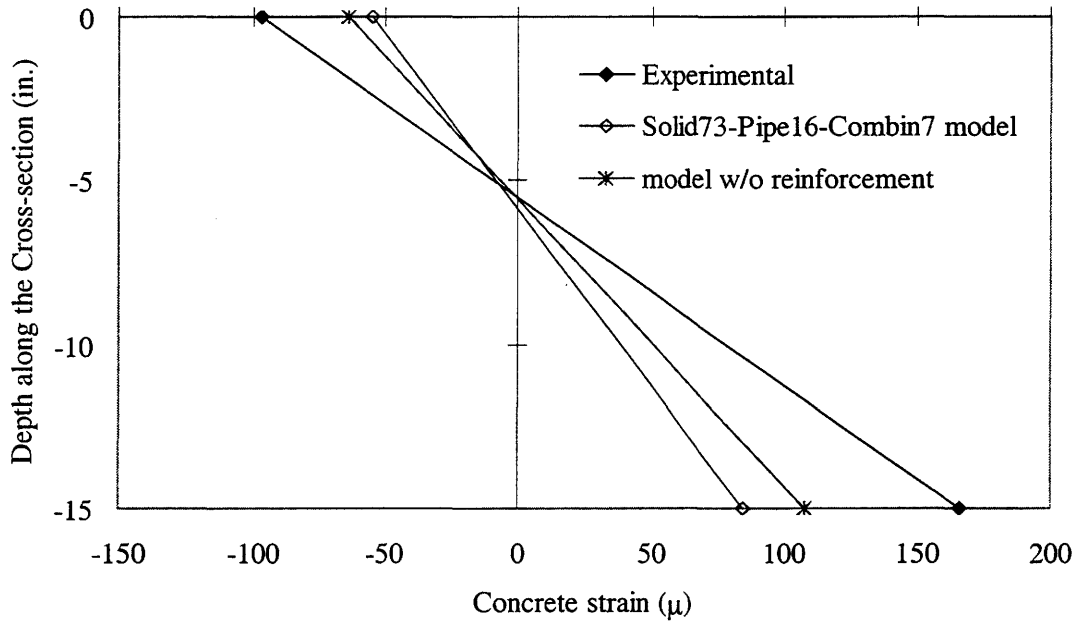

b. LC2

Figure 4.17. Comparison of strain profiles.

4.5. Discussion of Results

From Figure 4.16(a), it can be seen that the analytical models slightly underestimate the actual behavior of the laboratory bridge with bolt plus pipe connections. Under a load of 12 kip, Panel 1 deflected a maximum of 0.145 in. The analytical models predicted a maximum deflection of 0.095 in. and 0.12 in., underestimating by 34% and 17%, respectively. Similar results were obtained when the load was applied to Panel 2. Both of the models provided a close match to the experimental data representing the rotation of the adjoining beams.

Figure 4.17 presents the strain profiles along the depth of the panel on which the load was applied directly. Both of the finite element models underrated the actual structure. It is noted that for the absolute strain value, the two analytical models underestimated by 46% and 34%. With a neutral distance very similar to the analytical models, the laboratory test produced the maximum curvature.

Figure 4.18 illustrates the difference between the experimental and analytical results as the applied load was increased. It can be seen that larger differences occurred due to the nonlinear behavior of the structure. Compared to the experimental data, in this loading range, the maximum relative differences of the models with or without reinforcement are approximately 30% or 15%, respectively.

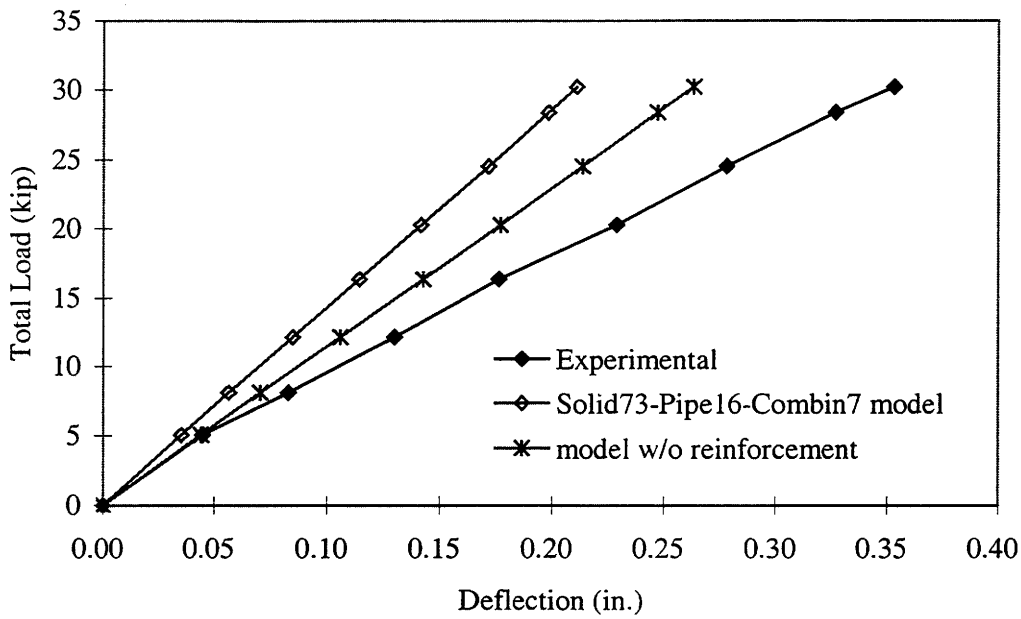

Figure 4.18. Difference on deflection.

4.6. Chapter Summary

After a careful comparison to the laboratory testing results, the Pipe16 element and the Combin7 element in ANSYS were determined to model the bolt and the pipe connections, respectively. Related sensitivity studies were conducted to determine the number of nodes connected by the bolt elements and the translational stiffness of the pipe connections. A 5-nodes-connection Pipe16 element was selected to model the bolts and a translational stiffness of K1=20 kip/in was assigned to the pipes since they predicted an appropriate rotation between the adjoining panels of the laboratory bridge.

Differences between the experimental and analytical results were investigated. Based on the beam analysis performed in Chapter 3, the stiffness of the structure was shown to be the main reason why the analytical models always slightly underestimate the actual structural

behavior. With a smaller stiffness, the analytical model neglecting reinforcement is more consistent with the laboratory bridge than the model including reinforcement. Due to existing deterioration, the field bridges should also have a smaller stiffness than the analytical models including reinforcement. However, since it is difficult to determine the decrease in stiffness due to deterioration, the models including reinforcement were used to analyze the field bridges.

5. MODELING OF FOUR FIELD BRIDGES

5.1. Introduction

Service load testing was conducted on four precast reinforced concrete multi-channel-beam bridges located in Butler, Story, and Delaware counties. Three of the bridges are single-span units; one of them is a two-span bridge. The layouts of the four bridges are presented in Chapter 1. The county engineer for the county in which each bridge was located provided the test vehicle. The test vehicle crossed the bridges with the centerline of each wheel line coinciding with the centerline of any panel. Deflections and strains at the midspan of the bridges were recorded. One may refer to Ingersoll's [1] paper for detailed information of the testing procedure.

Among the four tested bridges, only the Butler County Bridge was tested to obtain the material properties. All of the other bridges' material data were assumed. From the description in Chapter 1, it is noted that all individual channel beams of the four bridges, either interior or exterior, have the same cross-section, as illustrated in Figure 1.1. Differences among the four bridges lie in the panel number, span length, material properties, and the shear connection type. Table 5.1 presents a general summary of the four bridges.

Based on study presented in Chapter 4, the Solid73-Pipe16 model and the Solid73-Pipe16-Combin7 model were used to model the field bridges with only bolt connections and with bolt plus pipe connections, respectively. For all the analytical models, support conditions are that one end is hinged, the other is supported by a roller in the vertical direction. Span length was taken as the center-to-center distance between supports. The wheel loads applied on the model were positioned to produce a maximum longitudinal bending moment at the midspan of the panel. Deflections and strains predicted by the

analytical models and measured in the field tests were compared. Load distribution factors for these four bridges were provided to act as the bridge engineers' design reference.

Table 5.1. Summary of the four field tested bridges.

Bridge Name	Number of Spans	Span Length (ft)	Number of Panels	Material Property (ksi)	Shear Connection
Story County Bridge	1	25	9	E_c=4,415 E_s=29,000 (assumed)	bolts
Delaware County Dairy Bridge	1	36	8	E_c=5,700 E_s=29,000 (assumed)	bolts
Butler County Bridge	1	31	10	E_c=4,490 E_s=26,605 (measured)	bolts & pipes
Delaware County Trout Bridge	2	62	9	E_c=5,700 E_s=29,000 (assumed)	bolts & pipes

5.2. Loading Procedure

Tandem axle dump trucks were used in three of the field load tests and a truck tractor-simitrailer combination was used in the fourth test. For all test vehicles, the distance between the centerline of each wheel line was approximately the same as the width of two bridge panels. Therefore, the test vehicle could be positioned so that each wheel line of the test vehicle would track entirely on a single panel. A load position designation was used to describe the individual load position for each field load test and is defined as follows:

LC46

Transverse Position

The transverse position numbers refer to the panel numbers that the test vehicle was tracking on [1].

5.3. Story County Bridge

5.3.1. Testing Vehicle Description

Figure 5.1 illustrates the wheel configuration and weight distribution of the vehicle used to load test the Story Country Bridge.

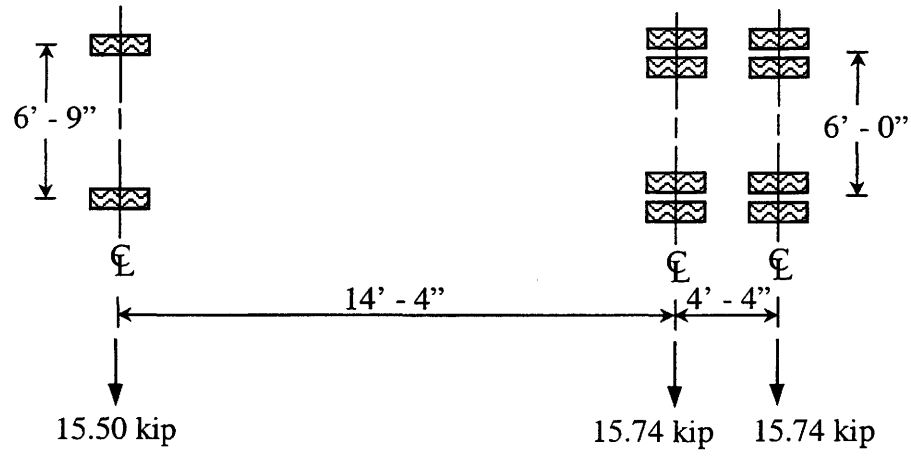

Figure 5.1. Wheel configuration and weight distribution of the vehicle.

5.3.2. Model Description

Based on the study performed on the laboratory bridge, the Solid73-Pipe16 model was used to analyze the Story County Bridge which has only bolt connections. The Solid73 element and Pipe16 element were used to model the concrete and reinforcement, respectively. The 5-nodes-connection Pipe16 element was used to model the bolt connections. Figure 5.2 illustrates the model constructed in the ANSYS program.

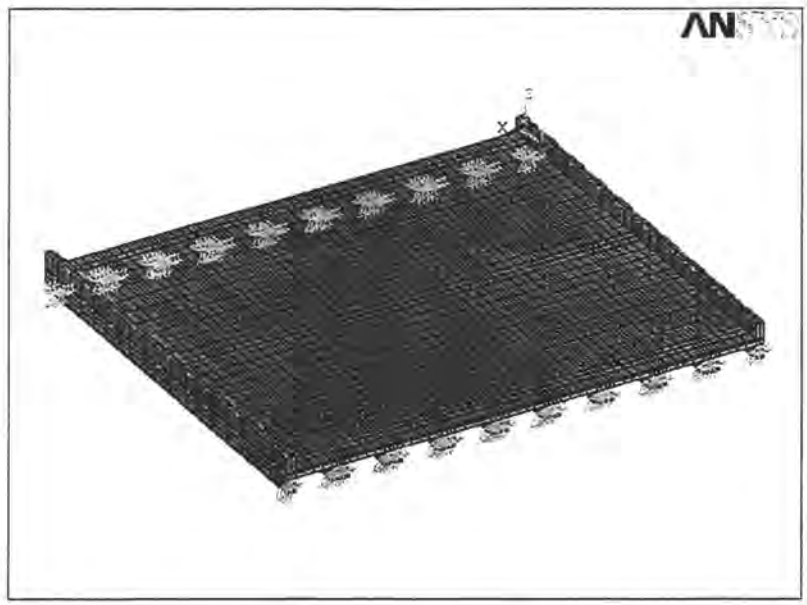

Figure 5.2. Model of the Story County Bridge.

5.3.3. Discussion of Results

5.3.3.1. Deflection Reading

Deflection profiles of the bridge predicted by the analytical model and measured in the field test were compared for the bridge under various transverse wheel load cases. The results are shown in Figure 5.3 for the midspan cross-section. Only four load cases are presented due to symmetry.

With a 25 ft end-to-end span, the Story County Bridge deflected a maximum of 0.16 in. under this vehicle loading. Slip is a common occurrence in this bridge which has only bolt connections. The maximum relative displacement of the bolt joint is 0.11 in. between Panels 2 and 3. The slip usually occurred between the panel directly received the load and its adjacent panels. The analytical model with 5-node-connection bolt elements cannot represent the slip behavior of the connections. From Figure 5.3, it can be seen that the model

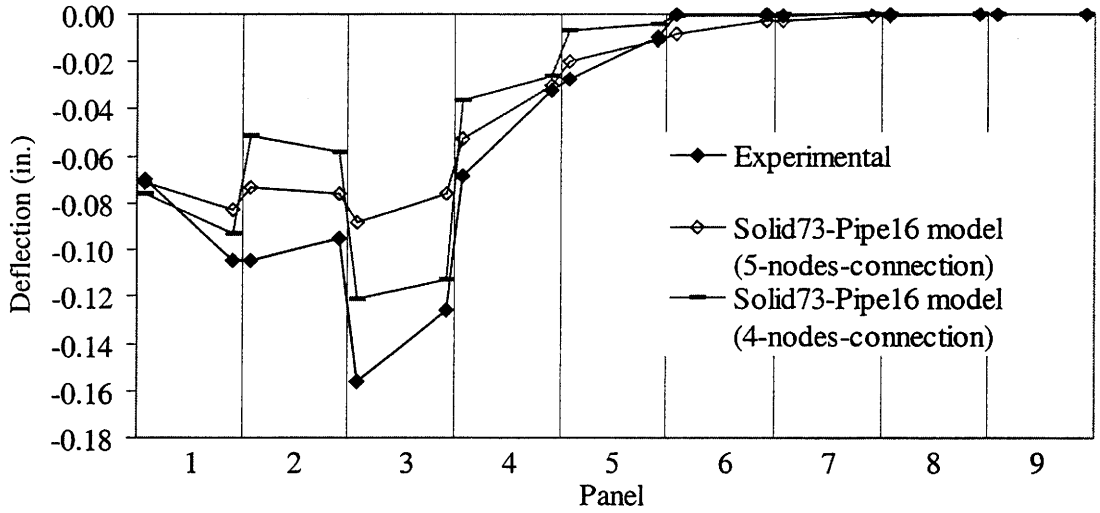

a. LC13

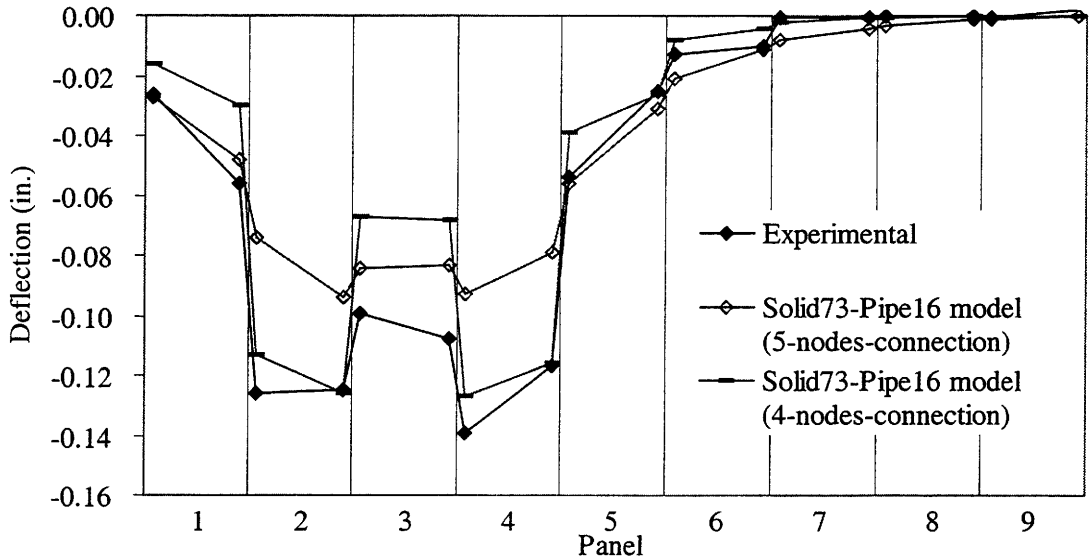

b. LC24

Figure 5.3. Deflection profiles of the Story County Bridge.

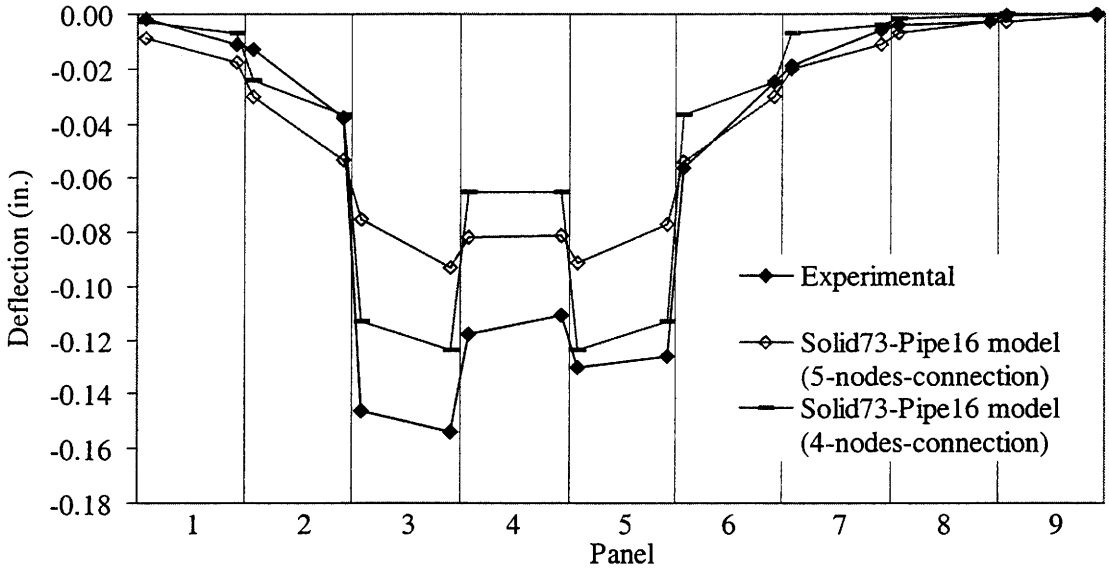

c. LC35

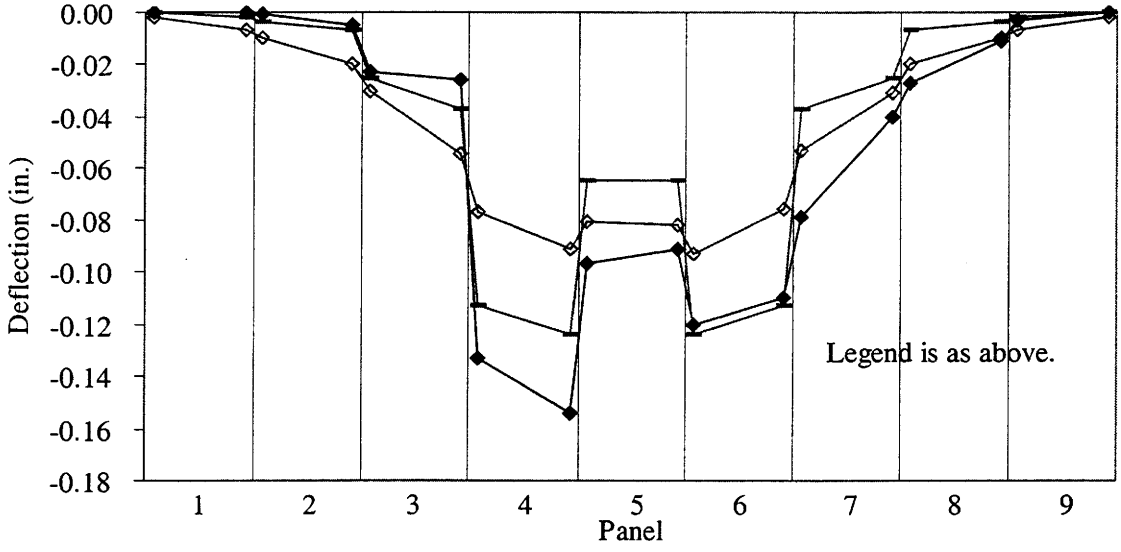

d. LC46

Figure 5.3. Deflection profiles of the Story County Bridge (continued).

underestimated the structure's behavior by 40%. The maximum relative displacement of the two joined panels predicted by the model is 0.03 in., which is 72% less than the experimental result. Based on this, a model with 4-nodes-connection Pipe16 elements was constructed. This model comes closer to predicting the relative displacements and rotations of the slipped joints, as shown in Figure 5.3. A maximum deflection of 0.13 in. was predicted by this model, which is 19% less than the experimental result. The difference between the 4-nodes-connection model and testing results may be due to the stiffer feature of the analytical models, as presented in Chapter 4.

5.3.3.2. Strain Reading

Figure 5.4 presents the bottom strain profiles at the midspan cross-section predicted by the analytical models and measured in the field test. A maximum measurement of 140 microstrain at the bottom reinforcing bars was obtained from the field test, while the model predicted a maximum of 150 microstrain. It can be seen that the analytical model with 4-nodes-connection bolt elements resulted in strain profiles that closely reflect the experimental data. The exception is that: (1) under LC13, a significant slip occurred between Panels 1 and 2 which made the model underestimated the bottom strain of Panel 1 by 33%, and that (2) under LC35, the model predicted a strain of 140 mocrostrain at the bottom which is 55% higher than the experimental result.

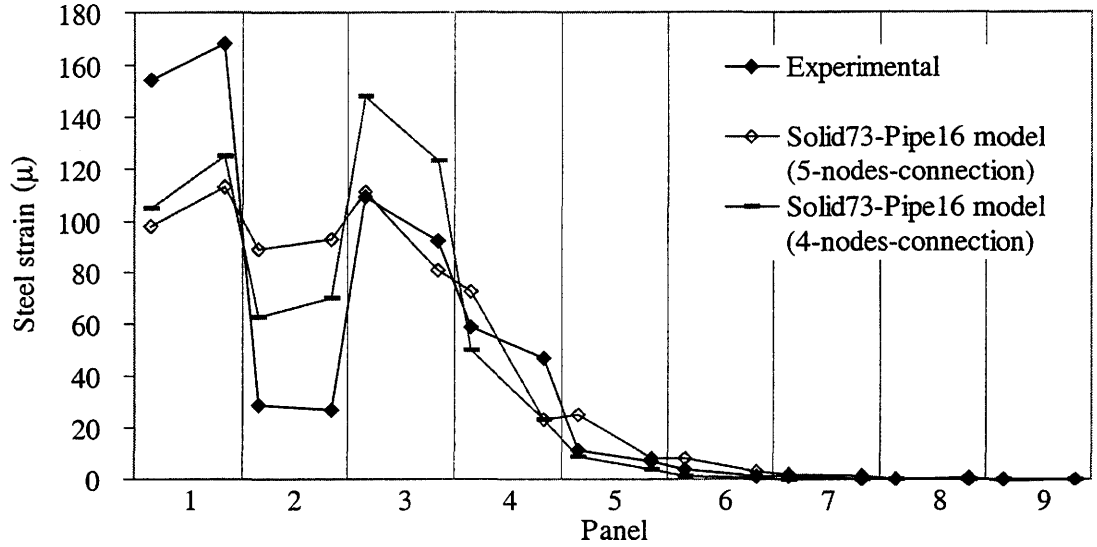

a. LC13

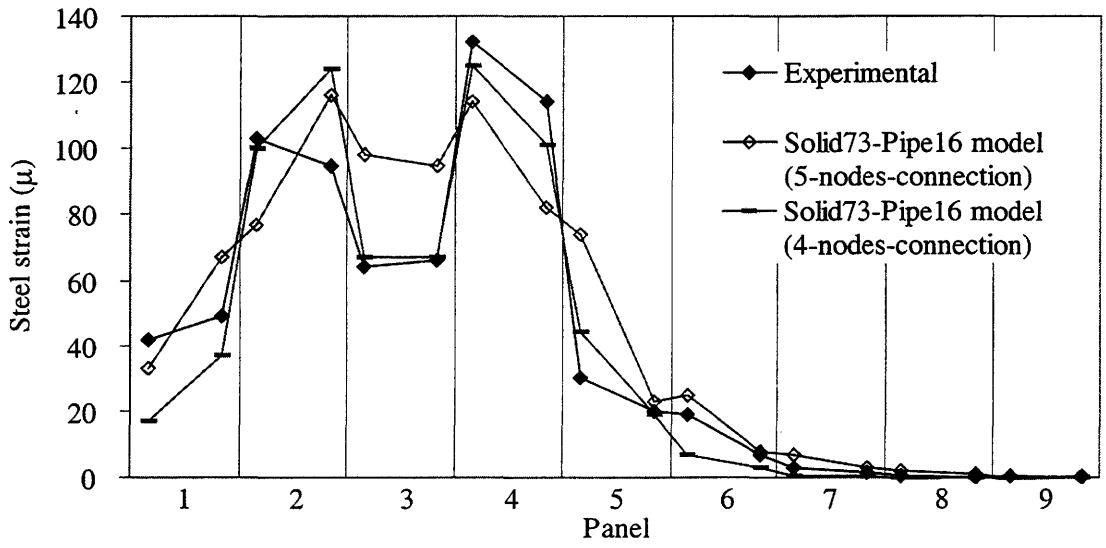

b. LC24

Figure 5.4. Bottom strain profiles of the Story County Bridge.

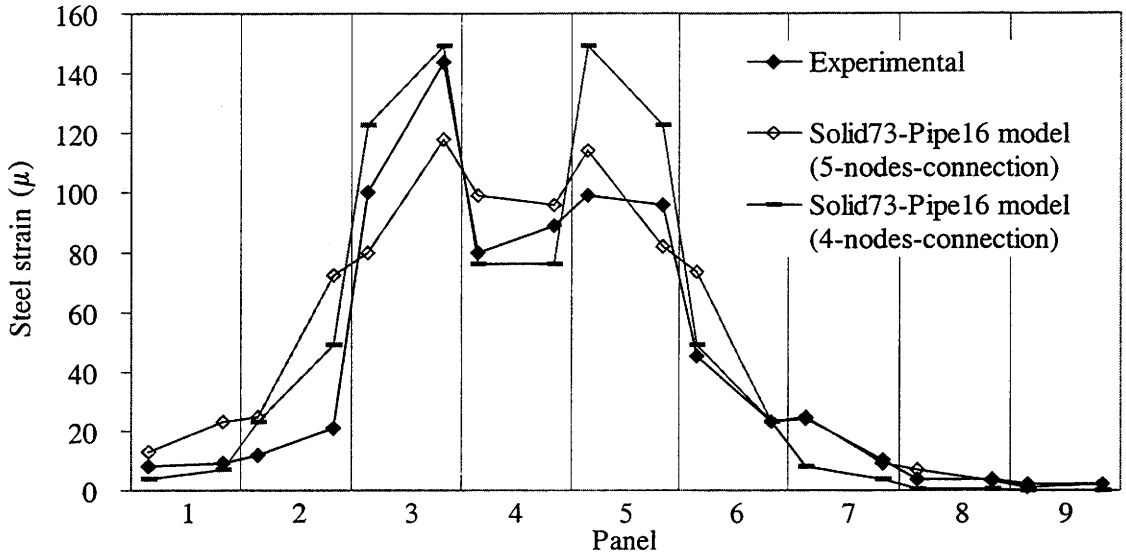

c. LC35

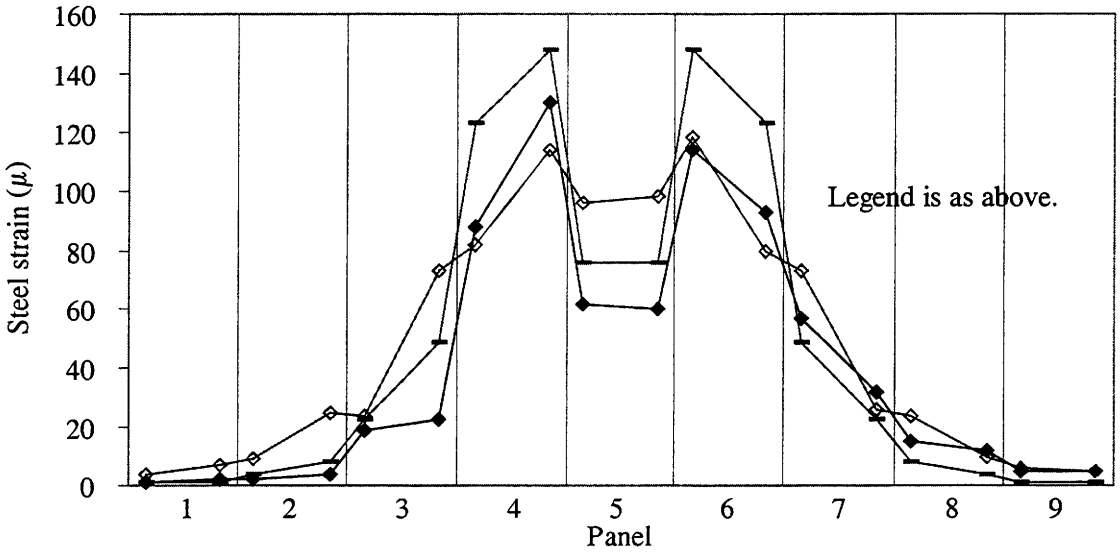

d. LC46

Figure 5.4. Bottom strain profiles of the Story County Bridge (continued).

5.4. Delaware County Dairy Bridge

5.4.1. Testing Vehicle Description

Figure 5.5 illustrates the wheel configuration and weight distribution of the vehicle used to load test the Delaware Country Dairy Bridge.

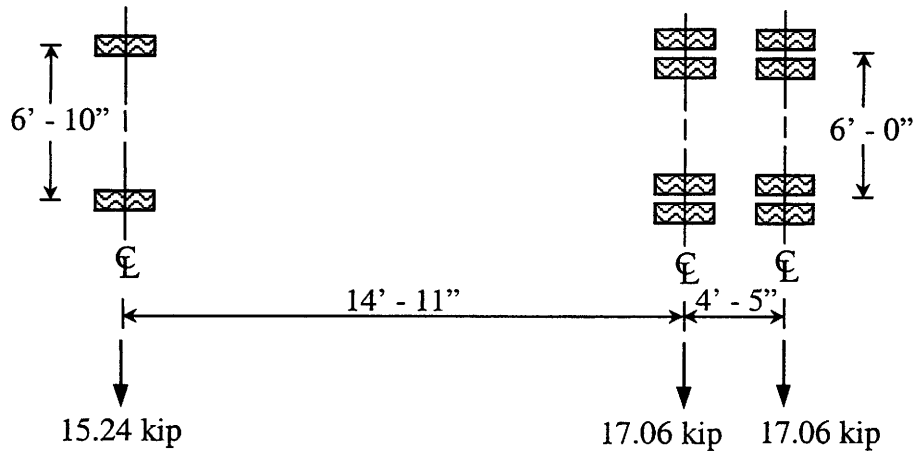

Figure 5.5. Wheel configuration and weight distribution of the vehicle.

5.4.2. Model Description

Two Solid73-Pipe16 models were used to analyze this Delaware County Dairy Bridge which has only bolt connections. One model uses the 5-nodes-connection Pipe16 elements to model the bolt connections; the other model uses the 4-nodes-connection Pipe16 elements. Figure 5.6 illustrates the model constructed in the ANSYS program.

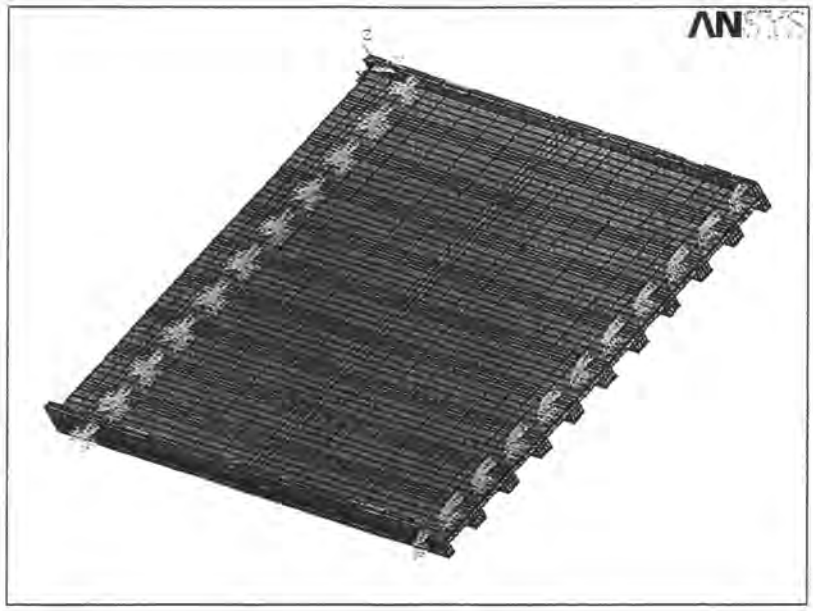

Figure 5.6. Model of the Delaware County Dairy Bridge.

5.4.3. Discussion of Results

5.4.3.1. Deflection Reading

Deflection profiles predicted by the analytical models and measured in the field tests were compared for the midspan cross-section, as shown in Figure 5.7. Only two load cases are presented due to the incompleteness of the experimental results for the other load cases.

Similar to the results compared in the Story County Bridge, the analytical model with 5-nodes-connection Pipe16 elements is not appropriate for the Dairy Bridge in which slip may have occurred significantly. The deflection profiles predicted by the model with 4-nodes-connection Pipe16 elements closely resemble the experimental results. Both the model and the field test produced a maximum deflection of 0.22 in. Under LC24, the model underestimated the deflection of Panel 1 by 32%, while overestimating the deflection of Panel 2 by 23%.

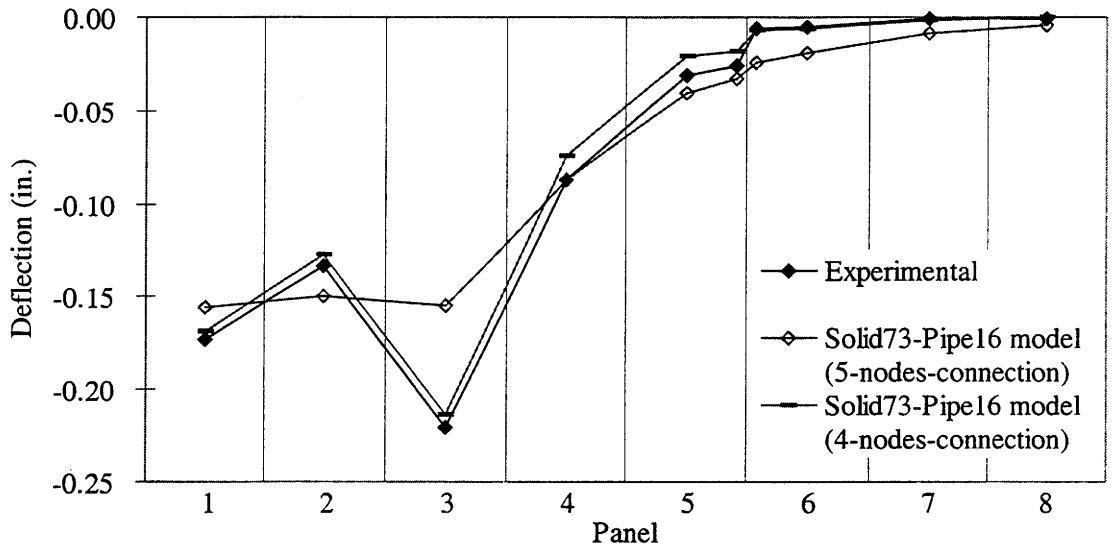

a. LC13

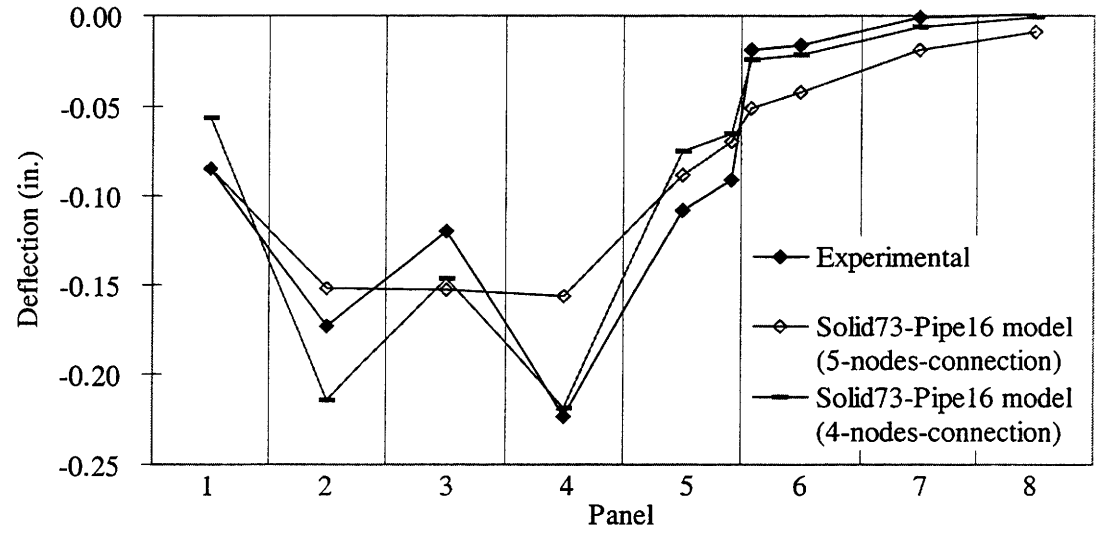

b. LC24

Figure 5.7. Deflection profiles of the Delaware County Dairy Bridge.

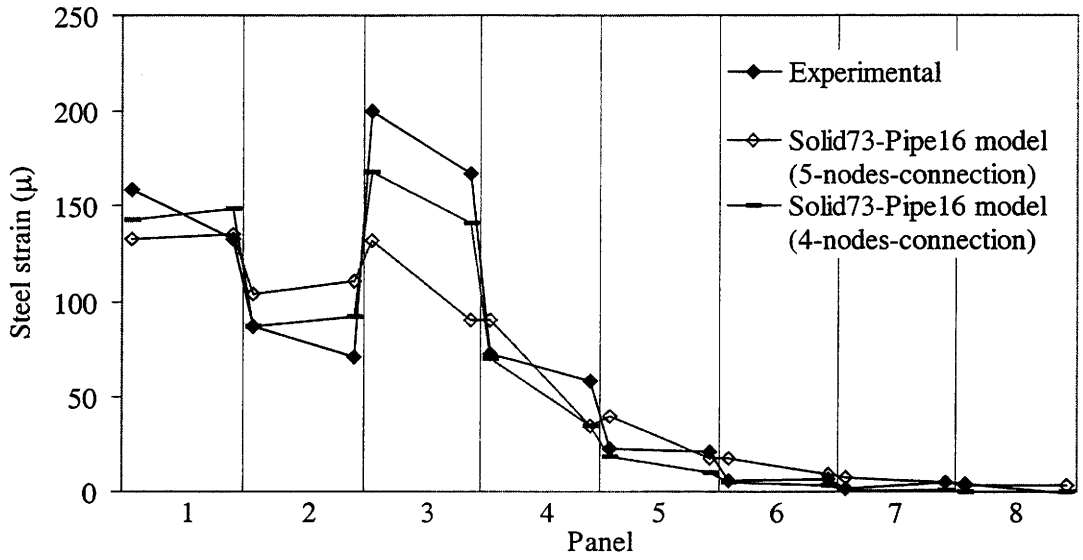

a. LC13

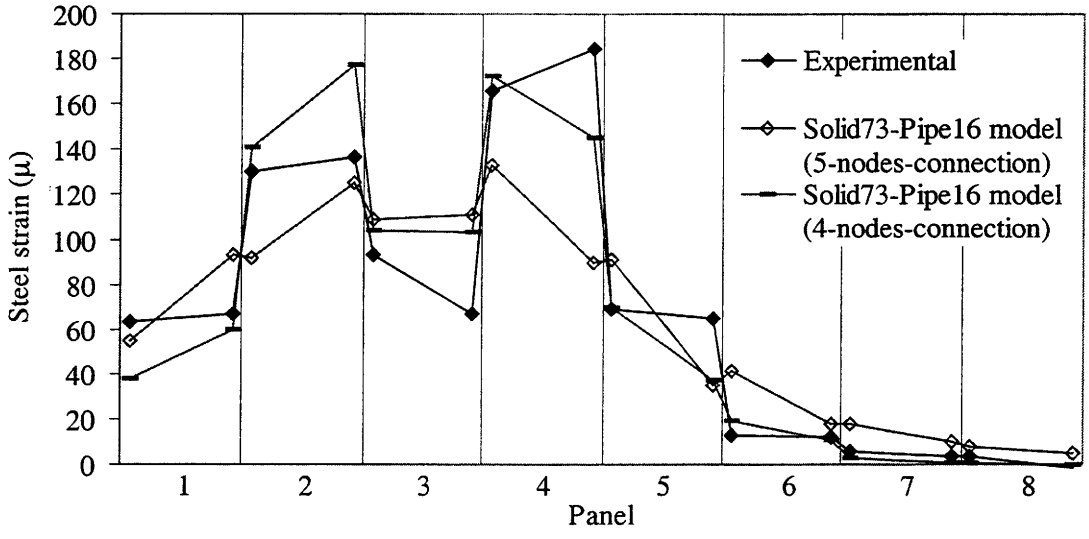

b. LC24

Figure 5.8. Bottom strain profiles of the Delaware County Dairy Bridge.

5.4.3.2. Strain Reading

Figure 5.8 presents the bottom strain profiles at the midspan cross-section predicted by the analytical models and measured in the field tests. A maximum reading of 200 microstrain at the bottom reinforcing bars was obtained from the field tests, while the model predicted a maximum of 165 microstrain. The results from the analytical model with 4-nodes-connection Pipe16 elements are similar to the experimental data.

5.5. Butler County Bridge

5.5.1. Testing Vehicle Description

A truck similar to the Type 3-S2 rating vehicle was used to load test the Butler County Bridge. The wheel configuration and weight distribution of the vehicle is shown in Figure 5.9.

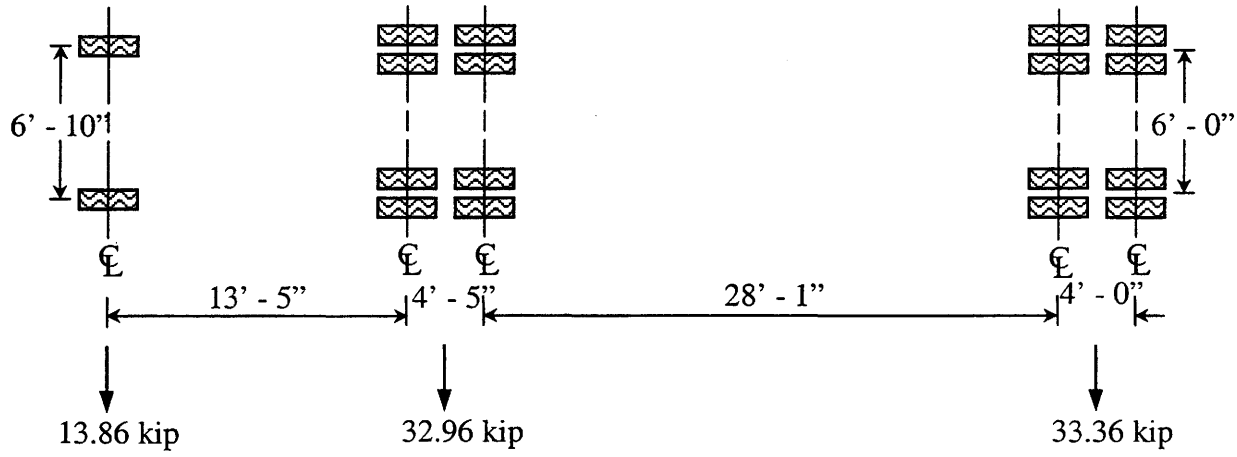

Figure 5.9. Wheel configuration and weight distribution of the vehicle.

5.5.2. Model Description

Based on the investigation of the laboratory bridge, the Solid73-Pipe16 model was used to analyze the Butler County Bridge which has both bolt and pipe connections. The Solid73 element and Pipe16 element were used to model the concrete and reinforcement, respectively. The Combin7 element with a translational stiffness K1=20 kip/in was used to model the pipe connections. Observing that the 4-nodes-connection Pipe16 element is more suitable than the 5-nodes-connection Pipe16 element to model the bolt connection in a field bridge in which slip usually occurs, the 4-nodes-connection Pipe16 element was selected in this model. It should be mentioned that the result from the model with 5-nodes-connection Pipe16 elements is very close to the result from the model with 4-nodes-connection Pipe16 elements when a translational stiffness of 20 kip/in is assigned to the Combin7 element used to model the pipe connections. Figure 5.10 illustrates the model constructed in the ANSYS program.

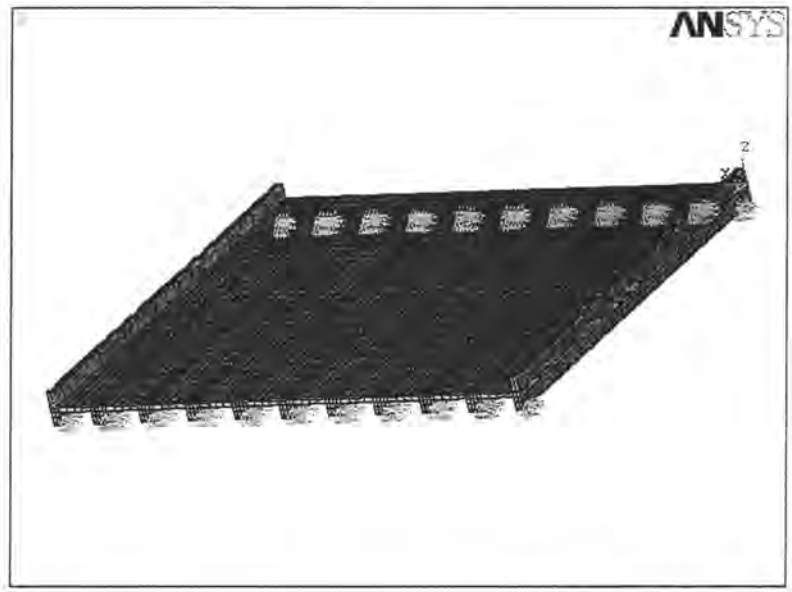

Figure 5.10. Model of the Butler County Bridge.

5.5.3. Discussion of Results

5.5.3.1. Deflection Reading

Deflection profiles from the analytical model and field tests were compared for the bridge under various transverse wheel load cases. The results are shown in Figure 5.11 for the midspan cross-section. Only four load cases are presented due to symmetry.

The maximum deflection of this bridge under this vehicle loading is approximately 0.24 in. The analytical model predicts a maximum deflection of 0.17 in., which is 29% less than the measured field test result. The analytical model predicted a similar rotation behavior of the connection to the experimental data. From Figure 5.11(b), it can be seen that a consistent slip occurred between Panels 2 and 3, 4 and 5, and Panels 5 and 6. The relative displacements of these slipped connections are 0.05 in., 0.07 in., and 0.1 in. The bridge's behavior at the connections was significantly affected by the occurrence of slip, but the overall behavior of the bridge is still similar to the prediction from the analytical model.

When the wheel loads were applied on the edge panel of the bridge, the edge-stiffening effect of the bridge was significant. However, the analytical model didn't adequately predict this effect even including the curbs and rails. Under LC13 (Figure 5.9(a)), the edge panel of the bridge deflected 0.125 in., while from the finite element model, a larger deflection of 0.15 in. was obtained. This represents a 20% increase. When the wheel loads were applied away from the edge panel, this edge-stiffening effect was negligible (Figure 5.11(b)(c)(d)).

5.5.3.2. Strain Reading

Figure 5.12 presents half of the bottom strain profiles at the midspan cross-section which resulted from the analytical model and field tests for the bridge under two transverse

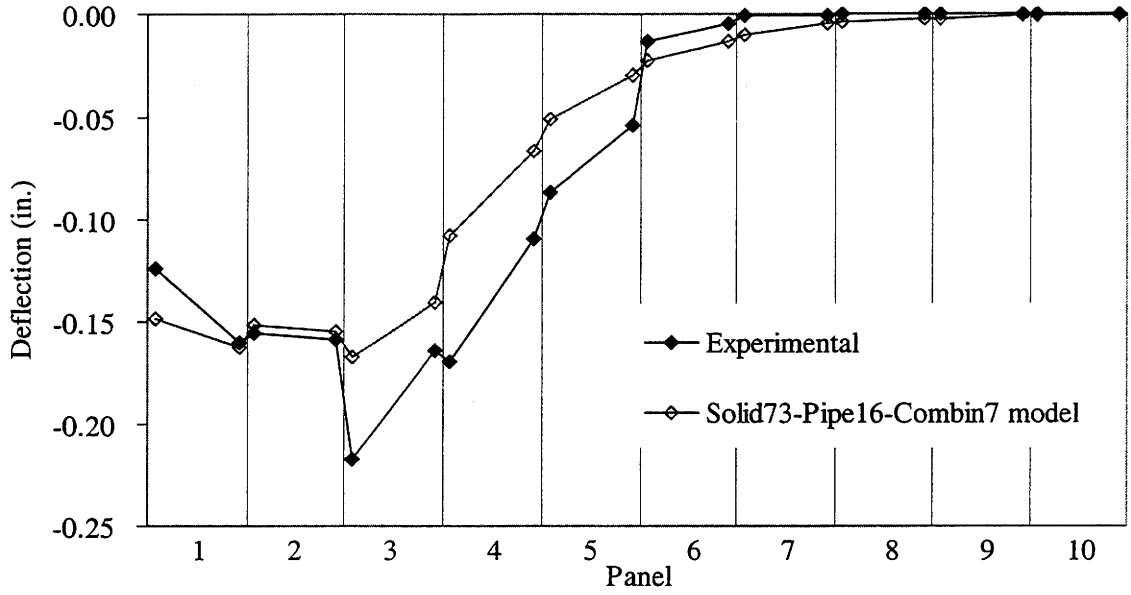

a. LC13

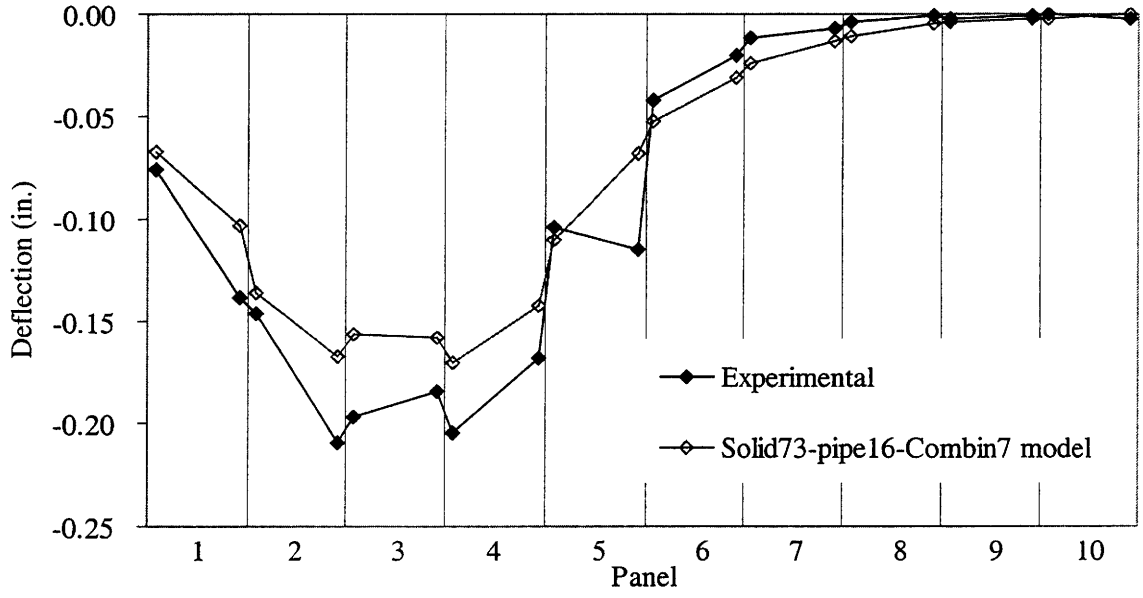

b. LC24

Figure 5.11. Deflection profiles of the Butler County Bridge.

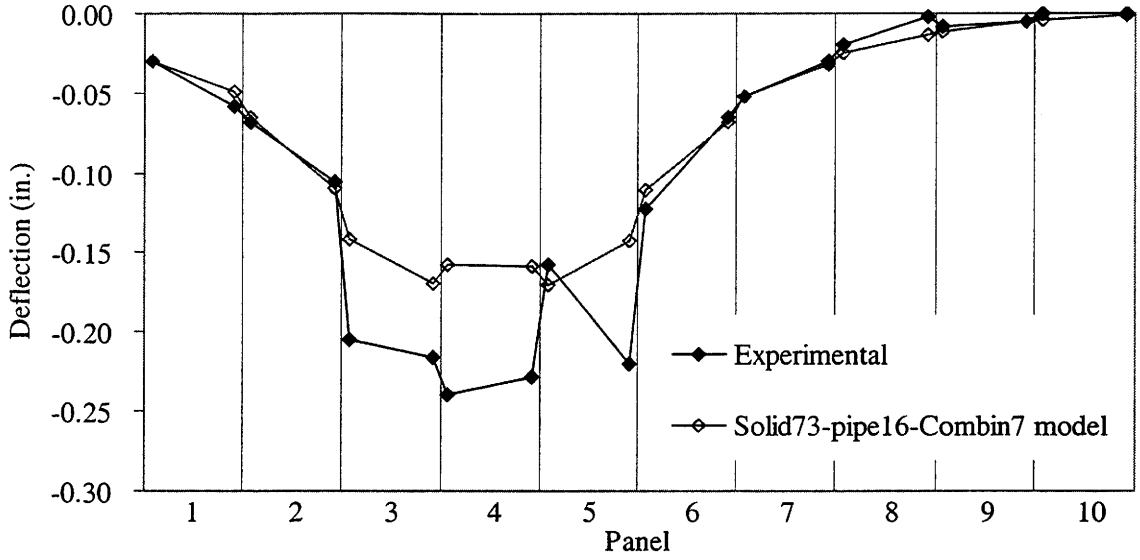

c. LC35

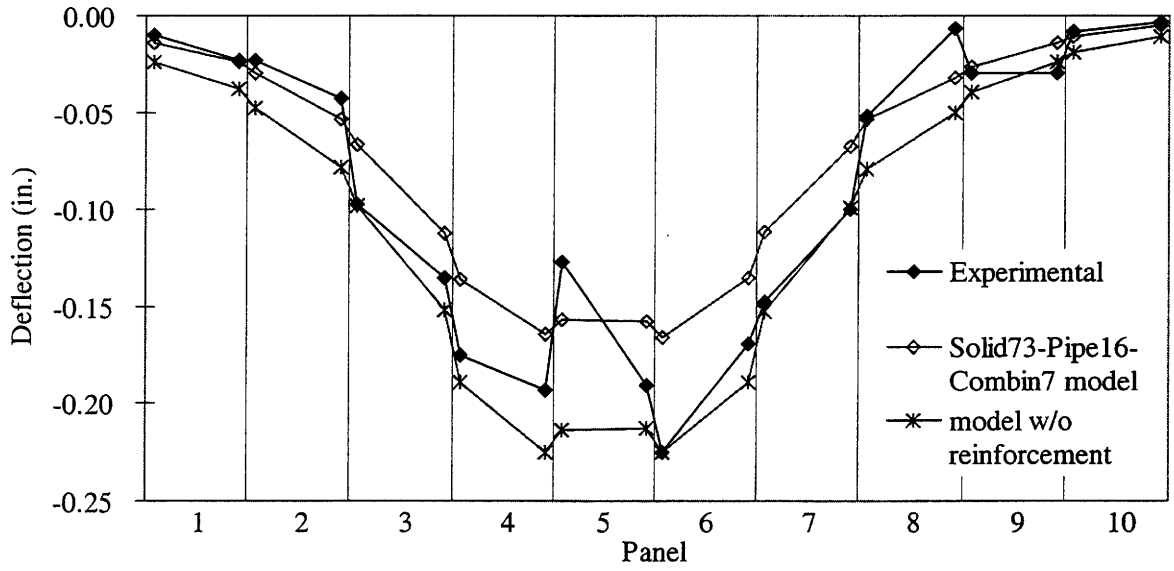

d. LC46

Figure 5.11. Deflection profiles of the Butler County Bridge (continued).

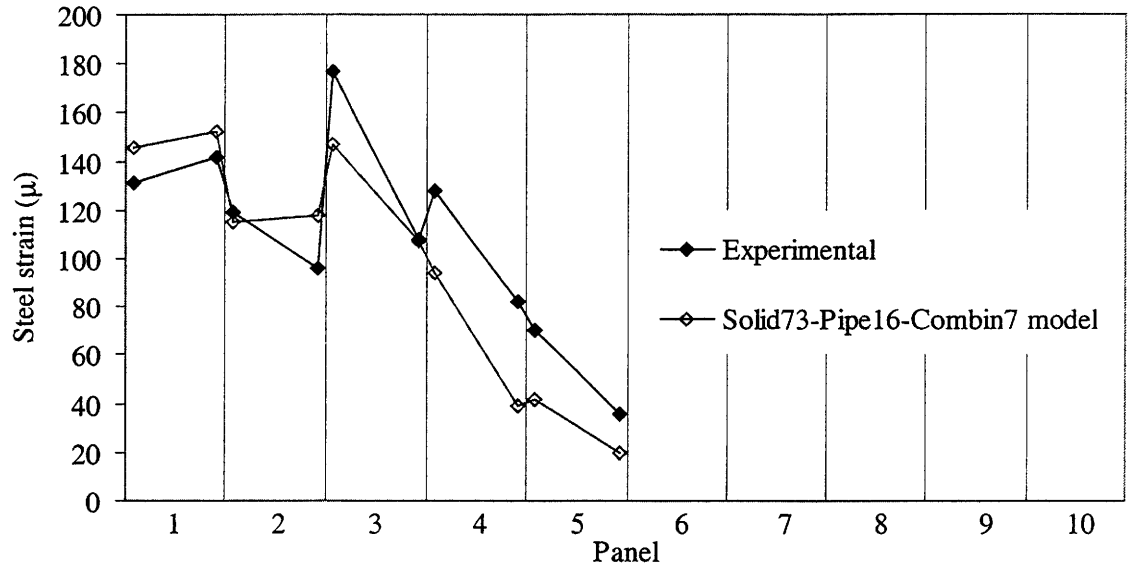

a. LC13

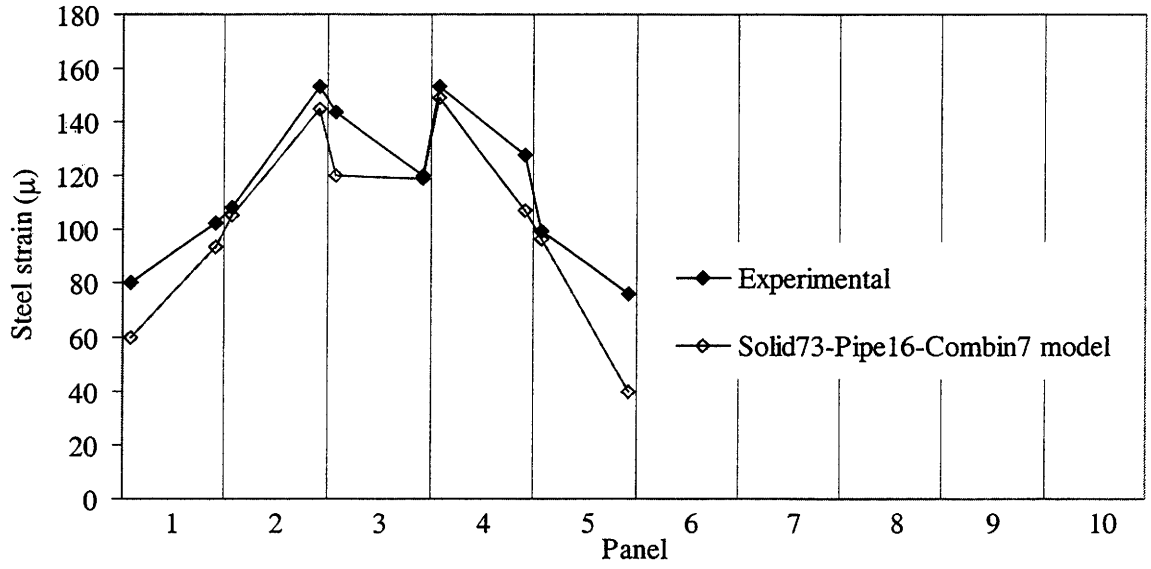

b. LC24

Figure 5.12. Bottom strain profiles of the Butler County Bridge.

wheel load cases. The bottom reinforcing bars reach a maximum of 185 microstrain, far less than the yielding strain of 1503 microstrain. A maximum of 148 microstrain was predicted by the elastic model with reinforcement, 20% lower than the measured field experiment. The comparison of the strain data from the analytical and experimental results is consistent with that of the deflection data. The occurrence of slip and an edge-stiffening effect are also observed.

5.6. Delaware County Trout Bridge

5.6.1. Testing Vehicle Description

Figure 5.13 illustrates the wheel configuration and weight distribution of the vehicle used to load test the Delaware Country Trout Bridge.

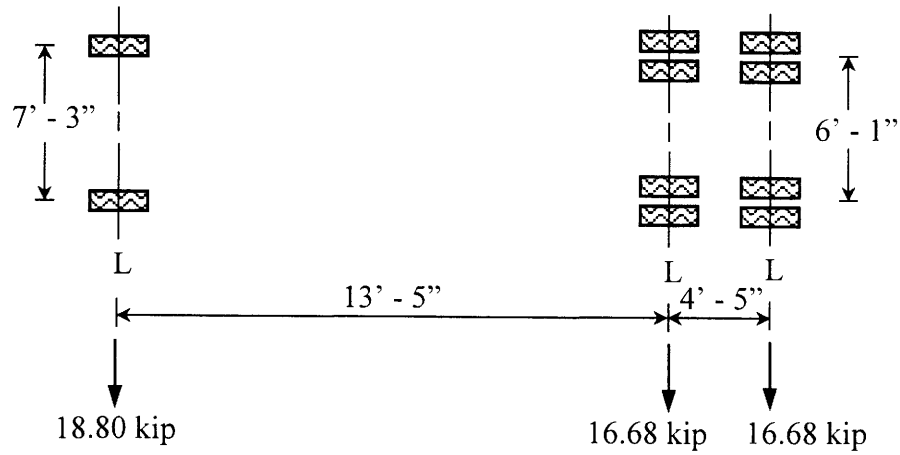

Figure 5.13. Wheel configuration and weight distribution of the vehicle.

5.6.2. Model Description

Although the Trout County Bridge has two spans, it is actually composed of two single-span bridges placed end to end. Each bridge has an end-to-end span of 31 ft, the same

as the Butler County Bridge. The model of this bridge has been simplified as a single span. The Solid73-Pipe16-Combin7 model with 4-nodes-connection bolt elements was used to analyze the Trout County Bridge which has both bolt and pipe connections. Figure 5.14 illustrates the model constructed in the ANSYS program.

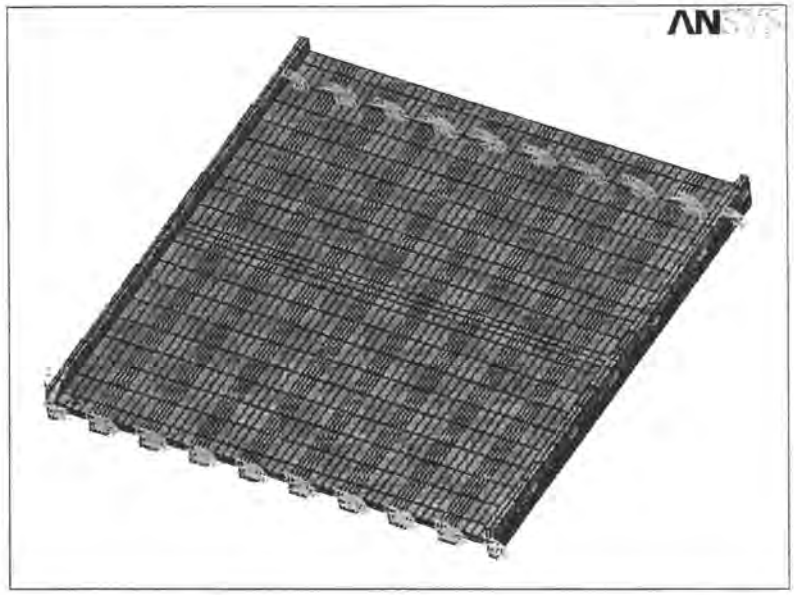

Figure 5.14. Model of the Delaware County Trout Bridge.

5.6.3. Discussion of Results

Figure 5.15 presents the comparison of the deflection profiles predicted by the analytical model and measured during the field tests for the midpan cross-section. Only four load cases are presented due to symmetry.

The maximum deflection of this bridge under this vehicle loading is approximately 0.16 in. Compared to the deflection obtained for Butler County Bridge, which is 0.24 in., this bridge is assumed to have a higher material strength than the Butler County Bridge since they have similar span length and load cases. With a maximum of 12.5% underestimation, the

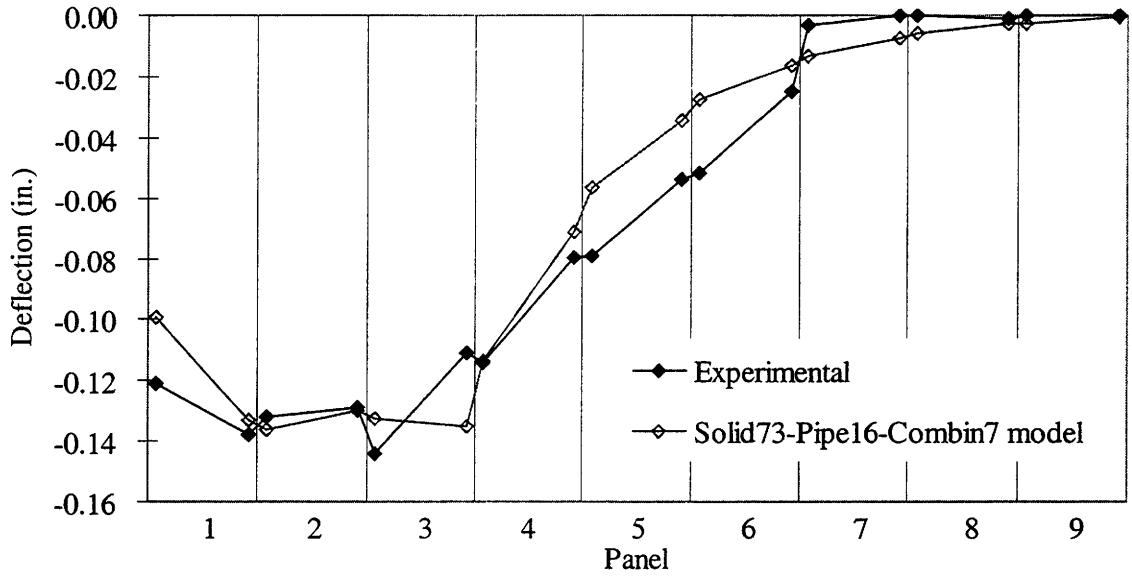

a. LC13

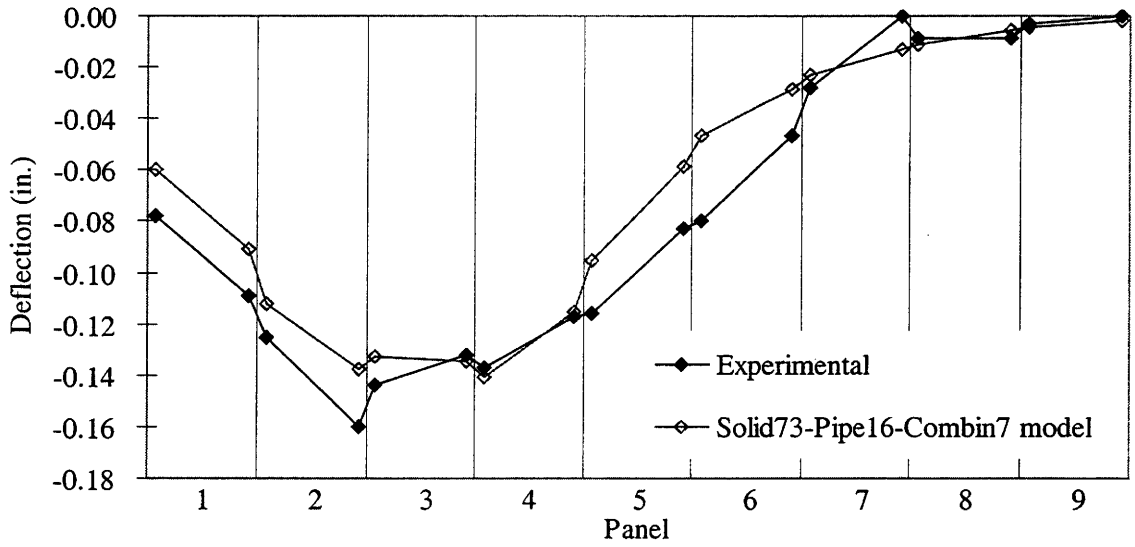

b. LC24

Figure 5.15. Deflection profiles of the Delaware County Trout Bridge.

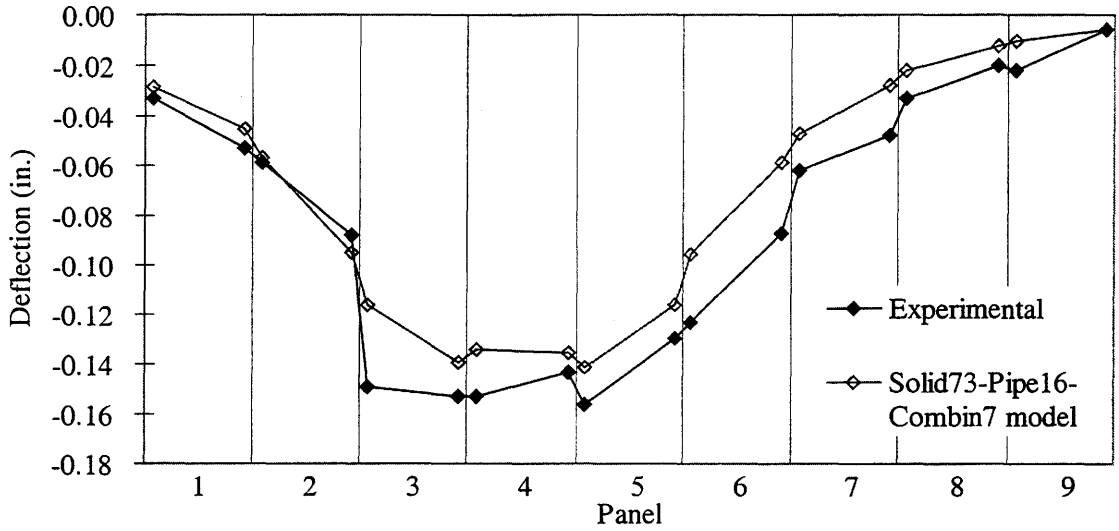

c. LC35

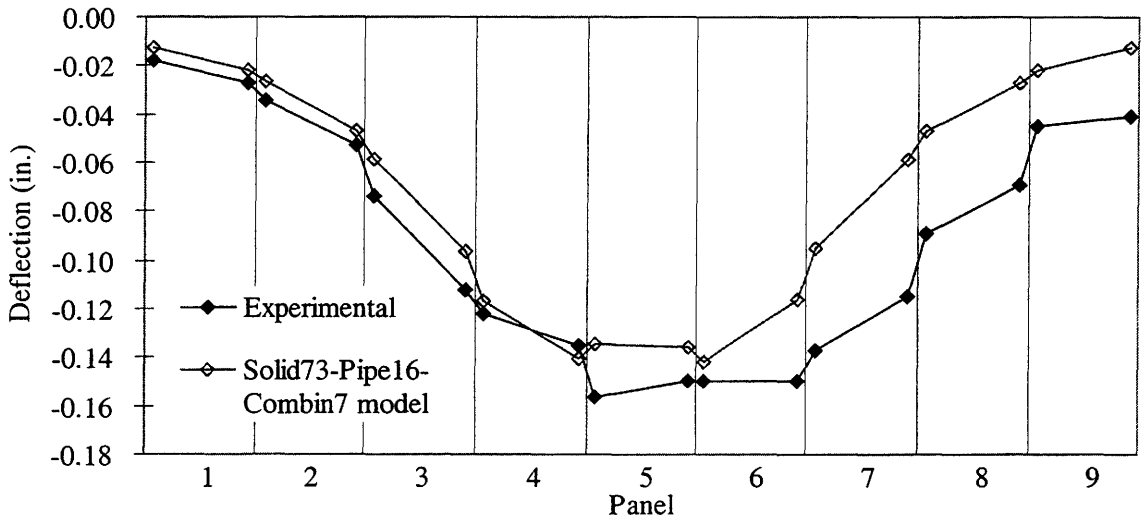

d. LC46

Figure 5.15. Deflection profiles of the Delaware County Trout Bridge (continued).

analytical model predicted rotations at the connections which are close to the experimental data.

The relative displacement of the adjoined panels is normally within 0.025 in., similar to the Butler County Bridge. It is noted that slip seldom occurred in this bridge. Only one obvious slip between Panels 2 and 3 was observed when the bridge is under LC35. The relative displacement of this slipped joint is 0.065 in.

Edge-stiffening effect of this bridge was observed. It is noted that Panels 6 through 9 deflected more than their symmetric panels. The possible reason includes the possibility of lower material properties in Panels 6 through 9. Due to the incompleteness of the strain data recorded in the field tests, no strain data are provided for this bridge.

5.7. Load Distribution Factor

Load distribution factor (LDF) is an important reference for bridge design. In this paper, it is defined as the percentage of deflection of each panel over the sum of each panel's deflection. Tables 5.2 through 5.5 present the load distribution factors of the four load tested bridges. The results are compared between the experimental data (Exp.) and the analytical results (Ana.).

It can be seen that load transfer of the bridge with bolt and pipe connections is more complete than the bridges with only bolt connections. The maximum LDF of the first two bridges is 0.27, while the maximum LDF of the latter two is 0.36. This indicates that in the bridges with bolt and pipe connections, the load directly applied to the panel has a higher distribution to the adjacent panels than in the bridges with only bolt connections. The panel may be designed taking only 27% or 36% of the total load applied to the bridge. However, a

more conservative result can be obtained from the AASHTO LRFD Bridge Design Specifications [17]. Based on this specification, an LFD of 0.61, 0.48, 0.60, and 0.40 was produced for the Butler, Trout, Story, and Dairy Bridge, respectively.

The analytical models predict a result that is close to the experimental data, especially for the bridges with bolt and pipe connections.

Table 5.2. Load Distribution Factor of the Butler County Bridge.

Loaded	Result's	Panel										Total
Panel	Source	1	2	3	4	5	6	7	8	9	10	Factor
1, 3	Exp.	0.20	0.22	0.27	0.20	0.10	0.01	0	0	0	0	1.00
	Ana.	0.25	0.25	0.25	0.14	0.07	0.03	0.01	0	0	0	1.00
2, 4	Exp.	0.13	0.22	0.23	0.23	0.13	0.04	0.01	0	0	0	0.99
	Ana.	0.12	0.21	0.22	0.22	0.13	0.06	0.03	0.01	0	0	1.00
3, 5	Exp.	0.05	0.09	0.23	0.26	0.21	0.10	0.04	0.01	0.01	0	1.00
	Ana.	0.05	0.12	0.21	0.21	0.21	0.12	0.05	0.02	0.01	0	1.00
4, 6	Exp.	0.02	0.04	0.13	0.21	0.18	0.22	0.14	0.03	0.03	0	1.00
	Ana.	0.02	0.05	0.12	0.20	0.20	0.20	0.12	0.06	0.03	0	1.00

Table 5.3. Load Distribution Factor of the Delaware County Trout Bridge.

Loaded	Result's	Panel								Total
Panel	Source	1	2	3	4	5	6	7	8	9	Factor
1, 3	Exp.	0.22	0.22	0.22	0.16	0.11	0.07	0	0	0	1.00
	Ana.	0.21	0.24	0.24	0.17	0.08	0.00	0.02	0	0	1.00
2, 4	Exp.	0.14	0.21	0.20	0.18	0.15	0.09	0.02	0	0	1.00
	Ana.	0.13	0.21	0.22	0.21	0.13	0.06	0.03	0.01	0	1.00
3, 5	Exp.	0.06	0.10	0.20	0.20	0.19	0.14	0.07	0.03	0.02	1.01
	Ana.	0.06	0.12	0.20	0.21	0.20	0.12	0.06	0.03	0.01	1.01
4, 6	Exp.	0.03	0.05	0.11	0.15	0.19	0.18	0.15	0.09	0.05	1.00
	Ana.	0.03	0.05	0.12	0.20	0.20	0.20	0.12	0.06	0.03	1.01

Table 5.4. Load Distribution Factor of the Story County Bridge.

Loaded Panel	Result's Source	Panel 1	2	3	4	5	6	7	8	9	Total Factor
1, 3	Exp.	0.22	0.25	0.36	0.13	0.05	0.00	0	0	0	1.01
	Ana.	0.29	0.19	0.40	0.11	0.02	0.00	0.00	0	0	1.01
2, 4	Exp.	0.09	0.28	0.23	0.29	0.09	0.03	0.00	0	0	1.01
	Ana.	0.06	0.32	0.18	0.33	0.09	0.02	0.00	0.00	0	1.00
3, 5	Exp.	0.01	0.05	0.31	0.24	0.27	0.08	0.03	0.01	0.00	1.00
	Ana.	0.01	0.08	0.32	0.17	0.32	0.08	0.02	0.00	0.00	1.00
4, 6	Exp.	0.00	0.01	0.05	0.31	0.20	0.26	0.13	0.04	0.00	1.00
	Ana.	0.00	0.01	0.08	0.31	0.18	0.31	0.09	0.02	0.00	1.00

Table 5.5. Load Distribution Factor of the Delaware County Dairy Bridge.

Loaded Panel	Result's Source	Panel 1	2	3	4	5	6	7	8	Total Factor
1, 3	Exp.	0.27	0.20	0.34	0.13	0.05	0.01	0	0	1.00
	Ana.	0.28	0.21	0.35	0.12	0.03	0.01	0.00	0	1.00
2, 4	Exp.	0.12	0.24	0.17	0.31	0.15	0.02	0.00	0	1.01
	Ana.	0.08	0.29	0.19	0.30	0.10	0.03	0.01	0.00	1.00

5.8. Chapter Summary

As presented in Chapter 4, the Solid73-Pipe16 model with 5-node-connection bolt elements is appropriate for the multibeam bridge with only bolt connections constructed in the laboratory. However, in the field bridges, due to many influences, the bolts cannot be guaranteed to stay tight and some slip may occur. This makes the 5-nodes-connection model inappropriate. The results from the testing on the field bridges proved that slip is a common

occurrence in the field bridges with only bolt connections. The 4-nodes-connection Pipe16 element is more suitable to model the bolt connections in the field bridges.

It was observed that slip is less likely to occur to the bridges with both bolt and pipe connections. Due to this behavior, the Solid73-Pipe16-Combin7 model predicts results similar to the experimental results. This includes the rotation of the connections, and the load distribution factor. Due to the larger stiffness, the analytical model usually underestimates the bridge's behavior by approximately 30%. But the deflection and strain profiles along the transverse cross-section obtained from the analytical model are consistent with the experimental results. The combination of the Pipe16 element with 4-nodes-connection and the Combin7 element with a translational stiffness of 20 kip/in proved to be appropriate when modeling the bolt and pipe connections. It should be mentioned here that another combination of the Pipe16 element with 5-nodes-connection and the Combin7 element with a translational stiffness of 20 kip/in produces a very similar result.

It is noted that the bridges with bolt and pipe connections have a more efficient load transfer than the bridges with only bolt connections. Based on deflection, a maximum LDF of 0.27, 0.22, 0.36, and 0.34 was obtained from the filed test for the Butler, Trout, Story, and Dairy Bridge, respectively. The analytical models resulted in a similar value of 0.25, 0.24, 0.40, and 0.35. The AASHTO LRFD Bridge Design Specifications [37] produced more conservative values of 0.61, 0.48, 0.60, and 0.40.

Edge-stiffening effect of the bridges was observed. Unfortunately, even including the curb and rail, the analytical models still cannot represent this effect properly.

6. SUMMARY AND CONCLUSIONS

6.1. Summary

A comprehensive literature review was initially conducted on analysis techniques for multibeam bridges. It was determined that the classical grillage method, plate theory and other derivations have limitations in representing the localized connection behavior of the multi-channel-beam bridges. The finite element method was thus chosen to be the analytical approach for this research project. The ANSYS program was selected to model the bridge structures and their components.

The Solid, Link and Pipe element types in ANSYS were used to model reinforced concrete beams. The Solid elements were used to model the concrete portion of the beam, while the Link or Pipe elements were used to model the reinforcing bars. Support condition and span length sensitivity studies were also conducted. Along with the laboratory testing, theoretical calculations based on ACI 318-99 were calculated to verify the models. To investigate the effect of reinforcement on the stiffness of the models, two models were constructed. One model included reinforcement to represent a structure with a stiffness of I_{uncr}, the other model neglected reinforcement to represent a structure with a stiffness of I_g.

A laboratory bridge, constructed of four reinforced concrete channel beams in Iowa State University, was modeled to investigate the modeling of bolt and pipe connections. The Link8 and Pipe16 elements were used to model the bolt connections and the Combin7 element was used to model the pipe connections. It was determined that the rotational degrees of freedom are critical in transferring load through the bolts. Because of this, the Link8 element is not appropriate to model the bolts since it has no rotational degrees of freedom. The Pipe16 element with additional rotational degrees of freedom is more

appropriate. A sensitivity study was performed to determine the number of connected nodes of the Pipe16 elements to best represent the bolts. Also, a sensitivity study to determine the translational stiffness of the Combin7 elements used to model the pipe connections was performed. By comparing to the laboratory testing results, it was determined that the Solid73-Pipe16 model was appropriate to model the bridges with only bolt connections and the Solid73-Pipe16-Combin7 model was appropriate to model the bridges with bolt and pipe connections.

Four field multi-channel-beam bridges were load tested for this research and the results were used to verify the finite element models. Two of them have both bolt and pipe connections, while the others have only bolt connections. Based on the study conducted on the laboratory bridge, the finite element models of these field bridges were constructed. Deflection and bottom stain profiles along the transverse cross-section of the bridges predicted by the analytical models and measured in the field tests were compared. Load distribution factors for each bridge predicted from the models were provided and compared to the results from the load tests and the AASHTO specifications. Slip was observed as a common occurrence to the bridges with only bolt connections. Edge-stiffening effects of the bridge were another observation.

6.2. Conclusions

It may be concluded that the finite element method has a number of advantages over the grillage method and plate theories analyzing the multibeam bridges with bolt or pipe connections. Localized information can be easily obtained and the connection behavior can be studied. Deflections and strains at any location of the bridge are available from the finite

element analysis. Using the general-purpose finite element software program, ANSYS, the multi-channel-beam bridges were modeled and the results were compared to the experimental data and available code calculations. The following list is a summary of the conclusions from this investigation:

1. Both of the Solid45-Link8 model and the Solid73-Pipe16 model are appropriate to model the individual reinforced concrete channel beams. In these models, the Solid elements were used to represent the concrete portion, while the Link or Pipe elements were used to represent the reinforcing bars. A perfect bond is assumed between the concrete and reinforcing bars. These models represent a structure with a stiffness of I_{uncr}. To represent a structure with a stiffness of I_g, reinforcing bars can be removed from the models.
2. Due to the lack of rotational DOFs, the Link8 elements cannot represent the bolt connections which transfers the load between the adjoined beams through its bending behavior. While with rotational DOFs, the Pipe16 elements are appropriate to model the bolts' behavior. Due to this behavior, the Solid73-Pipe16 model was used to model the multi-channel-beam bridges with only bolt connections. Nodal forces resulting from the models verifies that the more nodes connected, the more load is transferred. By comparing the results from the models to the experimental data, the 5-nodes-connection Pipe16 elements and the 7-nodes-connection Pipe16 elements were chosen to model the bolt connections for the laboratory bridge since they appropriately represent the rotation of the bolts. The 5-nodes-connection model was selected due to its simplicity and accuracy.

3. Based on the assumption that the pipe connections between the adjacent panels behave like hinges, the Combin7 elements were used to represent the pipe connections. After a sensitivity study, the translational stiffness of the Combin7 elements was determined to be 20 kip/in.
4. The analytical model with reinforcement usually underestimates the actual structure's behavior by up to 30%. Based on the observation that the experimental results are close to the ACI code calculations which uses I_e (not greater than I_g) instead of I_{uncr}, a model neglecting reinforcement, to represent a structure with a stiffness of I_g, was constructed to investigate the effect of the stiffness of the structures. It is noted that results from the model neglecting reinforcement are more consistent with the experimental data than the results from the model including reinforcement.
5. Slip is a common occurrence to the field bridges with only bolt connections. Due to this reason, the 4-node-connection Pipe16 elements were more suitable to model the Pipe16 connections than the 5-node-connection bolt elements. The Solid73-Pipe16 model with 4-node-connection bolt elements produced similar relative displacement and rotation of the bolt connections to the experimental data. It is noted that slip usually occurred between the panel directly receiving the load and its adjacent panels.
6. Load transfer of the bridges with bolt and pipe connections is more effective than in the bridges with only bolt connections. From the testing results, he maximum LDF of the two bridges with bolt and pipe connections is 0.27, while the maximum LDF of the two bridges with only bolt connections is 0.36. The analytical models

produced a corresponding LDF of 0.25 and 0.40 for the two kinds of bridges. More conservative results were obtained from the AASHTO specifications.

7. Edge stiffening effects of these tested multibeam bridges were observed. However, the analytical models constructed in this study cannot represent it sufficiently even though the curb and rail were included. Further investigation is recommended.

REFERENCES

1. Ingersoll, J. S., "Field and Laboratory Evaluation of Precast Concrete Bridges," M. S. thesis, Iowa State University, Ames, Iowa (in preparation).
2. *ANSYS User's Manual for Revision 5.1*, Swanson Analysis System, Inc., Houston, PA, 1992.
3. Barker, R. M., and Puckett, J. A., "Design of Highway Bridges," John Wiley & Sons, Inc., 1997, pp. 296-301.
4. Jategaonkar, R., Jaeger, L. G., and Cheung, M. S., "Bridge Analysis Using Finite Elements," *Canadian Society for Civil Engineering*, 1985, pp. 10-13.
5. Hambly, E. C., "Bridge Deck Behavior," Chapman and Hall, 1991, pp.35-42.
6. Bakht, B., and Jaeger, L. G., "Bridge Analysis Simplified," McGraw-Hill, Inc., 1985, pp. 1-4.
7. Euler, L., "De motu vibratorio tympanorum," *Novi Commentari Acad. Petropolit.*, 10 (1766), 243-260.
8. Huber, M. T., "Teoria sprezystoci, Theorie de l'elasticite," *Nakl. Polskiej Akademii Uniejetnosci*, Krakow 1948-1950, pp. 160-190.
9. Guyon, Y., "Calcul des ponts larges à poutres multiples solidariseés par des entretoises," *Annales des Ponts et Chausseés*, No. 24, September-October, 1946, pp. 553-612.
10. Massonnet, C., "Méthode de calcul des ponts à poutres multiples tenant compte de leur résistance à la torsion," Zurich, *International Association for Bridge and Structural Engineering, Publications*, Vol. 10, 1950, pp. 147-182.

11. Timoshenko, S. P., and Woinowsky-Krieger, S., "Theory of Plates and Shells," McGraw Hill Book Co. Inc., New York, N. Y., 2nd Edition, 1959, pp. 365.

12. Morice, P. B., and Little, G., "Load Distribution in Prestressed Concrete Bridge Systems," *The Structural Engineer*, Vol. 32, No. 3, March, 1954, pp. 83-111.

13. Rowe, R. E., "Concrete Bridge Design," John Wiley & Sons Inc., New York, N. Y., 3rd Impression, 1972.

14. Cusens, A. R., and Pama, R. P., "Design of Concrete Multibeam Bridge Decks," *Journal of the Structural Division*, ASCE, Vol. 91, No. ST5, October, 1965, pp. 255-278.

15. Best, B. C., "Tests of a prestressed Concrete Bridge Incorporating Transverse Mild-Steel Shear Connectors," *Research Report No. 16*, Cement & Concrete Assn., London, England, December, 1963.

16. Bakht, B., Jaeger, L. G., and Cheung, M. S., "Transverse Shear in Multibeam Bridges," *Journal of the Structural Engineering*, ASCE, Vol. 109, No. 4, April, 1983, pp. 936-949.

17. American Association of State Highway Officials (AASHTO), *Standard Specifications for Highway Bridges*, Washinton, D. C., 1977.

18. Ontario Ministry of Transportation and Communications, *Ontario Highway Bridge Design Code*, Downsview, Ontario, Canada, 1979.

19. Spindel, J. E., "A Study of Bridge Slabs Having No Transverse Flexural Stiffness," Ph. D. thesis, University of London, England, 1961.

20. Little, G., "Laboratory Tests for Load Distribution in a Model P.C. Bridge," *Civil Engineering & Public Works Review*, Vol. 50, No. 585, March, 1955, pp. 285-287, and No. 586, April, 1955, pp. 421-422.

21. Roesli, A., et al., "Field Tests on a prestressed Concrete Multibeam Bridge," *Proceedings*, Highway Research Bd., Natl. Research Council, Vol. 35, 1956, pp. 152-176.

22. Walther, R. E., "Investigation of Multibeam Bridges," *Journal of the American Concrete Institute*, Vol. 29, No. 6, December, 1957, Proceedings, Vol. 54.

23. Pama, R. P., and Cusens, A. R., "Edge Beam Stiffening of Multibeam Bridges," *Journal of the Structural Division*, ASCE, Vol. 93, No. ST2, April, 1967, pp. 141-161.

24. Duberg, J. E., Khachaturian, N., and Fradinger, R. E., "Method for Analysis of Multibeam Bridges," *Journal of the Structural Division*, ASCE, Vol. 86, No. ST7, July, 1960, pp. 109-138.

25. Khachaturian, N., Robinson, A. R., and Pool, R. B., "Multibeam Bridges with Elements of Channel Section," *Journal of the Structural Division*, ASCE, Vol. 93, No. ST6, December, 1967, pp. 161-187.

26. Powell, G. H., Ghose, A., and Buckle, I. G., "Analysis of Multibeam Bridges," *Journal of the Structural Division*, ASCE, Vol. 95, No. ST9, September, 1969, pp. 1953-1965.

27. Cusens, A. R., and Pama, R. P., "Discussion on Multibeam Bridges with Elements of Channel Section," *Journal of the Structural Division*, ASCE, No. ST8, August, 1968, pp. 2019-2021.

28. Jones, H. L., and Boaz, I. B., "Skewed Discretely Connected Multi-Beam Bridges," *Journal of Structural Engineering*, Vol. 112, No. 2, February, 1986, pp. 257-272.

29. Cook, R. D., Malkus, D. S., and Plesha, M. E., "Concepts and Applications of Finite Element Analysis," John Wiley & Sons Inc., New York, N. Y., 3rd Edition, 1989, pp. 4.

30. American Society of Civil Engineering, "Finite Element Analysis of Reinforced Concrete Structures II," New York, 1991.

31. Zienkiewicz, O. C., "The Finite Element Method in Engineering Science," McGraw Hill, London, 1971.

32. American Concrete Institute, *Building Code Requirements for Structural Concrete (318-99) and Commentary (318R-99)*, Farmington Hills, MI, 1999, pp. 97.

33. American Association of State Highway and Transportation Officials, *Manual for Condition Evaluation of Bridges*, Washington, D.C., 2001, pp. 74.

34. American Association of State Highway and Transportation Officials, *AASHTO LRFD Bridge Design Specifications*, Washington, D.C., 1994.

ACKNOWLEDGEMENTS

The research presented herein was sponsored by the Iowa Department of transportation. The instruction for the analyses given by Professor F. Wayne Klaiber and Professor Terry J. Wipf of Iowa State University is gratefully acknowledged. I am also indebted to J. Scott Ingersoll, a graduate student of Iowa State University, for making the experimental results available and providing all the photographs and some figures presented in this paper.

I wish to express my sincere appreciation to F. Wayne Klaiber, Terry J. Wipf, and Ann G. Sardo of Iowa State University and Chris Ramseyer of Star Building Systems for their careful editorial work. Mahmoud Halfawy is also greatly appreciated for his discussion on modeling during the beginning of this research.

Support from my husband, my parents, and my parents in law made this paper possible. I wish to thank them from the bottom of my heart for their love and patience.